ESL-TR-87-53

MODELING RESPONSE OF TANKS CONTAINING FLAMMABLES TO FIRE IMPINGEMENT

F.A. ALLAHDADI, C. LUEHR, T. MOREHOUSE, P. CAMPBELL

NEW MEXICO ENGINEERING RESEARCH INSTITUTE
P.O. BOX 25
UNIVERSITY OF NEW MEXICO
ALBUQUERQUE NM 87131

JULY 1988

FINAL REPORT

SEPTEMBER 1986 — FEBRUARY 1987

AFESC

ENGINEERING & SERVICES LABORATORY
AIR FORCE ENGINEERING & SERVICES CENTER
TYNDALL AIR FORCE BASE, FLORIDA 32403

NAVAIR

NAVAL AIR SYSTEMS COMMAND
DEPARTMENT OF NAVY,
WASHINGTON DC 20361

NOTICE

PLEASE DO NOT REQUEST COPIES OF THIS REPORT FROM HQ AFESC/RD (ENGINEERING AND SERVICES LABORATORY). ADDITIONAL COPIES MAY BE PURCHASED FROM:

NATIONAL TECHNICAL INFORMATION SERVICE
5285 PORT ROYAL ROAD
SPRINGFIELD, VIRGINIA 22161

FEDERAL GOVERNMENT AGENCIES AND THEIR CONTRACTORS REGISTERED WITH DEFENSE TECHNICAL INFORMATION CENTER SHOULD DIRECT REQUESTS FOR COPIES OF THIS REPORT TO:

DEFENSE TECHNICAL INFORMATION CENTER
CAMERON STATION
ALEXANDRIA, VIRGINIA 22314

UNCLASSIFIED

SECURITY CLASSIFICATION OF THIS PAGE

REPORT DOCUMENTATION PAGE

1a. REPORT SECURITY CLASSIFICATION Unclassified	1b. RESTRICTIVE MARKINGS
2a. SECURITY CLASSIFICATION AUTHORITY	3. DISTRIBUTION/AVAILABILITY OF REPORT Approved for public relase. Distribution unlimited.
2b. DECLASSIFICATION/DOWNGRADING SCHEDULE	
4. PERFORMING ORGANIZATION REPORT NUMBER(S) NMERI WA3-33 (3.05)	5. MONITORING ORGANIZATION REPORT NUMBER(S) ESL-TR-87-53
6a. NAME OF PERFORMING ORGANIZATION New Mexico Engineering Research Institute 6b. OFFICE SYMBOL (If applicable) NMERI	7a. NAME OF MONITORING ORGANIZATION Engineering and Services Laboratory
6c. ADDRESS (City, State and ZIP Code) Box 25, University of New Mexico Albuquerque, New Mexico 87131	7b. ADDRESS (City, State and ZIP Code) Air Force Engineering and Services Center Tyndall Air Force Base, Florida 32403
8a. NAME OF FUNDING/SPONSORING ORGANIZATION HQ AFESC/RD and NAVAIR 8b. OFFICE SYMBOL (If applicable) RDCF	9. PROCUREMENT INSTRUMENT IDENTIFICATION NUMBER Contract No. F29601-84-C-0080
8c. ADDRESS (City, State and ZIP Code) Tyndall AFB FL 32403-6001 Commander NAVAIR Washington DC 20361-5510	10. SOURCE OF FUNDING NOS. PROGRAM ELEMENT NO.: 62206F PROJECT NO.: 2673 TASK NO.: 0041 WORK UNIT NO.:
11. TITLE (Include Security Classification) MODELING RESPONSE OF TANKS CONTAINING FLAMMABLES TO FIRE IMPINGEMENT	
12. PERSONAL AUTHOR(S) Firooz A. Allahdadi, Charles Luenr, Thomas Morenouse, and Phyllis Campbell	
13a. TYPE OF REPORT Final Report 13b. TIME COVERED FROM 9/86 TO 2/87	14. DATE OF REPORT (Yr., Mo., Day) July 1988 15. PAGE COUNT 113
16. SUPPLEMENTARY NOTATION Availability of this report is specified on reverse of front cover.	
17. COSATI CODES FIELD / GROUP / SUB. GR.	18. SUBJECT TERMS (Continue on reverse if necessary and identify by block number) Boiling Liquid Expanding Vapor Explosion (BLEVE) Thermal loading, Runge Kutta method, Bisectional method, Heat transfer, Thermohydraulic processes, (continued)

19. ABSTRACT (Continue on reverse if necessary and identify by block number)

A prediction methodology has been developed for predicting the response of a tank containing liquid flammables to a uniform external heat flux from an accidental spill fire. The thermofluid physical processes for the "worst-case" condition, which results in a Boiling Liquid Expanding Vapor Explosion (BLEVE), were assumed. This analysis assumes that the tank is totally engulfed in the flame of a large, intense, turbulent fire. This development considers the response of the tank under thermal loading for two possible vented and unvented tank configurations. Keywords:

20. DISTRIBUTION/AVAILABILITY OF ABSTRACT UNCLASSIFIED/UNLIMITED ☐ SAME AS RPT. ☒ DTIC USERS ☐	21. ABSTRACT SECURITY CLASSIFICATION Unclassified
22a. NAME OF RESPONSIBLE INDIVIDUAL Joseph L. Walker	22b. TELEPHONE NUMBER (Include Area Code) (904) 283-6194 22c. OFFICE SYMBOL HQ AFESC/RDCF

DD FORM 1473, 83 APR EDITION OF 1 JAN 73 IS OBSOLETE.

UNCLASSIFIED

SECURITY CLASSIFICATION OF THIS PAGE

18. ~~SUBJECT TERMS~~ (Concluded)

Convective boundary layer, Vaporization, Circulation, ~~convection~~, (S.C.) Convection (Heat transfer).

EXECUTIVE SUMMARY

The following presents the development of a prediction methodology for assessing the response of a tank containing liquid flammables to a uniform external heat flux from an accidental spill fire. This analysis considers the assumed condition in which a tank is completely engulfed by the flame of a spill fire, the "worst-case" condition resulting in a Boiling Liquid Expanding Vapor Explosion (BLEVE). Common examples for the "worst-case" situation include a derailed tank car lying in a pool fire of flammable material released from a neighboring punctured tank, or an armed, mission-ready aircraft in a shelter or on the deck of an aircraft carrier exposed to an accidental jet fuel spill fire.

This model includes some of the inherent heat transfer phenomena that were ignored before. It considers the thermal effects caused by:

- Heat fluxes from total engulfment,
- Initial transient heating of the liquid inside the tank and formation of a convective turbulent boundary layer,
- Heat and mass transfer across the liquid/gas interface, and
- High intensity heat input.

Inclusion of the above parameters in the heat transfer model has improved the quality of prediction both in the liquid phase and the gaseous phase. It is recommended that efforts be continued to investigate other geometrical and structural aspects of the thermal tankage problem including:

- Tank initial filling density,
- Mechanical and physical integrity of the tank, and
- Structural response of the tank shell to fire impingement.

This analysis investigates and models the response of the tank under thermal loading for two possible vented and unvented tank configurations. It considers the thermofluid dynamic processes occuring inside the tank, including the initial turbulent boundary layer flow near the wetted wall of the tank; stratification of the tank bulk at the core; transport processes at the liquid/gas interface; convective heat transport in the ullage volume, and transfer of heat fluxes from the bottom of the tank. Each of these processes is defined, and the governing equations are derived and combined to provide an integrated physical response model. The system of governing integro/differential equations representing dynamics of the physical processes are solved numerically, and a model predicting the pressure rise inside the tank is developed. The prediction code provides the response of a tank containing flammables to a large turbulent spill fire and estimates the elapsed time before reaching the critical pressure for a given tank configuration. Also presented in this report is an evaluation of the code performance and comparison of its prediction with experimental results.

(The reverse of this page is blank.)

PREFACE

This final report was prepared by the New Mexico Engineering Research Institute (NMERI), University of New Mexico, Campus Box 25, Albuquerque, New Mexico 87131, under Contract F29601-84-C-0080 (Subtask 3.05) for the Air Force Engineering and Services Center, Engineering and Services Laboratory (AFESC/RDCF), Tyndall Air Force Base, Florida 32403-6001. This work was sponsored by the Naval Air Systems Command (NAVAIR) and the US Air Force Engineering and Services Center (AFESC). Mr Joseph T. Walker (AFESC), and Ms Phyllis Campbell (NAVAIR) were the Government technical program managers. This report summarizes work done between September 1986 and February 1987.

This report has been reviewed by the Public Affairs Office (PA) and is releasable to the National Technical Information Service (NTIS). At NTIS it will be available to the general public, including foreign nationals.

This technical report has been reviewed and is approved for publication.

EDWARD T. MOREHOUSE, Captain, USAF
Project Officer

LAWRENCE D. HOKANSON, Colonel, USAF
Director of Engineering and Services Laboratory

ROBERT J. MAJKA, Lt Colonel, USAF
Chief, Engineering Research Division

(The reverse of this page is blank.)

TABLE OF CONTENTS

TABLE OF CONTENTS (CONCLUDED)

LIST OF FIGURES

LIST OF FIGURES (Concluded)

LIST OF SYMBOLS

A_w	total unwetted surface area in the ullage volume
A_ℓ	liquid surface area
C_w	wall specific heat
$C_{a,v}$	specific heat of air at constant volume
$C_{v,v}$	specific heat of vapor at constant volume
$C_{v,p}$	specific heat of vapor at constant pressure
$\dot{q}''_f$	total incident heat flux for the fire
$\dot{q}''_{rr,i}$	reradiation inward from the wall
$\dot{q}''_{rr,o}$	reradiation outward from the tank
$\dot{q}''_{r,\ell}$	radiative heat flux incident on the liquid surface
$\dot{q}''_{c,\ell}$	conductive heat flux incident on the liquid
$\dot{q}''_{c,g}$	convective heat flux from the unwetted wall
$\dot{q}''_{cls}$	convective heat flux from the side walls
$\dot{q}''_{clb}$	convective heat flux from the bottom wall
T_g	gas temperature
$T_{\ell,s}$	substrate liquid temperature
T_i	liquid temperature at the interface
T_∞	temperature of ambient air
T_w	temperature of the wall
δ_w	thickness of the tank wall
δ	boundary layer thickness
ρ_w	density of the tank wall
σ	Stefan-Boltzmann constant
ϵ	emissivity coefficient
h	heat transfer coefficient

E	internal energy of the gas
$\dot{M}_i$	rate of mass addition due to vaporization
$\dot{M}_o$	mass outflow rate through the vent
ℓ	latent heat of vaporization
u	velocity distribution in the boundary layer
U	uniform counter flow velocity
H_ℓ	height of liquid
ψ	stream function
β	coeifecient of expansion of liquid
F_w	$\dfrac{g\dot{q}''_{c\ell s}}{\rho_p T_0}$
$\bar{F}_w$	$\dfrac{g\beta\dot{q}''_{c\ell s}}{\rho_0 C_p}$
Δ	$\dfrac{T - T_c}{T_0} g$
Δ_c	$\dfrac{T_c(z) - T_0}{T_0} g$
ν	kinematic viscosity
Pr	Prandtl number

SECTION I
INTRODUCTION

A. OBJECTIVE

The objective of this task encompasses two independent but interrelated parts: (1) development of a model for a large hydrocarbon pool fire,* and (2) development of a response prediction model for a fire-exposed tank containing flammables. Specifically, we are to determine the conditions under which a fire-exposed tank containing flammables fails and Boiling Liquid Expanding Vapor Explosion (BLEVE) occurs, and to determine the elapsed time before failure. The response of various thermophysical processes that occur inside a tank as a result of incident heat are combined and an integrated comprehensive computer prediction methodology is constructed. The prediction is to provide the pressure rise history profiles for a large range of flammables and fire/tank configurations. The prediction is essential to on-the-scene assessment of the fire environment and the safety of fire-fighting crews.

B. SCOPE/APPROACH

The scope of this effort is to develop an accurate heat transfer model for the liquid and gaseous phases of a fire-exposed, partially filled container. In this investigation, the governing equations describing the thermophysical processes that occur inside a tank are developed and solved numerically. Considered in this investigation are some of the heat transfer parameters that were ignored before. These include heat input from the tank bottom wall and initial transient heating of the liquid. The scope of this effort also requires conducting specially designed fire tank tests to validate and assess the model performance.

---

* Development of a large hydrocarbon pool fire model has been completed. It was reported in a 1986 Task Report (NMERI WA3-12) entitled **One-Dimensional Hydrocarbon Fuel Fire Model** prepared by New Mexico Engineering Research Institute for AFESC Engineering and Services Laboratory.

C. BACKGROUND

Large quantities of petroleum and volatile hazardous chemicals are routinely extracted, produced and transported, either by highway or rail. The possiblity of a major accident caused by human error or otherwise during transportation or maintenance of these facilities is quite real. The impetus behind this analysis is to formulate and model the thermodynamic phenomena that occur in a fire-engulfed tank and to predict the elapsed time before failure or the occurrence of BLEVE.

Before engaging in detailed mathematics regarding modeling response of a tank laden with flammables to a large sooty fire, it is instructive to use an illustrative example to define the sequence of events occurring in a fire/tank scenario and to demonstrate the processes that ultimately lead to BLEVE. Not all fire-engulfed flammable tanks conclude in BLEVE. Consider a large tank, e.g., a rail tank-car (Figure 1), partially filled with liquid propane and the remaining volume (ullage) occupied by propane vapor and air. The ullage volume in the tank is necessary to allow for swelling and expansion of the liquid that results from incident external heat fluxes.

When a tank partially filled with volatile liquid is exposed to a large turbulent sooty fire, the heat flux from the fire is partially stored in the walls of the tank, and is partially transferred to the contents, liquid and gas phases, of the tank. The total heat transferred to the tank consists of radiation from the plume and convection from the combustion gases. The contents of the tank are heated by natural convection. The tank wall next to the gas phase always has a higher temperature than the walls wetted by the liquid phase. Therefore, the temperature gradient sets up a conduction heat transport process along the wall of the tank.

The prevailing heat transfer from the tank wetted wall to the liquid is by convection. The heat transfer from the wall establishes a turbulent convective thermal and velocity boundary layer in the liquid next to the wall. The superheated turbulent boundary layer next to the wall raises the heated liquid along the wall and discharges into the subcooled main core at the liquid gas interface, creating a convective circulatory motion. This process continues until a near-uniform temperature field resulting from a

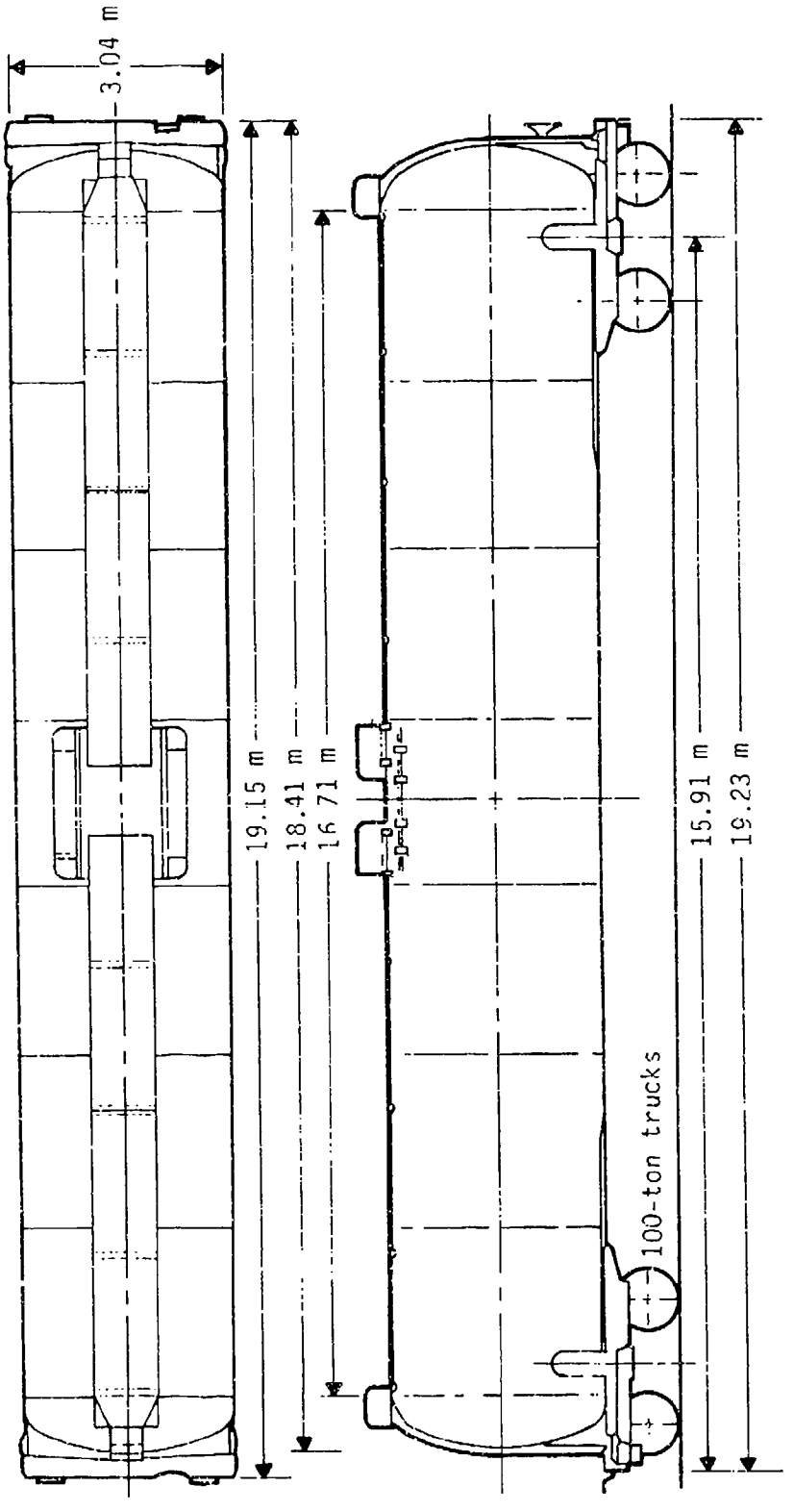

Figure 1. General Arrangement of a DOT 112A340W Tank Car

high rate of mixing is established. At this time, the heat transfer rate is quite high, and almost all of the incident heat transported to the wall is transferred to the liquid; very little goes into incr sing the temperature of the wali, and nucleate boiling occurs. As a result of this, the inner wall temperature in the liquid wetted region rarely exceeds the temperature of the liquid by more than 10 °C (Reference 1). Also, there is a transition region between the liquid wetted wall and the vapor wetted wall which will create a two-phase flow at the gas/liquid interface. The thickness of this region has not been determined and will depend on the strength of the boiling action. In this region, the magnitude of the heat transfer rates will be somewhere between those for the liquid wetted and vapor wetted surfaces, and as a result the wall temperature in this region will also be between those for the liquid and vapor wetted wall regions (Reference 1).

The prevailing heat transfers in the gas phase in the ullage volume are by convection and thermal radiation. The initial convective heat transfer rate in the vapor phase will be low because of the combined effect of the low thermal conductivity of the gas/vapor and the low flow velocities. Initial thermal radiation will also be small because of the low wall temperatures. As the temperature of the walls in the ullage volume increases, the energy transport from thermal radiation will also increase. The increase in the energy transport in the ullage volume is predominantly due to the radiation which is proportional to the fourth power of the wall temperature. The tank internal pressure rises as a result of an increase in the gas-phase temperature and surface vaporization of the liquid. When the temperature of the wetted walls reaches the saturation temperature, corresponding to the instantaneous tank pressure, vapor is generated rapidly and the pressure builds up quickly. At this time, the liquid portion of the tank expands as a result of thermal expansion. If the tank becomes completely filled with liquid as result of overexpansion, rupture will occur when the critical pressure is reached. The critical pressure is related to the decreasing strength of the tank shell as its wall temperature increases.

An operational tank is equipped with a pressure relief valve which would open to allow removal of mass from the tank, thus, keeping the internal pressure below the tank rupture pressure. However, the released vapor from the relief valve mixes rapidly with the ambient air, is ignited, and becomes

an additional source of heat flux incident on the tank. The additional heat flux that impinges directly on the unwetted wall, which is now increased as a result of the drop in the liquid level, deteriorates the mechanical strength of the tank. Under these conditions, depending upon the integrity of the physical structure of the tank, the tank will either safely continue to vent the lading or it will rupture. If the tank ruptures, the remaining liquid in the tank experiences a sudden depressurization. Since the remaining liquid cannot vaporize quickly enough to establish a stable saturated condition, the liquid becomes superheated. If the liquid is superheated sufficiently, a BLEVE results.

Some of the processes leading to the BLEVE have been defined by various researchers. Reference 2 describes this phenomenon in the following form. If a saturated liquid at high pressure suddenly experiences a rapid pressure decrease, as in the case of a rupturing tank car, then the liquid should boil until the temperature of the remaining liquid is reduced to the saturation temperature for the next pressure conditions. This requires sufficient nucleation sites for the boiling to take place, and these sites do not exist in sufficient quantities within the bulk of the liquid. This causes some of the liquid to become superheated for a brief period after the depressurization occurs. If the degree of superheating is sufficiently large, homogeneous nucleation takes place throughout the bulk of the liquid and the entire liquid mass vaporizes almost instantaneously. This rapid vaporization causes a vapor explosion which may cause the tank to be ripped open and sometimes propels tank fragments for large distances. In addition to the shock loads from the vapor explosion, the vapor rapidly mixes with the surrounding air and ignites, causing a fire ball which loads nearby structures with intense thermal radiation. Reid (Reference 3) suggests that a BLEVE is the result of homogeneous nucleation of a metastable superheated liquid.

Consistent with the definitions, occurence of BLEVE, although not totally independent of a pressure relief valve, is mostly controlled by the initial liquid filling density and by the magnitude of the incident heat fluxes. Various modes of response for tanks containing flammables have been studied by various researchers. A brief literature review is presented in the following.

D. LITERATURE REVIEW

The response of a tank engulfed in a pool spill fire has been studied under special conditions by various researchers. Roberts et al. (Reference 4) conducted experimental studies of insulated and uninsulated 500-liter tanks. The tanks were partially filled with liquid and exposed to a kerosene pool fire. In each test they measured the heat transfer rate to the total system, the contents of the tank, the boiling regime, and the tank wall temperature. They demonstrated that a response time of 3 minutes (the time needed for the pressure relief valve to activate) for an uninsulated propane tank could be extended to ranges of 12 to 90 minutes for insulated tanks of similar material.

Venart et al. (Reference 5) conducted a study of the physical behavior of tanks containing liquified fuel under accident conditions. They reached a number of conclusions that are believed to be true only for low-input heat flux, i.e., heat fluxes under 7 w/cm^2. Among the conclusions reached were: (1) prior to pressure relief valve action, the primary source of vapor generation originates in the liquid boundary layer, and (2) simple thermodynamic and heat transfer models may be used to predict the pressure response of such vessels.

The problem of evaporation rates of liquified natural gas in containers was considered by Hashemi and Wesson (Reference 6). They treat the system as a liquid layer heated from below and develop an empirical relationship between the boiloff rate and the supersaturation* pressure. This equation, which shows that the boiloff rate varies as the 4/3 power of the supersaturation pressure, is solved in conjunction with the energy equation for the liquid in the tank, resulting in an implicit algebraic equation in terms of evaporation rate.

---

* The supersaturation pressure of the liquid is defined as the product of the average pressure at the saturation temperature and the total difference between the temperature of the bulk of the liquid and the temperature at the surface.

Note that the natural convection patterns for a liquid layer will not exist for elevated pressure and the model will not yield realistic solutions for pressure rise cases.

The natural laminar convection of fluids in an enclosed cylindrical geometry has been considered by Barakat and Clark (Reference 7). The governing conservative equations pertinent to the fluid inside the tank were simplified by the use of stream functions, and numerical techniques are used for the solution of these equations. They demonstrated that steep velocity and thermal gradients exist in the vicinity of the sidewall and, hence, a boundary layer flow occurs. Analytical and experimental study of transient natural convection in a vertical cylinder has been reported by Evans and Reid (Reference 8). Their experimental effort consisted of monitoring transient temperature and flow patterns inside an exposed tank partially filled with a water-glycerin mixture. The tests were conducted for a range of Prandtl numbers from 2 to 8,000, and for L/D ratio (L = mixture depth, D = cylinder distance) and Grashof numbers from 10^3 to 10^{11} encompassing both laminar and turbulent regimes. They considered the problem analytically. The system was divided into three regions: (1) a boundary layer region near the wall, (2) the mixing region at the top of the gas/liquid interface, and (3) a main core region where the bulk fluid slowly falls down in plug flow. The resulting equations are solved numerically to obtain the temperature profile in enclosed fluids subject to wall heating. It was observed that after measurement of the initial transient temperature, the core temperature increased linearly with time--a characteristic of low heat flux input.

Transient thermal stratification in heated, partially filled horizontal cylindrical tanks was considered by Aydemire et al. (Reference 9). They extended the analytical technique for boundary layer analysis to account for the presence of a covering of aluminum foil mesh on the inside walls of the tank. Results with and without ExploSafe were compared with experimental data for Freon-113™. Although fairly good agreement between the experimental and analytical results is obtained, the procedure appears to be valid only for low-input heat fluxes. Virk and Venkataramana (Reference 10) studied the transient boiloff rates of a liquified natural gas from large industrial storage tanks subjected to the perturbation of ambient atmospheric pressure.

Their theoretical model closely tracks the procedure covered in References 6-9. The model demonstrates that constant heat input to the tank maintains a steady boiloff rate of LNG from the tank. It establishes that a natural convection boundary layer exists in the vicinity of the wall, and that hot fluid, upon reaching the liquid surface, diffuses radically inward toward the center, losing part of its mass and energy as boiloff. They also demonstrated that step changes in ambient pressure (i.e., rise or drop) could affect the boiloff rate by as much as 1000 percent.

Birk and Oosthuizen (Reference 11) outlined a computer model of a rail tank car with its exterior surface exposed to a spill fire. Their model is two-dimensional, capable of predicting tank pressure, wall temperatures, wall stresses, vapor and liquid mean temperatures, flow rates through the relief valve, and liquid level as a function of time.

Delichatsios (Reference 12) conducted analytical and experimental studies of fire-exposed containers containing different solvents prior to rupture. He modeled the thermohydraulic process occurring inside the container in terms of a set of physical dimensionless prameters. He also measured the container internal pressure and temperature rise resulting from incident heat for different solvents using 55-gallon steel drums. In this investigation he concludes that, for most solvents, the time for tank rupture is equal to the time for the tank's wetted walls to reach the solvent boiling temperature.

SECTION II
MODELING PRINCIPLES

The description and sequence of events that occur inside a fire-engulfed tank are illustrated pictorially in Figure 2. Figure 2a shows the fire engulfment of a rail tank-car. As shown in the figure, the tank is nearly filled with the flammable liquid and the remaining volume is occupied by vapor. The radiative and convective heat fluxes from the external fire are conducted through the wall into the tank lading. The heat input raises the temperature of the wall next to the liquid, and a convective turbulent thermal and velocity boundary layer is established. With increasing time, the temperature of the wall next to the gas increases sufficiently to radiate. The radiative heat flux, combined with the convective current, causes vaporization of the liquid at the interface. At this time, the liquid expands and swells, further increasing the internal pressure of the tank. If the tank is equipped with a pressure relief valve and if the tank's internal pressure exceeds the valve operational pressure, the valve will open to allow the venting of lading. This will reduce the internal pressure of the tank, but at the expense of increasing the surface of the unwetted wall in the ullage volume (see Figure 2b).

Simultaneous with the expulsion of lading, two important phenomena that significantly contribute to occurrence of the BLEVE will take place:

1. The vented combustible vapor mixes with the surrounding air and ignites; therefore, the total radiative heat incident on the tank is increased.

2. The radiation heat that impinges directly on the continuously increasing unwetted wall will result in further reduction of the tank shell mechanical strength.

The additional radiative heat from the unwetted wall causes extensive surface evaporation, a phenomenon which further raises the pressure considerably. At this time, the wetted wall temperature has reached the saturation temperature, and copious vapor from nucleate boiling is generated. With increasing time, the tank's internal pressure rises quickly, and rapid

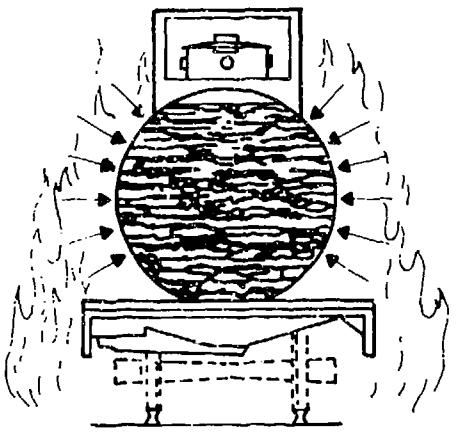

(a) External fire begins. Heat is conducted into tank loading.

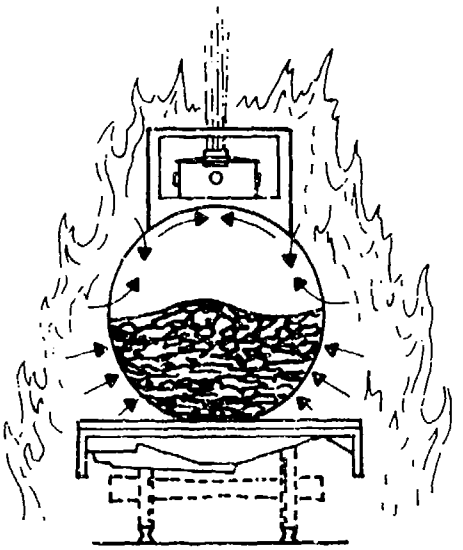

(b) Relief valve opens. Venting of of lading increases the vapor space.

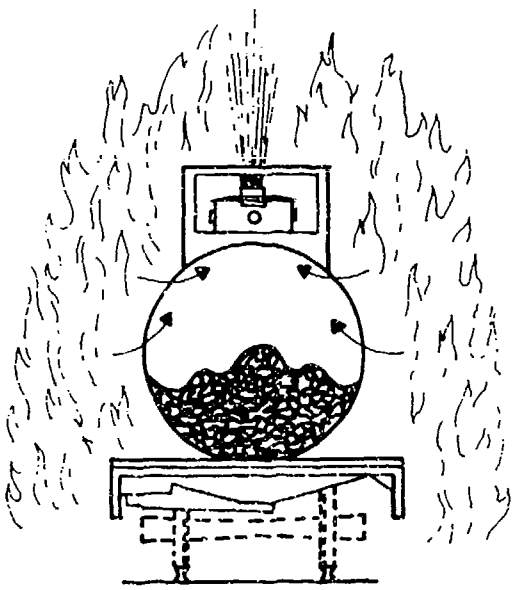

(c) Wall adjacent to vapor space heats up because vapor is a poor conductor of heat.

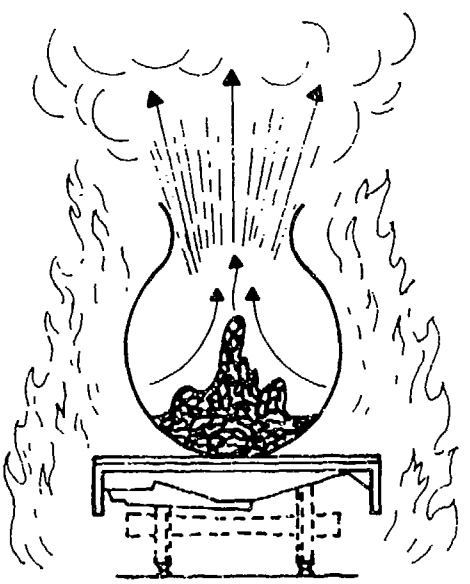

(d) Wall temperatures rise to a point where the steel weakens and the wall ruptures.

Figure 2. Pictorial Representation of Bleve (from Ref. 11)

generation of vapor and further expulsion of lading occur (Figure 2c). At this time, the strength of the unwetted wall has deteriorated to its critical value and the tank will rupture (Figure 2d). At the moment of rupture when the tank is depressurized to ambient pressure, if the remaining liquid in the tank is at saturation temperature, a violent explosion, BLEVE, occurs.*

The thermofluid mechanics of the physical processes before BLEVE were discussed earlier. They are determined by the following interacting transport phenomena:

1. Heating of the walls of the tank.
2. Heating of the gaseous phase in the ullage volume.
3. Heating of the liquid phase.
4. Transport of heat and mass across the liquid/gas interface.

The analysis of the mathematical model describing each of these processes is presented in the following sections.

A. GOVERNING TRANSPORT EQUATIONS IN THE ULLAGE VOLUME

Figure 3 depicts the cross section of an arbitrary tank. This figure describes interactive processes that occur in the ullage volume. The parameters indicated are:

$\dot{q}''_{rr,o}$: reradiation outward from the tank

$\dot{q}''_{rr,i}$: reradiation inward from the wall

$\dot{q}''_{f}$: total heat flux from the fire incident on the tank

$\dot{q}''_{r,\ell}$: radiative heat flux incident on the liquid

$\dot{q}''_{c,\ell}$: conductive heat flux incident on the liquid

$\dot{q}''_{c,g}$: convective heat transfer from the wall

A_w : total unwetted surface area in the ullage volume

A_ℓ : liquid surface area

---

*For more explanation of the phenomena refer to the paragraph entitled "Background" in Section I.

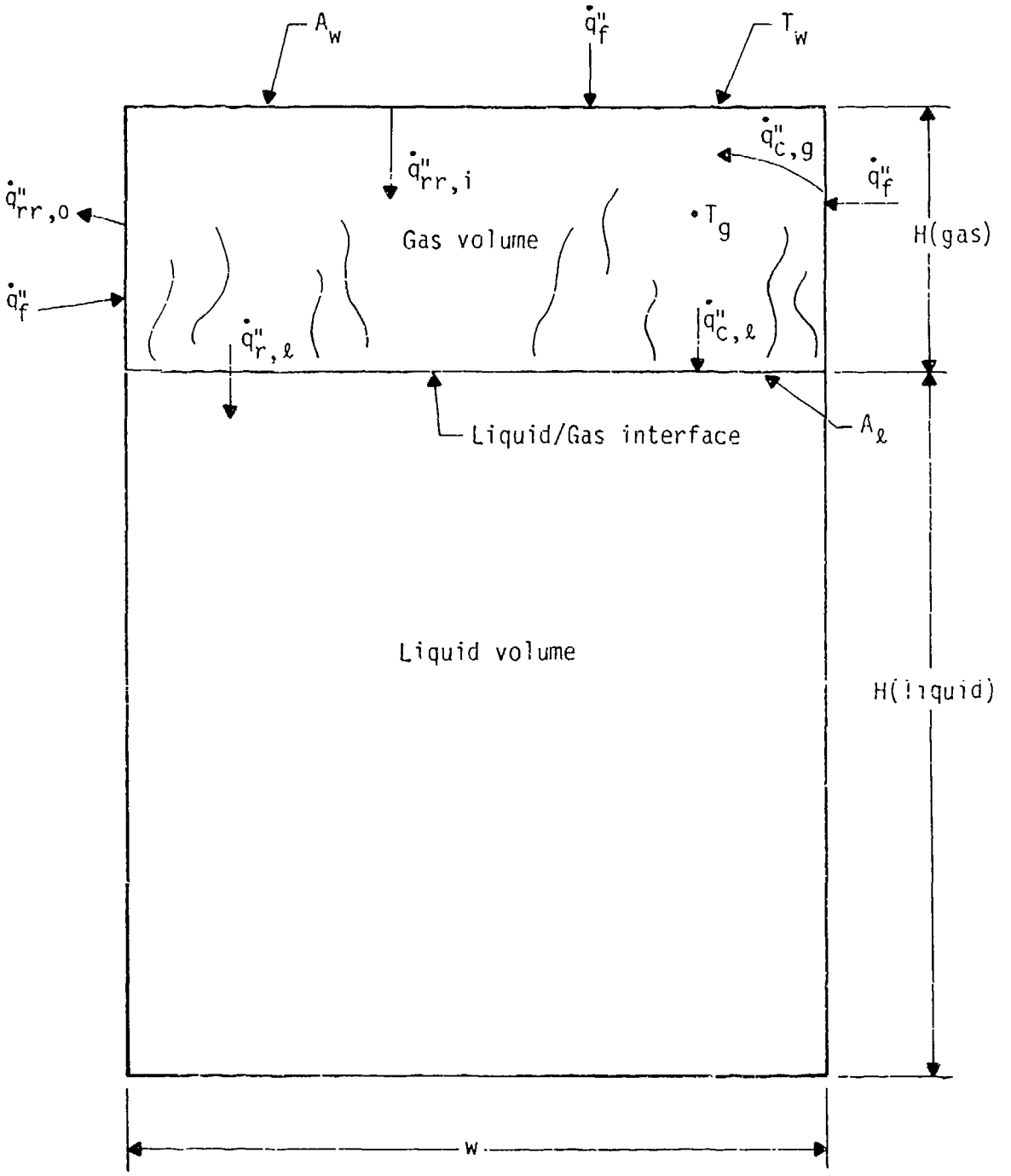

Figure 3. Heat Transfer Interaction in the Ullage Volume

T_g : gas temperature

T_i : liquid temperature at the interface.

T_{wg} : unwetted tank wall temperature.

In the derivation of the governing equations describing the transport process in the gas phase, the following assumptions have been made:

1. The thickness of the tank wall is very small compared with its other dimensions. Therefore, the temperature variation across the thickness is negligible.
2. Vapor and air in the ullage volume behave as perfect gases.
3. Temperature and concentration distributions in the ullage volume are homogenous, since the mixing occurs relatively quickly.
4. In spite of the large temperature gradients in the wall near the liquid meniscus, the total heat flow rate by conduction along the wall is assumed negligible.
5. The heat flux imposed by the fire is uniformly applied on the tank walls.

B. UNWETTED WALL HEAT TRANSFER PROCESS

The total heat stored in the walls of the ullage volume is given by the following thermal energy balance equation:

$$\rho_w C_w \delta_w \frac{dT_{wg}}{dt} = \dot{q}''_f - \dot{q}''_{rr,o} - \dot{q}''_{rr,i} - \dot{q}''_{c,g} \qquad (1)$$

where ρ_w, C_w and δ_w are density, specific heat, and thickness of the wall, respectively. The reradiation heat loss to the outside is given by

$$\dot{q}''_{rr,o} = \sigma\varepsilon \, (T^4_{wg} - T^4_{\infty}) \qquad (2)$$

In Equation (2), T_∞ is the ambient temperature, $\sigma = 0.1713 \times 10^{-8}$ BTU/ft^{2}hrR^4 is the Stefan-Boltzmann constant, and $\varepsilon = 0.99$ is the coefficient of emissivity. Similarly, the radiation heat losses to the interior of the tank impinging on the liquid surface reads

$$\dot{q}''_{rr,i} = \sigma\varepsilon \, (T^4_{wg} - T^4_{i}) \qquad (3)$$

The total convective heat transfer rate in the ullage volume is represented by $\dot{q}''_{c,g}$. It can be shown (Reference 13) that the total convective heat transfer for a given surface coefficient, i.e., h, is given by:

$$\dot{q}''_{c,g} = h\,(T_{wg} - T_g) \tag{4}$$

where h is the tank surface heat transfer coefficient, and, as defined earlier, T_{wg} and T_g are the unwetted tank wall temperature and gas temperature, respectively. The surface heat transfer coefficient, h, can be calculated from the data given in Reference 13, and the convective heat transfer equation becomes

$$\dot{q}''_{c,g} = C_g(T_{wg} - T_g)^{4/3} \tag{5}$$

In Equation (5) the coefficient, C_g, depends on the property values of the gas inside the ullage volume. The value of the C_g is defined in Section IV.

C. ENERGY CONSERVATION IN THE GASEOUS PHASE

The conservation of energy in the gaseous phase is a statement of energy balance between the internal energy of the gas and the energy transport across the boundary and the gas/liquid interface. The conservation of energy balance reads

$$\frac{dE}{dt} = \dot{q}''_{c,g} A_w - \dot{q}''_{c,\ell} A_\ell + \dot{M}_i h_i \tag{6}$$

In deriving this equation, it is assumed that gas inside the ullage volume does not absorb any thermal radiation. The parameters in Equation (6) are:

- E : is the internal energy of the gases in the ullage volume
- $\dot{M}_i$: is the mass addition rate of vapor owing to the evaporation from the liquid surface.
- h_i : is the enthalpy of the vapor

The energy equation in the ullage volume can be written in terms of air and vapor mass fractions. It follows that

$$M_a = M\, Y_a$$

$$M_v = M\, Y_v \qquad (7)$$

where

M_a: mass of air in the ullage volume
M_v: mass of vapor in the ullage volume
Y_a: mass fraction of air in ullage volume
Y_v: mass fraction of vapor in ullage volume

Note that

$$Y_a + Y_v = 1 \qquad (\ )$$

and the total mass of gases in the ullage volume is given by

$$M = M_a + M_v \quad \text{total mass} \qquad (9)$$

It is evident that for a closed tank configuration

$$\frac{dM_a}{dt} = 0 \qquad (10)$$

Therefore,

$$\frac{dM}{dt} = \frac{dM_v}{dt} = \dot{M}_i \qquad (11)$$

In the open tank configuration, the total mass balance equation for the ullage volume will take the following form:

$$\frac{dM}{dt} = \dot{M}_i - \dot{M}_o \qquad (11a)$$

where dM/dt is the rate of change of total mass in the ullage volume and $\dot{M}_i$ is the rate of mass addition at the interface due to the boiling and vaporization. The quantity $\dot{M}_o$ represents the mass rate of outgoing air and vapor, collectively. The mass rate of change of each species in the ullage volume is calculated based on the mass fraction of the outgoing gases. For example, the mass rate of change of air and vapor in the ullage volume is given by the following equations, respectively:

$$\frac{d}{dt}(Y_a M) = -Y_a \dot{M}_o \tag{11b}$$

$$\frac{d}{dt}(Y_v M) = \dot{M}_i - Y_v \dot{M}_o \tag{11c}$$

Using Equations (11a), (11b), and (11c), the rate of change of air mass fraction can be calculated as

$$\frac{d}{dt}(Y_a) = -Y_a \left(\frac{\dot{M}_i}{M} \right) \tag{11d}$$

It can be shown from Bernoulli's law that the outflowing mass is related to the pressure drop in the tank:

$$\dot{M}_o = A\, C_d \left[2 \left(P - P_{atm} \right) \rho \right]^{1/2} \tag{11f}$$

where A represents the vent cross-sectional area and C_d is the coefficient of discharge.

Considering the closed tank configuration, the total internal energy term in the gas phase can be written as the sum of the specific energy of air, e_a, and vapor, e_v:

$$E = M_a e_a + M_v e_v \tag{12}$$

After taking the time derivative of Equation (12) and substituting for the mass fractions from Equations (10) and (11), one obtains

$$\frac{dE}{dt} = M_a \frac{de_a}{dt} + M_v \frac{de_v}{dt} + \dot{M}_i e_v \tag{13}$$

Substituting for $\frac{dE}{dt}$ from Equations (12) and (13) into Equation (6) results in

$$M_a \frac{de_a}{dt} + M_v \frac{de_v}{dt} = \dot{q}''_{c,g} A_w - \dot{q}''_{c,\ell} A_\ell + \dot{M}_i (h_i - e_v). \tag{14}$$

Because of the high rate of mixing, the air/vapor mixture in the ullage volume remains at a uniform and homogeneous temperature. Based upon this conclusion and the definitions of internal energy, e, and enthalpy of ideal gas, h, one can modify Equation (14). We have

$$\frac{de_a}{dt} = C_{a,v} \frac{dT_g}{dt} \quad ; \quad \frac{de_v}{dt} = C_{v,v} \frac{dT_g}{dt} \tag{15}$$

$$h_i = C_{v,p} T_i \quad ; \quad h_v = C_{v,p} T_g = e_v + \frac{P_v}{\rho_v} \tag{16}$$

The time rate of change of gas temperature, i.e., dT_g/dt, can be obtained from the energy equation (Equation (14)) after substituting for de_a/dt, de_e/dt and h_i from Equations (15) and (16).

It follows that

$$\frac{dT_g}{dt} = \frac{\dot{q}''_{cg} A_w - \dot{q}''_{c\ell} A_\ell + \dot{M}_i [C_{v,p}(T_i - T_g) + P_v / \rho_v]}{M_a C_{a,v} + M_v C_{v,v}} \tag{17}$$

Similarly, for the vented configuration the rate change of gas temperature becomes

$$\frac{dT_g}{dt} = \left(M_a C_{a,v} + M_v C_{v,v}\right)^{-1} \left[\dot{q}''_{cg} A_w - \dot{q}''_{cl} A_\ell + \dot{M}_i C_{v,p} T_i - C_{v,v} T_g - \dot{M}_o PV / \left(M_a + M_v\right)\right] \tag{17a}$$

In arriving at the above equation we have made use of the following thermodynamic relationship

$$C_{v,p} - C_{v,v} = \frac{R}{(mol)_v} = \frac{P_v}{\rho_v T_g}$$

D. PRESSURE HISTORY IN THE ULLAGE VOLUME

The total pressure in the ullage volume at any time is the sum of the partial pressure of air and the partial pressure of the vapor. Therefore, the total pressure becomes

$$P = P_a + P_v \tag{18}$$

and the time derivative of the total pressure becomes

$$\frac{dP}{dt} = \frac{dP_a}{dt} + \frac{dP_v}{dt} \tag{19}$$

Using ideal gas law relations, one can write

$$P_a = \frac{M_a}{(mol)_a} \times \frac{RT_g}{V} \tag{20a}$$

$$P_v = \frac{M_v}{(mol)_v} \times \frac{RT_g}{V} \tag{20b}$$

For a closed tank configuration, the ullage volume, V, remains nearly constant and the time rate of change of total pressure yields

$$\frac{dP}{dt} = \frac{RT_g}{V(mol)_v} \dot{M}_i + \left[\frac{RM_v}{V(mol)_v} + \frac{RM_a}{V(mol)_a} \right] \frac{dT_g}{dt} \tag{21}$$

In the derivation of Equation (21), the identities describing a closed tank configuration, Equations (10) and (11) have been used. For the vented configuration, the internal pressure of the tank at any time is determined by

$$P(t) = \left[\frac{M_a(t)}{(mol)_a} + \frac{M_v(t)}{(Mol)_v} \right] \frac{RT_g(t)}{V}$$

Here

$(mol)_v$: molecular weight of vapor

$(mol)_a$: molecular weight of air

R: universal gas constant

E. MASS TRANSFER ACROSS THE INTERFACE

The gas temperature in the ullage volume is much higher than the liquid temperature. Evaporation at the interface between the liquid and the gas occurs because of the convective heat transfer in the gas and radiative heat flux from the unwetted wall impinging on the liquid at the interface with the vapor volume. By using stagnant film theory (Reference 14), one can find that the evaporation rate per unit surface area is

$$\dot{m}'' = \frac{h_c}{C_{p,g}} \mathrm{Ln}\left[1 + \frac{C_{p,g}(T_g - T_i)}{L_{eff} - \dot{q}''_{r,\ell}/\dot{m}''} \right] \qquad (22)$$

Derivation of Equation (22) is shown in Appendix A. In Equation (22), the parameters are

h_c : convective heat transfer coefficient from a horizontal surface

$C_{p,g}$: specific heat transfer of the gas mixture

L_{eff}: effective heat of gasification

$C_{p,\ell}$: specific heat of liquid

T_i : surface temperature of liquid

T_ℓ : substrate liquid temperature

$\mathfrak{L}$: latent heat of vaporization

L_{eff}: $\mathfrak{L} + C_{p,\ell}(T_i - T_\ell)$ (23)

F. ENERGY TRANSFER ACROSS THE INTERFACE

The heat transfer across the liquid vapor interface is a statement of energy balance between the conduction and radiative heat transfers incident on the surface and the energy associated with the vaporized mass. Assuming no radiation energy is absorbed by the vapor in the ullage volume, the interface energy equation reads

$$\dot{q}''_{c,\ell} + \dot{q}''_{r,\ell} = \dot{m}'' L_{eff} \tag{24}$$

The radiative heat transfer incident on the liquid surface, $\dot{q}''_{r,\ell}$, is directly related to the total inward radiation energy emanating from the side walls. It follows that

$$\dot{q}''_{r,\ell} = \frac{\dot{q}''_{rr,i} A_w}{A_\ell}$$

where, as defined previously, $\dot{q}''_{rr,i} = \sigma\varepsilon(T^4_{wg} - T^4_i)$.

SECTION III
ANALYSIS OF THERMOHYDRAULIC PROCESSES OCCURRING INSIDE THE LIQUID PHASE

Heat from the external fire is partially stored in the wall next to the liquid and partially transmitted to the liquid through convective currents. The heat through the vertical walls establishes a turbulent natural convective velocity and temperature boundary layer. The analyses of physical phenomena considered in this investigation are:

1. Determination of boundary layer flow produced by natural convection.
2. Evaluation of the core temperature variation.
3. Analysis of liquid top layer where the boundary layer turns horizontally and the flow descends into the liquid mass.

The kinetic energy and the momentum of the boundary layer near the surface characterize the flow in the core. They determine whether the flow at the tank core consists of large mixing eddies or a slow stratified motion (Reference 15). The thermohydraulic processes that occur in the liquid phase are shown in Figure 4. The parameters indicated in the figure are

δ	:	boundary layer thickness
$T_c(z)$	:	core temperature (stratification) distribution
T, u	:	temperature and velocity distribution in the boundary layer (defined later)
U	:	uniform downward counter flow velocity
H_ℓ	:	liquid height in the tank
A_ℓ, L_ℓ	:	area and perimeter of the liquid surface

The mathematical models descriptive of the above physical processes are developed in the following sections.

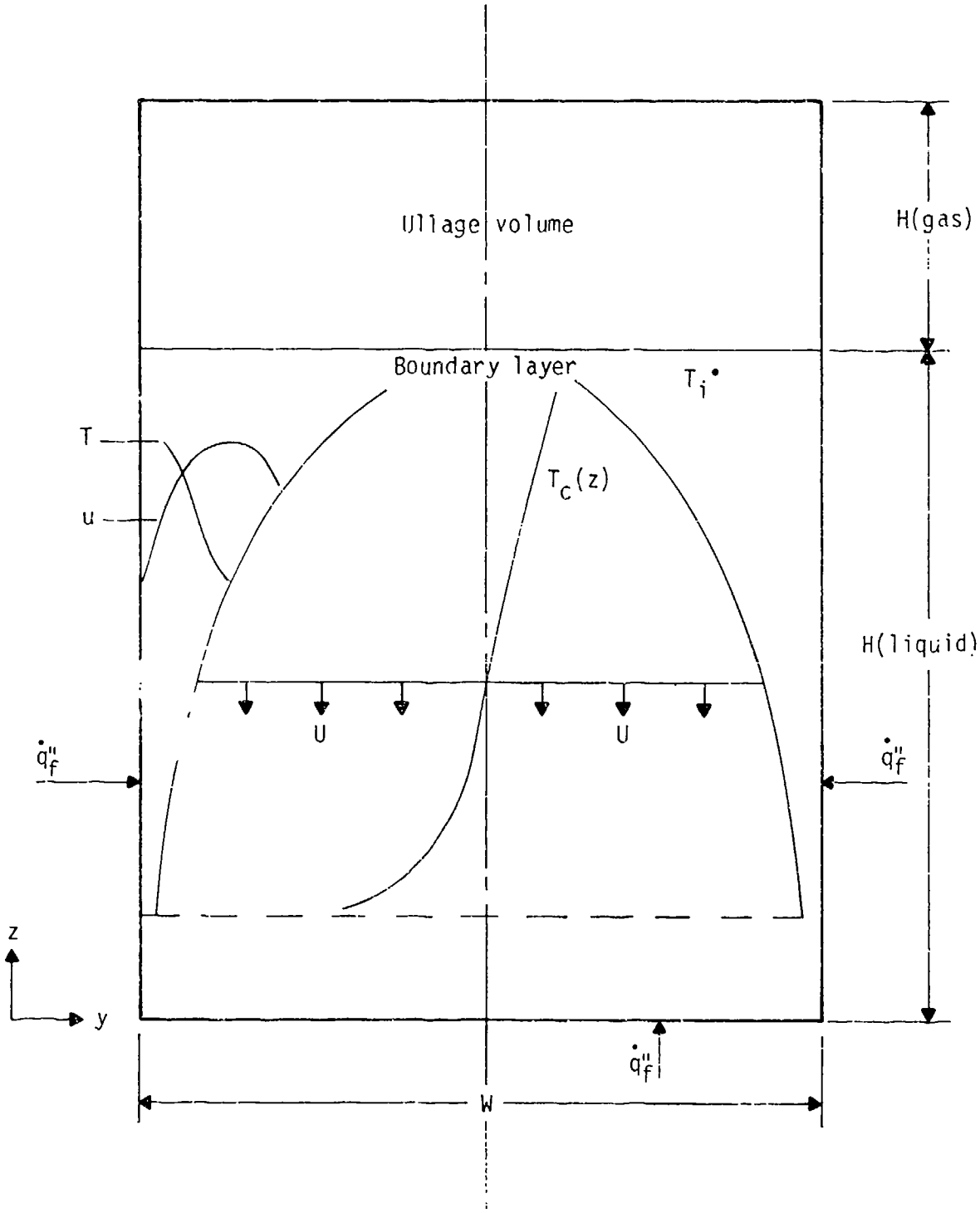

Figure 4. Thermohydraulic Processes in the Liquid Phase

A. HEATING OF THE WETTED WALLS

Analogous to the heating of the wall in the gaseous volume, it is assumed that the temperature across the thickness of the wall is uniform. Then, the thermal balance* equation for the walls can be written as

$$\rho_w C_w \delta_w \frac{\partial T_{ws}}{\partial t} = \dot{q}''_f - \dot{q}''_{rros} - \dot{q}''_{c\ell s} \tag{25}$$

In Equation (25), $\dot{q}''_{c\ell s}$ is the convective heat loss to the liquid and T_{ws} is the side wall temperature.

Similar to the derivation of Equation (5), the convective, $\dot{q}''_{c\ell s}$, and the re-radiation, $\dot{q}''_{rros}$, heat transfer terms can be written respectively as

$$\begin{aligned} \dot{q}''_{c\ell s} &= C_s \left(T_{ws} - T_c\right)^{4/3} \\ \dot{q}''_{rros} &= \varepsilon o \left(T_{ws}^4 - T_\infty^4\right) \end{aligned} \tag{25a}$$

where the coefficient C_s depends on the physical properties of the liquid (Reference 13), given as

$$C_s = \rho_o C_p \left\{ \nu_c \beta\, g/[(5.3)^4\, Pr^2] \right\}^{1/3} \tag{25b}$$

B. CONVECTIVE FLOW FIELD INSIDE THE LIQUID

A mathematical description of the heating of the liquid by convective currents is presented. This development ignores the possibility of laminar boundary layer which may occur late in time. It is also assumed that the core of the vessel does not contain large eddies, and that the boundary layer region can be described continuously by turbulent boundary layer equations. The governing equations for the boundary layer are based on the integral representation and are appropriately coupled with the core flow. In view of initially weak buoyant flow in the boundary layer, the Boussinesq approximation has been implemented.

---

*It is assumed that the flames surrounding the tank are radiatively thin.

C. CONSERVATION OF MASS

The principle of conservation of mass is applied to an elemental volume of boundary layer (see Figure 5).

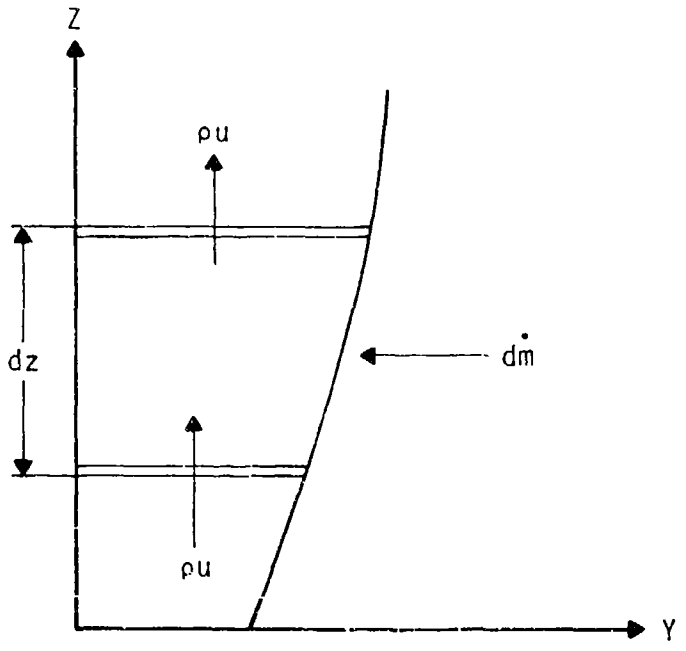

Figure 5. Mass Balance For Boundary Layer Elemental Volume

The conservation of mass states that the entrainment rate is equal to the difference between mass efflux and influx in the boundary layer. Therefore the mass rate, $d\dot{m}$, entrained in the boundary layer by convective currents is equal to the amount of mass leaving the boundary at any cross section. It follows that

$$\int_0^{\delta} \left[\rho u dy + \frac{d}{dz}(\rho u dy)\ \Delta z\right] - \rho u dy = d\dot{m} \tag{26}$$

where, after simplification, it becomes

$$\frac{d\dot{m}}{dz} = \frac{d}{dz}\int_0^{\delta} \rho u dy \tag{27}$$

D. BUOYANCY CONSERVATION

The buoyancy equation is a description of the energy associated with the upward flow in the boundary layer caused by the temperature gradient. The integral form of the buoyancy equation is written for an elemental volume of boundary layer (see Figure 6). It follows that the rate of change of energy per unit length in the boundary layer is equal to the algebraic sum of the heat input (Reference 16).

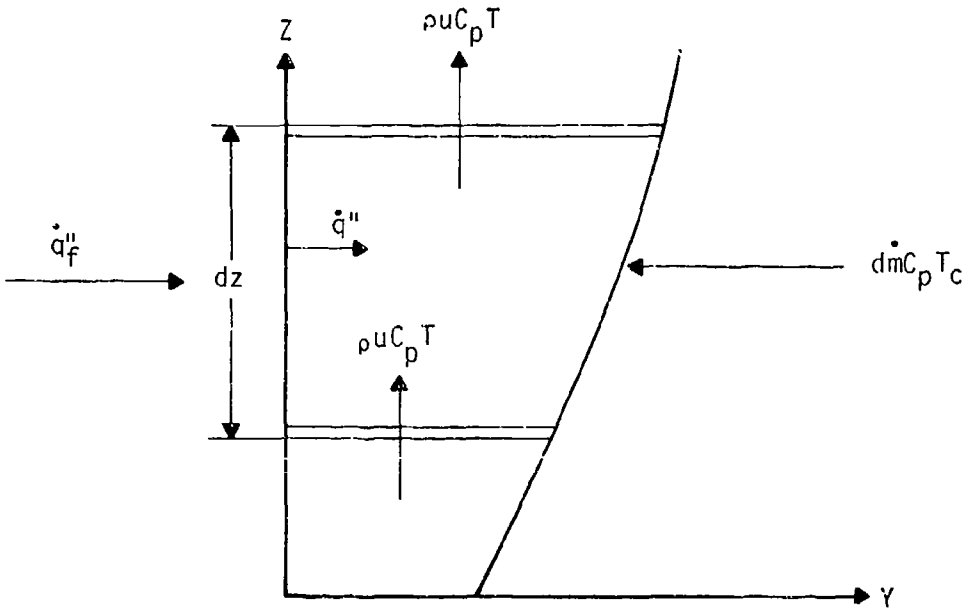

Figure 6. Energy Balance for Boundary Layer Elemental Volume

The governing buoyancy equation for a tank having an orthogonal cross section reads

$$\dot{q}''dz = d\left(\int_0^{\delta} \rho u C_p T dy\right) - d\dot{m}\, C_p T_c \qquad (28)$$

In Equation (28), dz is a differential length in the vertical direction, u is the velocity of the fluid in the boundary layer, and T_c is the temperature of the entrained core liquid. Equation (28) can be rewritten as

$$\dot{q}''/C_p = \frac{d}{dz}\left(\int_0^{\delta} \rho u T dy\right) - \frac{d\dot{m}}{dz} T_c$$

Substituting for $\dot{m}/dz$ from conservation of mass, Equation (27), one obtains

$$\dot{q}''/C_p = \frac{d}{dz}\left(\int_0^\delta \rho u T dy\right) - \frac{d}{dz}\left(\int_0^\delta \rho u dy\right).T_c \qquad (29)$$

Since the core temperature T_c varies with the liquid height, the last term in the right side of Equation (29) is modified to reflect this behavior. It follows that

$$\frac{d}{dz}\left(\int_0^\delta \rho u dy\right).T_c = \frac{d}{dz}\int_0^\delta T_c\, \rho u dy - \frac{dT_c}{dz}\int_0^\delta \rho u dy.$$

Substitution of the above relation into Equation (29) gives the buoyancy equation

$$\frac{d}{dz}\int_0^\delta \rho u(T-T_c)\, dy = \frac{\dot{q}''}{C_p} - \left(\int_0^\delta \rho u dy\right)\frac{dT_c}{dz} \qquad (30)$$

Equation (30) can be modified to a more useful form if it is multiplied through by $g/(\rho T_0)$. Here, g is the gravitational acceleration and T_0 is some reference temperature. This yields

$$\frac{d}{dz}\int_0^\delta ug\frac{T - T_c}{T_0}dy = \frac{\dot{q}''g}{\rho C_p T_0} - g\frac{d}{dz}\left(\frac{T_c(z)-T_0}{T_0}\right)\int_0^\delta u dy \qquad (31)$$

Define:

$$\Delta = \frac{T - T_c(z)}{T_0}\, g \qquad \Delta_c = \frac{T_c(z) - T_0}{T_0}\, g$$

$$\tilde{\Delta} = \beta T_0 \Delta; \quad \tilde{\Delta}_w = \beta\,(T_{ws} - T_c)\, g \qquad (31a)$$

$$\tilde{F}_w = \frac{\beta g \dot{q}''_{c\ell s}}{\rho C_p} = \left[\frac{\nu_c}{(5.3)^4 Pr^2}\right]^{1/3} \tilde{\Delta}_w^{4/3}$$

$$\dot{q}'' = \dot{q}''_{c\ell s}$$

Also, after replacing the y coordinate with a stream function, ψ, one obtains,

$$\psi = \rho_0 \int_0^y u dy \tag{31b}$$

where $\psi_t = \rho_0 \int_0^\delta u dy$ is the total flow rate.

Then the governing buoyancy equation reads

$$\frac{\partial}{\partial z}\left(\int_0^{\psi_t} \tilde{\Delta}\, d\psi\right) = \rho_0 \bar{F}_w - \psi_t \frac{\partial \tilde{\Delta}_c}{\partial z} \tag{32}$$

E. CONSERVATION OF MOMENT OF MOMENTUM

Because the wall friction parameter in the boundary layer region is not well known, especially for slow buoyant flows, the motion of the fluid in the boundary layer is characterized by the moment of momentum instead of the conventionally used momentum equation (Reference 17). This method is quite appropriate for flows attached to vertical surfaces. Rigorous derivation and justification of this method is beyond the scope of this work. However, observe that its acceptability may be based on physical argument, intuition, and considerable recent research (References 18, 19, and 20).

In deriving the moment of momentum equation, it is assumed that: (1) the flow is a boundary layer type flow, (2) the average pressure in the plume is the same as the ambient pressure at sea level, which is the consequence of the Buossinesq approximation, and (3) the flow is two-dimensional. We start with the Navier-Stokes turbulent boundary layer equation (References 21 and 22).

$$\tilde{\rho}\,\tilde{u}\frac{\partial \tilde{u}}{\partial z} + \tilde{\rho}\,\tilde{v}\frac{\partial \tilde{u}}{\partial y} = \frac{\partial}{\partial y}\left(-\overline{\rho\, u''v''} + \mu \frac{\partial \tilde{u}}{\partial y}\right) + \Delta\rho g \beta T_0 \tag{33}$$

In Equation (33) z is the vertical direction, y is the distance normal to the wall, μ is the viscosity, and the quantity $\overline{\rho u'' v''}$ is the Reynolds Stress. The coefficient β is the thermal expansion coefficient for liquid, and T_o is a reference temperature. Every variable in Equation (33) is represented by its Favre average (Reference 23):

$$\vec{u} = \tilde{u} + u''$$

$$\tilde{u} = \frac{\overline{\rho u}}{\rho} \tag{34}$$

where the velocity field $\vec{u}$ is the algebraic sum of mean, $\tilde{u}$ and fluctuation velocity u". The bar over the symbols denotes the time or the ensemble average. Again we make use of stream function, i.e., ψ, to replace the y coordinate:

$$\tilde{\rho}\,\tilde{u} = \rho_o \frac{\partial \psi}{\partial y} \tag{35}$$

$$\tilde{\rho}\,\tilde{v} = -\rho_o \frac{\partial \psi}{\partial z}$$

With this change of variable $[(z,y) \rightarrow (z,\psi)]$ and neglecting gradients of stresses in the direction of flow, the momentum equation, Equation (33), takes the form

$$\frac{\partial \tilde{u}}{\partial z} = \frac{\partial \tau}{\partial \psi} + \beta\, \bar{T}_o\, \bar{\Delta} / \tilde{u} \tag{36}$$

which is a more useful form. In this equation

$$\tau = -\rho / \overline{\rho_o\, u''\, u''} + (\mu/\rho) \frac{\partial \tilde{u}}{\partial \psi} (\rho/\rho_o)^2\, \tilde{u}$$

$$\bar{\Delta} = \overline{\Delta\rho} / \bar{\rho}\, g$$

To obtain the moment of momentum equation, first integrate Equation (36) over ψ from ψ to ψ_t (total flow rate):

$$\int_{\psi}^{\psi_t} \frac{\partial \tilde{u}}{\partial z} = \int_{\psi}^{\psi_t} \frac{\partial \tau}{\partial \psi} \, d\psi + \beta T_o \int_{\psi}^{\psi_t} \bar{\Delta} / u d\psi \tag{37}$$

Since

$$u = 0 \quad @ \quad \psi = \psi_t$$

$$\tau = 0 \quad @ \quad \psi = \psi_t$$

we have

$$\frac{\partial}{\partial z} \int_{\psi}^{\psi_t} u d\psi = -\tau_{\psi} + \beta T_o \int_{\psi}^{\psi_t} \bar{\Delta} / \tilde{u} d\psi \tag{38}$$

Next integrate over ψ from 0 to ψ_t . One obtains

$$\int_{o}^{\psi_t} d\psi \frac{\partial}{\partial z} \int_{o}^{\psi_t} u d\psi = - \int_{o}^{\psi_t} \tau d\psi + \int_{o}^{\psi_t} d\psi \, \bar{\Delta} / \tilde{u} d\psi \tag{39}$$

using the Leibnitz rule (Reference 24)

$$\frac{\partial}{\partial z} \int_{o}^{\psi_t} d\psi \int_{o}^{\psi_t} \tau d\psi + \beta T_o \int_{o}^{\psi_t} d\psi \int_{o}^{\psi_t} \bar{\Delta} / \tilde{u} d\psi$$

which after partial integration reads

$$\frac{\partial}{\partial z} \int_{o}^{\psi_t} \tilde{u}_{\psi} d\psi = \beta T_o \int_{o}^{\psi_t} \bar{\Delta} / \tilde{u}_{\psi} d\psi - \int_{o}^{\psi_t} \tau d\psi \tag{40}$$

Equation (40) is the desired moment of momentum equation. In general, the second term at the right side of Equation (40) is small relative to the first term at the right side of the same equation; its magnitude is slightly negative for turbulent flows.

Equation (40) demonstrates that the core stratification affects the momentum of the boundary layer only indirectly through the temperature difference Δ . In Equation (40), β is the coefficient of thermal expansion for the liquid and has the units of inverse temperature.

In deriving the moment of momentum equation, it is assumed that the core velocity, u, is significantiy small indeed, since the width of the tank is much larger than the boundary layer thickness (see Figure 4). Finally, the shear stress term in Equation (40), although small, must be included in the present application because the velocities and the growth of the boundary layer are slowed down by stratification. An approximate development of the shear stress is given in Reference 22. It reads

$$\int_0^{\psi_t} \tau d\psi = 10\rho(F_w\nu)^{1/2}\psi_t$$

Thus, Equation (40) may be written as

$$\frac{\partial}{\partial z}\int_0^{\psi_t} \tilde{u}\psi d\psi = \int_0^{\psi_t} \frac{-}{\Delta} / \tilde{u}\psi d\psi - 10\rho(\tilde{F}_w\nu)^{1/2}\psi_t \qquad (41)$$

where u is the flow velocity in the boundary layer, n is the kinematic viscosity of liquid, and F_w is as defined in Equation (31a).

F. WALL HEAT FLUX TEMPERATURE RELATION

Analogous to the principles defined earlier for the gaseous phase, the wetted wall heat transfer is based on calculation of turbulent free convection over a vertical plate (Reference 25 and Reference 13, pp. 197-207). The convective heat transfer coefficient, h_c, for a large range of Prandtl numbers ($Pr = C_p\mu/k$) is given by

$$Nu = C_T(Gr.Pr)^{1/3} \qquad (42)$$

where the symbol Nu is the Nusselt number, ($Nu = h_cL/K$), and Gr is the Grashof number ($Gr = g\beta\Delta TL^3\rho^2/\mu^2$). Using the experimental data given in Reference 13, one obtains the following wall heat flux temperature relation:

$$\tilde{\Delta}_w = 5.3\left(\frac{\tilde{F}_w^3}{\nu}\right)^{1/4}(Pr)^{1/2} \qquad (43)$$

G. VARIATION OF CORE TEMPERATURE

The variation of the core temperature has been considered for heating and nonheating of the tank bottom surface. In the absence of the bottom heating, the core temperature will increase because the hot layer near the interface moves down the center of the tank. In this case the variation of the core temperature can be readily obtained from the general diffusion heat transfer equation. Neglecting the second-order diffusion terms and the viscous effects, the tank core temperature variation equation reads

$$\frac{\partial \tilde{\Delta}_c}{\partial t} = -U(z) \frac{\partial \tilde{\Delta}_c}{\partial z} \tag{44}$$

In Equation (44) $\tilde{\Delta}_c = \beta g(T_c - T_o)$, where β is the expansion coefficient and $U(z)$ is the core main counter flow velocity. Note that $U(z)$ can be obtained from the following continuity argument. Since the boundary layer thickness, δ, is much smaller than the tank diameter, the flow velocity in the boundary layer must be much larger than core velocity. Therefore, based upon the conservation of mass argument, the core velocity can be calculated by setting the upward total mass flow $\psi_{\ell} L_{\ell}$ in the boundary equal to the downward total mass flow $-\rho A_{\ell} U(z)$ in the core. It follows that

$$U(z) \rho A_{\ell} = - \psi_t(z) L_{\ell} \tag{45}$$

If the bottom of the tank is also exposed to an external heat flux, additional heat is transferred to the bulk of the liquid. In this case, similar to the previous analysis, one must consider the additional heat transfer processes:

1. Heating of the bottom "horizontal" surface (similar to the analysis for "vertical" wall).

2. Convective heat loss from the bottom to the liquid (similar to Equation (5). We have

$$\rho_w C_w \delta_w \frac{dT_{wb}}{dt} = \dot{q}''_f - \dot{q}''_{rrob} - \dot{q}''_{c\ell b} \tag{46}$$

where

$$\dot{q}''_{c\ell b} = C_b (T_{w,b} - T_{\ell,b})^{4/3}$$

$T_{w,b}$: wall temperature at the bottom

$T_{\ell,b}$: core liquid temperature near the bottom

The additional heat from the bottom is distributed by the buoyant thermals near the bottom of the tank. We assume that these thermals are "buoyantly" strong enough to transfer the heat uniformly through the bulk of the fluid while the boundary layers remain unaffected. Under this condition the governing heat transfer equation, Equation (14), becomes

$$\frac{\partial \tilde{\Delta}_c}{\partial t} = -U(z) \frac{\partial \tilde{\Delta}_c}{\partial z} + \frac{A_b g \beta}{\rho C_p V_T} \dot{q}''_{c\ell b} \tag{47}$$

In Equation (47), A_b is the bottom surface area and V_T is the tank volume.

The following empirical expressions (Reference 25) describe the profiles of velocity and temperature in the boundary layer:

$$u = 1.8 u_m \left(\frac{\psi}{\psi_t}\right)^{1/4} \left(1 - \frac{\psi}{\psi_t}\right)$$

$$\tilde{\Delta} = 1.23\, \tilde{\Delta}_w \left(\frac{\nu}{\psi}\right)^{1/4} \left(1 - \frac{\psi}{\psi_t}\right) Pr^{-1/2} \tag{48}$$

The governing equations that have been developed for each zone together with the boundary layer velocity and temperature profiles, Equation (48), constitute a set of deterministic integro-differential equations that are solved numerically. The solutions provide internal pressure rise history and boiling temperature which determines the tank response.

SECTION IV
NUMERICAL SOLUTION

A. NUMERICAL SCHEME

A special numerical scheme is developed to solve the governing thermo-hydrodynamic equations of processes occuring inside the tank. This scheme utilizes a stationary and a moving grid that are essential to temporal and spatial calculations of the liquid parameters under thermal load. The numerical scheme also includes a rezoning procedure necessary to model the variation of the temperature in the descending liquid inside the tank as a function of height.

The governing partial differential Equations (1), (10), (11), (17), (22), (25), (32), (46), (47) are solved, and the height-dependent variables are approximated in either of the two grid systems using a time-dependent staircase (i.e., piecewise constant) function of height z. The staircase function is restricted to jump only at the grid points. Figure 7 illustrates an instantaneous plot of a staircase function of the core temperature $T_c(t,z)$ in a stationary grid z_0, z_1,...z_n, as well as a moving time-dependent grid, z'_0, $z'_1(t)$,...$z'_n(t)$, z'_{n+1}. The prime sign indicates the moving grid. The vertical axis measures the two corresponding staircase approximations for the core temperature $T_c(t,z)$. The time axis, not shown in this figure, is perpendicular to the plane.

Equation (25), describing the temperature of the wetted wall, can be easily solved by using a stationary grid. However, a moving grid which follows the motion of the descending liquid is required to evaluate the core temperature variation. It is important to note that the temperature $T_c(t,z)$, which is a function of time and height, is the only variable that needs to be calculated in terms of both grids. This is because of the convective heat transfer term, $\dot{q}''_{c\ell s}$, in Equation (25) which depends on $T_c(t,z)$. Therefore, $T_c(t,z)$ is calculated once in terms of the moving grid for the core temperature equation and a second time in terms of the stationary grid for the wetted wall equation.

A rezoning procedure has been devised to couple the two grid systems. This procedure converts a staircase function in a moving grid to a staircase function in a stationary grid. Therefore the rezoning procedure enables one to convert from one grid system to the other. Details of this procedure are presented in the following section.

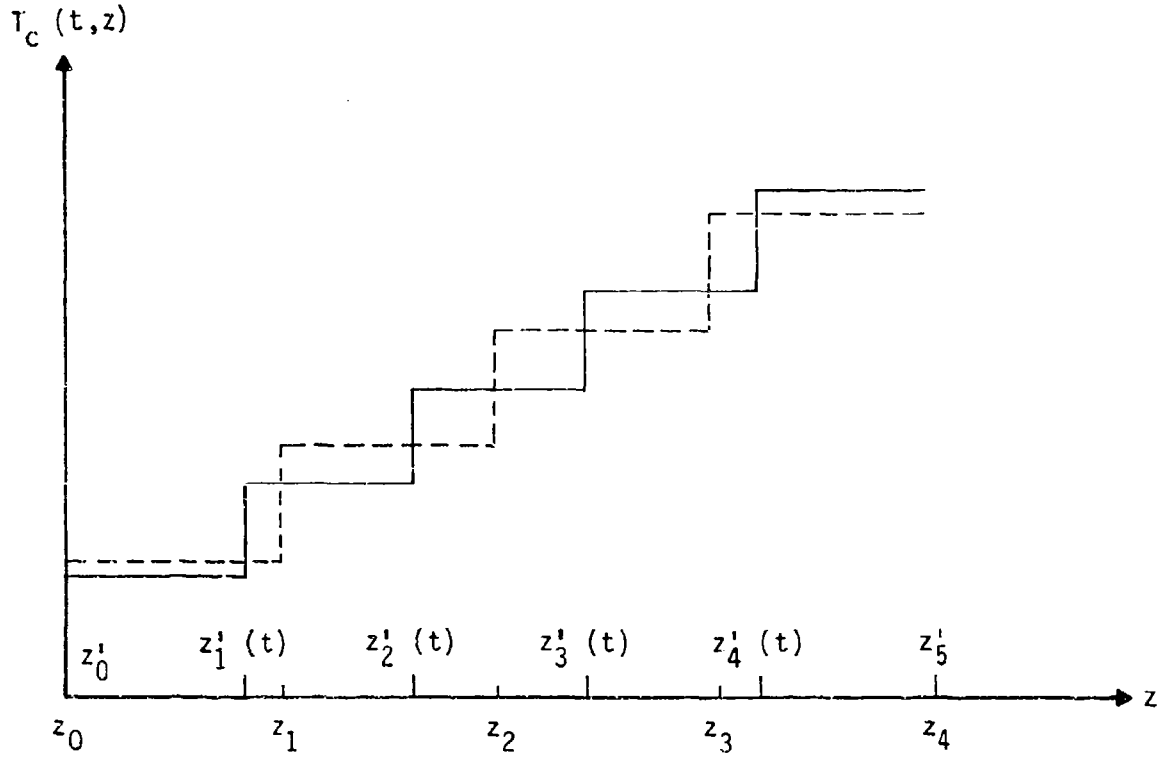

Figure 7. Staircase Representation of the Core Temperature in Terms of a Moving and Stationary Grid. n = 4

B. COMPUTATIONAL GRID

The variation of the wetted wall temperature as a function of height is calculated numerically, based on a stationary grid given as

$$z_k = kH_\ell/n \qquad \text{for } k = 0,1,\ldots,n.$$

In this equation the height of liquid, H_ℓ, is divided into n cells of equal size in the interval $0 \leq z \leq H_\ell$. Once the stationary grid is set up, the wetted wall temperature T_{ws} can be approximated using a staircase function.

$$T_{ws}(t,z) = T_{ws,k}(t) \qquad \text{for } z_{k-1} < z < z_k$$

$$\text{for } k = 1,2,\ldots,n.$$

As discussed earlier, the staircase function is restricted to jumps only at points $z_1, z_2, \ldots, z_{n-1}$.

The variation of the core temperature, $T_c(t,z)$, due to the motion of descending liquid is modeled by using the following moving grid,

$$0 = z'_0 < z'_1(t) < z'_2(t) < \ldots < z'_n(t) < z'_{n+1} = H_\ell.$$

In this expression the grid moves with the liquid, and $z'_0 = 0$ and $z'_{n+1} = H_\ell$ are the fixed end points corresponding to the bottom of the tank and top of the liquid, respectively. Then the core temperature T_c can be approximated using a staircase function in the moving grid

$$T_c(t,z) = T'_{c,k}(t) \qquad \text{for } z'_{k-1}(t) < z < z'_k(t)$$
$$\text{for } k = 1,2,\ldots,n+1.$$

A similar approach is taken in a related problem by Germeles (Reference 26).

The wetted wall temperature equations, Equations (25) and (25a), contain a convective heat transfer term which depends on the core temperature, T_c. Therefore, analogous to the discretization of the wetted wall temperature, T_{ws}, the core is described in the same manner using a staircase function in a stationary grid. Hence, T_c in a stationary grid becomes

$$T_c(t,z) = T_{c,k}(t) \qquad \text{for } z_{k-1} < z < z_k \text{ for } k = 1,2,\ldots,n.$$

A rezoning procedure is employed to convert the staircase function in the moving grid into a staircase function approximation in a stationary grid. The application of the two grid systems for calculating the liquid core temperature $T_c(z,t)$ as a function of height is presented in the following.

Assume the following time grid

$$t_k = t_0 + k\Delta t \qquad \text{for } k = 0,1,2,\ldots$$

and consider the time step from t_j to t_{j+1}.

Initially, at time t_j, the liquid core temperature, $T_c(z,t)$, is known and is defined in terms of a staircase function in the stationary grid. In other words, the values of $T_{c,k}(t_j)$ are known for all k's.

STEP 1. Define the moving grid z'_k in the same time interval, i.e., $t_j < t < t_{j+1}$, so that

(a) at the start of the time step, $t = t_j$, the moving grid coincides with the stationary grid for all values of k, i.e.,

$$z'_k(t_j) = z_k \qquad \text{for } k = 0,1,2,\ldots,n$$
$$z'_{n+1} = z_n$$

(b) the moving grid points $z'_1(t), z'_2(t), \ldots, z'_n(t)$ move with the liquid core, while the endpoints z'_0 and z'_{n+1} remain fixed. Note that the moving grid is redefined at the start of each time step.

STEP 2. Next, express the core temperature $T_c(z,t)$ at time t_j in terms of a staircase function in the moving grid . Since the moving grid coincides originally with the stationary grid, it follows that

$$T'_{c,k}(t_j) = T_{c,k}(t_j) \qquad \text{for } k = 1,2,\ldots,n.$$

STEP 3. Iterate the discretized differential equations for $T_c(z,t)$ over time to calculate the staircase expression for the core temperature in the moving grid, i.e., $T'_{c,k}(t_{j+1})$ for $k = 1,2,\ldots,n+1$.

STEP 4. The discretized side wall temperature, T_{ws}, Equation (25), is solved numerically. This iterative procedure takes the staircase representation of T_{ws} at time t_j in a stationary grid and calculates the expression for T_{ws} at the next time, t_{j+1}. The values of $T_{c,k}(t_j)$ are needed for this calculation of the side wall temperature.

STEP 5. Using the rezoning method, the staircase function for $T_c(z,t)$ at time t_{j+1} in the moving grid is converted into a staircase function in the stationary grid. Therefore, the values of $T'_{c,k}(t_{j+1})$ are used for calculating the values of $T_{c,k}(t_{j+1})$ for $k = 1,2,\ldots,n$ in the stationary grid.

This procedure is repeated to calculate the variables for the subsequent time steps.

A detailed description of the rezoning method is presented in the following. Consider the kth stationary cell $z_{k-1} < z < z_k$, and assume the simple case where it overlaps only with kth moving cell $z'_{k-1} < z < z'_k$ and the (k+1)th moving cell $z'_k < z < z'_{k+1}$. In other words, one has the situation where

$$z'_{k-1} < z_{k-1} < z'_k < z_k < z'_{k+1}.$$

Then the core temperature, $T_{c,k}$, in the kth stationary cell given by the rezoning method is

$$T_{c,k} = (z_k - z_{k-1})^{-1} \left[(z'_k - z_{k-1})\, T'_{c,k} + (z_k - z'_k) T'_{c,k+1} \right]$$

In the above relation $T_{c,k}$ is a weighted average of the temperatures $T'_{c,k}$ and $T'_{c,k+1}$ in the kth and (k+1)th moving cells, respectively. The weights are proportional to the lengths of overlap $z'_k - z_{k-1}$ and $z_k - z'_k$ of the stationary cell with the moving cells. Figure 8 shows the relationship between the moving and stationary grid systems.

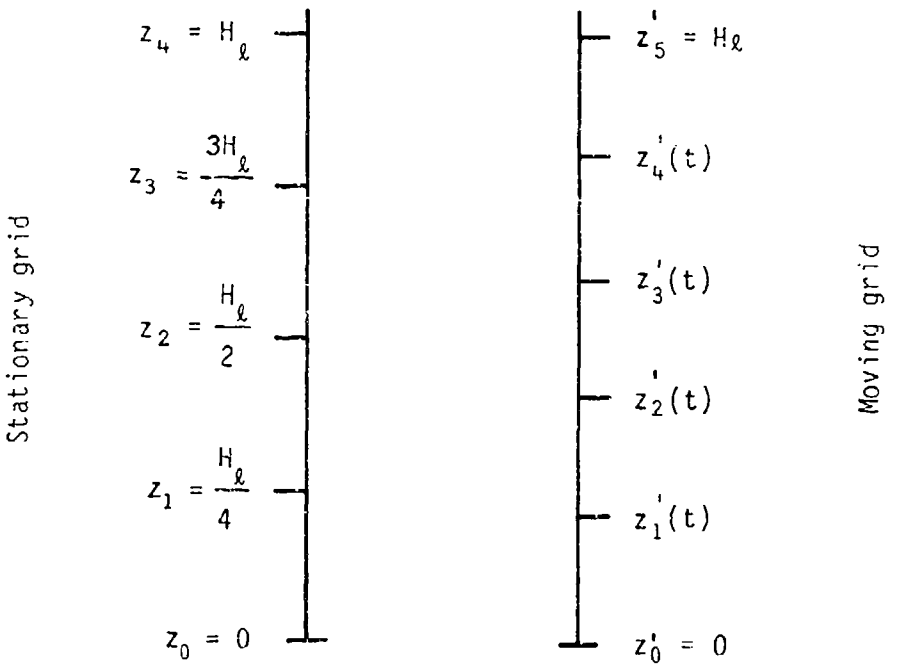

Figure 8: Moving and Stationary Grid Systems

C. MODELING TEMPERATURE OF THE WETTED WALL

The governing temperature equation for the side wall next to the liquid $T_{ws}(t, z)$ was derived earlier in Equation (25). It satisfies the following partial differential equation

$$\rho_w C_w \delta_w \frac{\partial T_{ws}}{\partial t} = \dot{q}''_f - \dot{q}''_{rros} - \dot{q}''_{c\ell s} \tag{49}$$

where

$$\dot{q}''_{rros} = \varepsilon\sigma (T_{ws}^4 - T_\infty^4)$$

$$\dot{q}''_{c\ell s} = C_s (T_{ws} - T_c)^{4/3}$$

$$C_s = \rho_o C_p \left[\frac{\nu_c \beta g}{(5.3)^4 Pr^2}\right]^{1/3} = C_{1v} \rho_o C_p \left(\frac{\nu_c \beta g}{Pr^2}\right)^{1/3}$$

$$C_{1v} = (5.3)^{-4/3} = 0.11$$

The above partial differential equation contains a derivative explicitly with respect to time t but not z. Therefore, it can be replaced by a system of ordinary differential equations involving ordinary derivatives with respect to t. Furthermore, the z dependent variables in Equation (49) are all replaced by their corresponding staircase functions in a stationary grid.

The governing expressions for the z dependent variables as staircase functions in the stationary grid are

$$T_{ws}(t, z) = T_{ws,k}(t) \qquad \text{for } z_{k-1} < z < z_k$$

$$T_c(t, z) = T_{c,k}(t) \qquad \text{for } z_{k-1} < z < z_k$$

$$\dot{q}''_{rros}(t, z) = \dot{q}''_{rros,k}(t) \qquad \text{for } z_{k-1} < z < z_k$$

$$\dot{q}''_{c\ell s}(t, z) = \dot{q}''_{c\ell s,k}(t) \qquad \text{for } z_{k-1} < z < z_k.$$

and the partial differential equation for $T_{ws}(t, z)$ in the staircase function approximation becomes the following system of ordinary differential equations,

$$\rho_w C_w \delta_w \frac{dT_{ws,k}}{dt} = \dot{q}''_f - \dot{q}''_{rros,k} - \dot{q}''_{c\ell s,k} \tag{50}$$

where

$$\dot{q}''_{rros,k} = \varepsilon\sigma \left(T_{ws,k}^4 - T_\infty^4\right)$$

$$\dot{q}''_{c\ell s,k} = C_s (T_{ws,k} - T_{c,k})^{4/3} \qquad \text{for } k = 1,2,\ldots,n.$$

The ordinary differential equation for the temperature $T_{wb}(t)$ of the bottom wall, Equation (46), reads

$$\rho_w C_w \delta_w \frac{dT_{wb}}{dt} = \dot{q}''_f - \dot{q}''_{rrob} - \dot{q}''_{c\ell b} \tag{51}$$

where

$$\dot{q}''_{rrob} = \varepsilon\sigma \left(T_{wb}^4 - T_\infty^4\right)$$

$$\dot{q}''_{c\ell b} = C_b (T_{wb} - T_{cb})^{4/3}$$

$$C_b = C_{1h}\rho_o C_p \left(\frac{\nu_c \beta g}{Pr^2}\right)^{1/3} = (C_{1h}/\ C_{1v})C_s$$

$$C_{1h} = 0.06$$

The constants C_{1h} and C_{1v} are coefficients within the heat transfer coefficients corresponding to the horizontal and vertical walls of the tank, respectively. The quantity T_{cb} is the liquid core temperature at the bottom. The quantity $T_{cb}(t)$ equals the value of $T_c(t,z)$ in the first step of its staircase approximation,

$$T_{cb}(t) = T_{c,1}(t)$$

A fourth-order Runge Kutta numerical method (Reference 27) is used for solving the set of ordinary differential equations, Equations (50) and (51). The quantities $T_{c,k}$ are kept constant during the calculation of a single time step. However, they are updated to new values at the end of each iteration.

D. MODELING OF LIQUID CORE TEMPERATURE

The partial differential equations for the liquid core temperature $T_c(t,z)$ was derived earlier in Equation (47); it reads,

$$\frac{\partial T_c}{\partial t} + U \frac{\partial T_c}{\partial z} = \frac{A_b}{\rho C_p V_T} \dot{q}''_{c\ell b} \tag{52}$$

where V is the tank total liquid volume and the vertical velocity U(t, z) of the core is given by Equation (45) as,

$$U(t, z) = -\psi_t(t, z)\, L_\ell / (\rho_o A_\sim) \tag{53}$$

Here L_ℓ is the perimeter of the horizontal cross section and $\psi_t(t, z)$ is the boundary layer mass flux. Detailed description of $\psi_t(t,z)$ is presented in the next section. The left side of the Equation (52) is the material derivative DT_c/Dt (also called total derivative) of T_c with respect to time. Therefore, for a grid which moves with the liquid, the total derivative is replaced in the discretized equations by an ordinary derivative $dT'_{c,k}/dt$. Hence, the discretized expression for $T_c(t, z)$ as a staircase function in the moving grid becomes

$$T_c(t, z) = T'_{c,k}(t) \qquad \text{for } z'_{k-1}(t) < z < z'_k(t)$$
$$\text{for } k = 1, 2, \ldots, n+1.$$

and the governing partial differential equation, Equation (52), in the staircase function approximation will become the following system of ordinary differential equations.

$$\frac{dT'_{c,k}}{dt} = \frac{A_b}{\rho C_p V_T} \dot{q}''_{c\ell b} \qquad \text{for } k = 1,2,\ldots,n \tag{54}$$

Equation (52) must satisfy the boundary condition at the top, $z = H_\ell$;

$$T_c(t,H_\ell) = T_{c\ top}(t)$$

The quantity $T_{c\ top}$, core temperature at the top, is determined by the rate that the mass and heat are being added to the core top from the convective boundary layer flow. Corresponding to the transformation of partial differential Equation (52) into the system of ordinary differential equations shown in Equation (54) by application of the staircase approximation, the above boundary condition will take the following form:

$$T'_{c,n+1}(t) = T_{c\ top}(t).$$

The variables appearing in the liquid core velocity equation, Equation (53), are defined in a stationary grid as:

$$\psi_{t,k}(t) = \psi_t(t, z_k)$$

$$U_k(t) = U(t, z_k) \qquad \text{for } k = 0,1,\ldots,n.$$

Note that, unlike the core temperature, $\psi_t(t,z)$ and $U(t,z)$ are not being represented as staircase functions, and are not constant between the grid points. Then Equation (53) at the grid points becomes

$$U_k(t) = -\psi_{t,k}(t)L_\ell / (\rho_0 A_\ell) \tag{55}$$

Euler's method (Reference 27) is used for numerically updating the values of $T'_{c,k}$ during each time increment Δt. Also, the values of the moving grid points z'_k at the end of a time increment for all values of k are calculated from:

$$z'_k(t_j + \Delta t) = z'_k(t_j) + \Delta t\, U_k(t_j) = z_k + \Delta t\, U_k(t_j)$$

and $z'_{n+1} = z_n$.

The rezoning procedure is used to convert $T'_{c,k}$ in the moving grid into $T_{c,k}$ in a stationary grid at the end of each time step.

E. MODELING OF CONVECTIVE BOUNDARY LAYER

In the convective boundary layer, a continuous upward flow of mass and heat takes place. The motion of the mass in the boundary layer is defined by the buoyancy equation, Equation (29). The buoyancy equation was recast into the more useful form in terms of total mass flux ψ_t in Equation (32). In a similar fashion, the upward heat flux is defined and expressed in terms of ψ_t. The values of mass and heat flux at the top of the boundary are used to estimate the temperature $T_{c\ top}(t)$ at the top of the core. The buoyancy equation together with the temperature profile (Reference 28) and the heat flux temperature relations, in the boundary layer, are given in Equations (56), (57), and (58), respectively.

$$\frac{\partial}{\partial z}\left(\int_0^{\psi_t} \tilde{\Delta}\, d\psi\right) = \rho_0 \tilde{F}_w - \psi_t \frac{\partial \tilde{\Delta}_c}{\partial z} \tag{56}$$

$$\tilde{\Delta} = 1.23\, \tilde{\Delta}_w\, Pr^{-1/2} \left(\frac{\nu_c}{\psi}\right)^{1/4} \left(1 - \frac{\psi}{\psi_t}\right) \tag{57}$$

$$F_w = \left(\frac{\nu_c}{(5.3)^4 Pr^2}\right)^{1/3} \tilde{\Delta}_w^{\,4/3} \tag{58}$$

where

$$\tilde{\Delta}_w = \beta g\, (T_{ws} - T_c)$$

Integrating Equation (57) from $\psi = 0$ to $\psi = \psi_t$ gives,

$$\int_0^{\psi_t} \tilde{\Delta} d\psi = 0.937\, \tilde{\Delta}_w\, Pr^{-1/2}\, \nu_c^{1/4}\, \psi_t^{3/4} \tag{59}$$

Using Equations (58) and (59), the buoyancy equation, Equation (56), reduces to

$$\frac{\partial}{\partial z}\left(\tilde{\Delta}_w\, \psi_t^{3/4}\right) = C_0 \tilde{\Delta}_w^{4/3} - C_1 \psi_t \frac{\partial \tilde{\Delta}_c}{\partial z} \tag{60}$$

where

$$C_o = \rho_o \nu_c^{1/12} / \left[(.937)(5.3)^{4/3} Pr^{1/6} \right]$$

$$C_1 = Pr^{1/2} / \left[(0.937)\ \nu_c^{1/4} \right]$$

This is a form of the buoyancy equation with ψ_t (t, z) as a dependent variable. Note that $\psi_t(t,z)$ is the total upward mass flux in the boundary layer integrated over the thickness, δ, of the boundary layer.

The new form of the buoyancy equation, Equation (60), can be solved for the total mass flux, ψ_t, once the variables $\tilde{\Delta}_c$ and $\tilde{\Delta}_w$ are properly determined. Analogous to the previous procedure, $\tilde{\Delta}_w$ and $\tilde{\Delta}_c$ are expressed in terms of staircase functions in the stationary grid.

$$\tilde{\Delta}_w(t, z) = \tilde{\Delta}_{w,k}(t) \qquad \text{for } z_{k-1} < z < z_k \text{ and } k = 1,2,\ldots,n.$$

$$\tilde{\Delta}_c(t,z) = \tilde{\Delta}_{c,k}(t)$$

where by definition $\tilde{\Delta}_{w,k}(t)$ and $\tilde{\Delta}_{c,k}(t)$ are

$$\tilde{\Delta}_{w,k} = g\,\beta\,(\bar{T}_{ws,k} - T_{c,k})$$

$$\tilde{\Delta}_{c,k} = g\,\beta\,(T_{c,k} - T_o)$$

After substituting for $\tilde{\Delta}_w$ and $\tilde{\Delta}_c$ in Equation (60), and noting that they are constant in the interval $z_{k-1} < z < z_k$, the buoyancy equation will take the following form:

$$\frac{\partial}{\partial z}(\psi_t)^{3/4} = C_o \tilde{\Delta}_{w,k}^{1/3} \qquad \text{for } z_{k-1} < z < z_k \qquad (61)$$

Integration of the modified buoyancy equation, Equation (61), results in

$$\psi_t^{3/4}(t,z) = \psi_{t,k-1}^{3/4}(t) + C_o \tilde{\Delta}_{w,k}^{1/3}(t)(z - z_{k-1}) \text{ for } z_{k-1} < z < z_k$$

and evaluating it at $z = z_k$ for all $k = 1,2,\ldots,n$ yields

$$\psi_{t,k}(t) = \left[\psi^{3/4}_{t,k-1}(t) + C_o \tilde{\Delta}^{1/3}_{w,k}(t)(z_k - z_{k-1})\right]^{4/3} \qquad (62)$$

Equation (62) is the general solution of the buoyancy equation, Equation (61). It calculates the value of the total mass flux, i.e. $\psi_{t,1}$, $\psi_{t,2}$,..., at any grid point along the boundary layer. Obviously, since there is no flow in the bottom of the tank, $\psi_{t,0} = 0$.

A more accurate form of the bouyancy equation may be obtained once the variables $\tilde{\Delta}_w$ and $\tilde{\Delta}_c$ are expressed as staircase function approximations. The resulting form of the bouyancy equation, Equation (61), would be supplemented by a jump condition on ψ_t at each z_k, i.e., the assumption of continuity of ψ_t at each z_k would be relaxed. This jump condition could be derived as follows: Integrate each term of Equation (60) from $z_k - \delta$ to $z_k + \delta$ where $\delta>0$. Then let $\delta\to 0$. The result would be an expression from which the jump in ψ_t at z_k can be calculated.

Another quantity essential to calculation of the core top temperature is the upward heat flux $\dot{q}'_{bnd}(t, z)$, with $T_c(t, z)$ as its reference temperature, integrated over the thickness, δ, of the boundary layer. It is

$$\dot{q}'_{bnd}(t, z) = C_p \int_o^{\psi_t} (T - T_c)\, d\psi = \frac{C_p}{\beta g} \int_o^{\psi_t} \tilde{\Delta}\, d\psi$$

After substituting from Equation (59), the above equality becomes:

$$\dot{q}'_{bnd}(t,z) = C_2\, \tilde{\Delta}_w\, (t,z)\psi^{3/4}_t(t,z) \qquad (63)$$

where

$$C_2 = \frac{0.937\ \nu_c^{1/4} C_p}{\beta\, g (Pr)^{1/2}}$$

At the core top the total mass and the convective heat issuing from the boundary layer are defined as;

$$\psi_{t\ top}(t) = \psi_t(t, H_\ell) \tag{64}$$

$$\dot{q}'_{bnd\ top}(t) = \dot{q}'_{bnd}(t, H_\ell) \tag{65}$$

The two quantities given by Equations (64) and (65) determine the temperature $T_{c\ top}(t)$ of the liquid flowing onto the top core from the boundary layer according to the following equation

$$T_{c\ top}(t) = T_c(t, H_\ell) + \frac{\dot{q}'_{bnd\ top}(t)}{C_p \psi_{t\ top}(t)} \tag{66}$$

The equations describing the flow variables at the core top, Equations (64), (65), (66), written in terms of their corresponding staircase representation, will take the following form; the total mass flux becomes

$$\psi_{t\ top}(t) = \psi_{t,n}(t) \tag{67}$$

Similarly, the expression for the heat flux at the top of the boundary layer, written in staircase form after substituting from Equation (63) into Equation (65), becomes

$$\dot{q}'_{bnd\ top}(t) = C_2 \tilde{A}_{w,n}(t)\ \ \psi^{3/4}_{t,n}(t) \tag{68}$$

Following the same procedure, the expression for the core top temperature in the staircase form becomes

$$T'_{c,n+1}(t) = T_{c,top}(t) = T_{c,n}(t) + \frac{\dot{q}'_{bnd\ top}(t)}{C_p \psi_{t,top}(t)} \tag{69}$$

F. MODELING OF VAPORIZATION RATE

The relation describing the vaporization and the mass transfer across the gas liquid interface is given in Equation (22). This equation can be put in the form

$$\dot{m}'' = a \ln\left(1 + \frac{b\,\dot{m}''}{\dot{m}'' - c}\right) \tag{70}$$

or

$$\dot{m}'' = a \ln\left(1 + b + \frac{b\,c}{\dot{m}'' - c}\right)$$

where

$$a = \frac{h_c}{C_{p,g}} = \frac{C_g}{C_{p,g}} (T_g - T_i)^{1/3}$$

$$C_g = k_g\, C_{lh}\left(\frac{g\,\beta_g}{\nu_g \alpha_g}\right)^{1/3}$$

$$b = \frac{C_{p,g}(T_g - T_i)}{\ell_{eff}}$$

$$c = \frac{\dot{q}''_{r\ell}}{\ell_{eff}}$$

$$\ell_{eff} = L + C_{p,\ell}\,(T_i - T_{c\ top})$$

$$\dot{q}''_{r\ell} = \frac{\dot{q}''_{rri} A_w}{A_\ell}$$

The surface temperature $T_i(t)$ is estimated according to the following relationship:

$$T_i = \min\left[\left(1/2\right)\left(T_g + T_{c\ top}\right),\ T_b\right].$$

The boiling temperature T_b is determined by the Clausius-Clapeyron relation

and is discussed in the next section.

Parameters not previously defined are

k_g = thermal conductivity of the gas
C_{lh} = dimensionless constant for horizontal orientation of surface
β_g = thermal expansion coefficient of the gas
ν_g = kinematic viscosity of the gas
α_g = thermal diffusivity of the gas

Equation (70) is a nonlinear equation that needs to be solved for $\dot{m}''$. This problem is a particular case from a general class of problems in which roots are to be found for an equation of the form

$$f(x) = 0$$

Numerical methods for solving such problems are discussed extensively in the literature. To convert Equation (70) to this form, transpose the right side to the left side of this equation, and replace $\dot{m}''$ by the symbol x. This result; in the following expression for the function $f(x)$.

$$f(x) = x - a \ln \left(1 + \frac{bx}{x - c}\right) \tag{71}$$

Then the value $x = x_0$, where $f = 0$ is the solution, $\dot{m}''$, of the transcendental equation, Equation (70), i.e., $\dot{m}'' = x_0$.

To develop a numerical method of solution, some properties of the function $f(x)$ need to be determined. Assume that $a > 0$, $b > 0$, $c > 0$, which will normally be the case. Note the properties,

$f(x)$ undefined for $0 < x < c$

$f \to -\infty$ as $x \to c$ from the right

$f \to +\infty$ as $x \to +\infty$

$\frac{df}{dx} > 1$ for $c < x$

It follows that there is one solution

$$x_0 > c$$

and

$$f(x) < o \text{ for } c < x < x_0$$
$$f(x) > 0 \text{ for } x_0 < x$$

An iterative scheme* which is a combination of Newton's method and the bisection method (Reference 29) is used in the numerical solution of this equation. For any iterate x, if $f(x) > o$, then the next iterate is taken half way between the points c and x, unless Newton's method gives a point closer to x. This procedure is continued until an iterate x is reached where $f(x) < 0$. After reaching an iterate that gives $f < 0$, Newton's method is used for calculating all the remaining iterates. It can be shown that if $f < 0$ for one iterate, then all the remaining iterates from Newton's method will also give $f < 0$.

The input quantity f_{tol} is the absolute degree of accuracy desired in the solution x_0. If $|f| < f_{tol}$, then it follows that $|x-x_0| < f_{tol}$ because $\frac{df}{dx} > 1$ for $x > c$.

G. MODELING OF GAS AND THE UNWETTED WALL TEMPERATURE

The equation for the unwetted wall temperature $T_{wg}(t)$ was derived earlier, Equation (1). It satisfies the following ordinary differential equation,

$$\rho_w C_w \delta_w \frac{dT_{wg}}{dt} = \dot{q}''_f - \dot{q}''_{rro} - \dot{q}''_{rri} - \dot{q}''_{cg} \qquad (72)$$

---

* The method was developed only to the point where it satisfied the present needs. Further investigation would be desirable to assess its limitations and its capability. The method of solving the vaporization equation can easily be improved. The bisection method, which was used in part of this calculation, is slow. The number of iterations can be reduced by modifying this part of the calculation.

where

$$\dot{q}''_{rro} = \varepsilon\sigma\left(T^4_{wg} - T^4_{\infty}\right)$$

$$\dot{q}''_{rri} = \varepsilon\sigma\left(T^4_{wg} - T^4_{i}\right)$$

$$\dot{q}''_{cg} = C_g\left(T_{wg} - T_g\right)^{4/3}$$

The coefficient C_g was defined earlier, it reads,

$$C_g = k_g\, C_{1h}\left(\frac{g\beta_g}{\nu_g \alpha_g}\right)^{1/3}$$

The gas temperature equation, Equation (17), is modified to allow also for an open vent configuration. The gas temperature T_g satisfies the following ordinary differential equation:

$$\frac{dT_g}{dt} = \left(M_a\, C_{a,v} + M_v\, C_{v,v}\right)^{-1}\left[\dot{q}''_{cg}\, A_w - \dot{q}''_{c\ell} A_\ell + \dot{M}_i\left(C_{v,p}\, T_i - C_{v,v}\, T_g\right)\right.$$

$$\left. - \dot{M}_o PV/\left(M_a + M_v\right)\right] \qquad (73)$$

where

$$\dot{q}''_{c\ell} = \dot{m}''_{eff}\, L - \dot{q}''_{r\ell}$$

The mass inflow rate $\dot{M}_i$ into the ullage volume due to the evaporation is

$$\dot{M}_i = A_\ell\, \dot{m}'' \qquad (74)$$

The mass outflow rate $\dot{M}_o$ from the ullage volume through the vent is

$$\dot{M}_o = \begin{cases} 0 & \text{for } P \leq P_{vnt} \\ \left(\dot{M}_o\right)_{max}\left(P - P_{vnt}\right)/\Delta P_{vnt} & \text{for } P_{vnt} < P < P_{vnt} + \Delta P_{vnt} \\ \left(\dot{M}_o\right)_{max} & \text{for } P_{vnt} + \Delta P_{vnt} \leq P \end{cases} \quad (75)$$

where

$$\left(\dot{M}_o\right)_{max} = AC_d\left[2\left(P - P_{atm}\right)\left(M_v + M_a\right)/V\right]^{1/2}$$

and P_{vnt} is the vent activation pressure such that the vent is closed and open for $P < P_{vnt}$ and $P > P_{vnt}$, respectively. The quantity ΔP_{vnt}, when it is set greater than zero, gives a model of a vent that is partly open in the pressure range $P_{vnt} < P < P_{vnt} + \Delta P_{vnt}$.

The mass $M_v(t)$ and $M_a(t)$ of vapor and air, respectively, in the ullage volume satisfies the following ordinary differential equations

$$\frac{dM_v}{dt} = \begin{cases} \dot{M}_i & \text{for } P \leq P_{vnt} \\ \dot{M}_i - \dot{M}_o M_v / \left(M_v + M_a\right) & \text{for } P_{vnt} < P \end{cases} \quad (76)$$

and

$$\frac{dM_a}{dt} = \begin{cases} 0 & \text{for } P \leq P_{vnt} \\ -\dot{M}_o M_a / \left(M_a + M_v\right) & \text{for } P_{vnt} < P \end{cases} \quad (77)$$

The four simultaneous ordinary differential equations, numbered (72), (73), (76), and (77), are solved by a fourth-order Runge Kutta numerical method (Reference 27).

H. MODELING OF PRESSURE AND BOILING TEMPERATURE

According to Equations (18) and (20), the total pressure, $P(t)$, of the gas is

$$P(t) = \left[\frac{M_a(t)}{(mol)_a} + \frac{M_v(t)}{(mol)_v}\right]\frac{RT_g(t)}{V} \tag{78}$$

The boiling temperature $T_b(t)$ of the liquid at the total pressure $P(t)$ is given by the Clausius-Clapeyron equation,

$$T_b(t) = \left[\frac{1}{T_1} - \frac{R}{(mol)_v L_v}\ln\frac{P(t)}{P_1}\right]^{-1} \tag{79}$$

where P_1 is the vapor pressure at the reference temperature T_1; i.e., T_1 is the boiling temperature when the total pressure is P_1.

I. INITIAL VALUE CALCULATION

The initial values of the physical parameters in the ullage volume, i.e., vapor pressure $P_v(0)$, vapor mass $M_v(0)$, and the amount of air $M_a(0)$ are calculated using Clausius-Clapeyron and ideal gas law relations.

Using the Clausius-Clapeyron equation, the initial vapor pressure in the tank is obtained from the following relation:

$$P_v(0) = P_1 \exp\left[\frac{(mol)_v L_v}{R}\left(\frac{1}{T_1} - \frac{1}{T_g(0)}\right)\right] \tag{80}$$

The corresponding initial mass $M_v(0)$ of the vapor in the tank is calculated by substituting $P_v(0)$ from Equation (80) in the ideal gas law relation;

$$M_v(0) = \frac{(mol)_v V\, P_v(0)}{RT_g(0)} \tag{81}$$

Assuming that the initial total pressure inside the tank is equal to the ambient atmospheric pressure P_{atm}, the initial mass $M_a(0)$ of the air is obtained from:

$$M_a(0) = \frac{(mol)_a V\left[P_{atm} - P_v(0)\right]}{RT_g\ (0)} \qquad (82)$$

J. DESCRIPTION OF THE CODE

A modular code using the FORTRAN 77 language was written to numerically solve the governing equations. The code was developed in the VUE (VOS UNIX™ Environment) operating system on a Harris 800 computer. The code consists of one main program and seventeen subroutines. A description of each of these program units is presented below. A copy of the source code is given in Appendix B.

Program TANK is the main program. To allow flexibility, the program has two time variables, t_g and t_ℓ, for gas and liquid, respectively. The two corresponding time increments can be related so that $\Delta t_\ell = m\ \Delta t_g$, where m is a positive integer. However, in this calculation m = 1 was used.

The main program performs the following:

1. Initially, it calls the INPUT1, INPUT2, INPUT3, and INITVAL subroutines.

2. It carries out the iterative numerical procedure by calling GKUTTA for each updating of the gas variables by a time increment, Δt_g, and by calling the BUOY, CORE, LKUTTA, and REZCORE subroutines for each updating of the liquid variables by a time increment, Δt_ℓ.

3. It controls the output time by the variable t_{pr}. When t_ℓ becomes larger than t_{pr}, the program calls WL and DVG to complete the calculations. It then outputs the desired liquid variables as well as the desired gas variables on the VOS files called OUTL and OUTG, respectively. Similarly, it outputs the interface and the remaining variables on the VOS file OUTI. Finally, it increments t_{pr} by the amount Δt_{pr} to determine the next output time.

4. The program stops when t_{pr} exceeds t_{max}.

Subroutine INPUT1 assigns and calculates constants and initial values. The initial values assigned in this subroutine are the initial time, t_o = TIMZ, and the initial temperature, T_o = TZ. To change the values to be assigned in INPUT1, the source file which has this subroutine is edited and recompiled.

Subroutine INPUT2 reads the VOS file INTK to get the following values: the maximum time t_{max} = TIMMX; the time increments Δt_ℓ = DTIML, Δt_g = DTIMG, and Δt_{pr} = DTIMPR; the parameters $T_{dfto\ell}$ = TDFTOL, x_{tol} = XTOL, f_{tol} = FTOL, and n_{tol} = NTOL which determine the accuracy of the iterative calculation in Subroutine EVNEWT; the number n = N of computational cells in the stationary grid $z_o, z_1, \ldots, z_n$; and the vent parameters V_{opt} = VOPT = VENTOPT = ("Y" for vented option, "N" for unvented option), P_{vnt} = PVNT, and ΔP_{vnt} = DPVNT. It then outputs all these input values to the VOS file OUTTK.

Subroutine INPUT3 interactively obtains either a fire diameter, DIAMF, which it converts to heat flux by a table (when provided), or the heat flux, $\dot{q}''_f$ = QF, directly. It then outputs these input values to the terminal and also to the VOS file OUTTK.

Subroutine INITVAL initializes the temperature variables T_{wb}, $T_{ws,k}$, $T_{c,k}$, T_{wg}, T_g and T_{ct}. It also intializes the two time variables t_ℓ and t_g. It calls INITM to calculate initial values for some gas variables. It calculates the stationary vertical grid points $z_o, z_1, \ldots, z_n$ for the liquid part of the system.

Subroutine INITM calculates the initial values for the vapor pressure P_v, for the mass M_v of vapor in the ullage volume, and for the mass M_a of air in the ullage volume.

Subroutine GKUTTA updates the gas variables T_{wg}, T_g, M_v and M_a over a time increment Δt_g by using a fourth-order Runge Kutta method for solving the system of simultaneous ordinary differential equations for the gas variables. It obtains the first derivative with respect to time of the gas variables by calling subroutine DVG.

Subroutine DVG calculates $\dot{M}_i$, $\dot{M}_o$, and the first derivative with respect to time of the gas variables T_{wg}, T_g, M_v and M_a. It calls subroutine WG to evaluate other variables appearing in the differential equations of the gas variables. The other variables are functionally dependent on the gas variables and on T_{ct}.

Subroutine WG calculates the variables which are functionally dependent on the gas variables T_{wg}, T_g, M_v, M_a and also on T_{ct}. First, it calculates $\dot{q}''_{rro}$, $\dot{q}''_{cg}$, P_a, P_v, P, and T_b. It calls subroutine SURFTEMP to obtain the interface surface temperature T_i. It then calculates $\dot{q}''_{rri}$, $\dot{q}''_{r\ell}$, and L_{eff}. It calls subroutine EVAP to obtain the value of the evaporation rate $\dot{m}''$. Then it calculates $\dot{q}''_{c\ell}$.

Subroutine EVAP calculates the value of the evaporation rate $\dot{m}''$. It calls subroutine EVNEWT to solve the transcendental equation for $\dot{m}''$.

Subroutine EVNEWT numerically solves the transcendental equation for the evaporation rate $\dot{m}''$ using a combination of Newton's method and the bisection method.

Subroutine SURFTEMP gives an estimate of the value of the surface temperature T_i.

Subroutine BUOY calculates the boundary layer mass flux $\psi_{t,k}(t_\ell) = \psi_t(t_\ell, z_k)$ for $k = 0,1,\ldots,n$ at the stationary grid heights z_0, $z_1,\ldots,z_n$ by using the analytical solution of the discretized buoyancy equation in which the side wall temperature $T_{ws}(t, z)$ and the liquid core temperature $T_c(t, z)$ are expressed as staircase functions in the stationary grid. It then assigns the value for the boundary layer mass flux at the top $\psi_{t\ top}(t_\ell) = \psi_{t,n}(t_\ell)$. It calculates the value for the boundary layer heat flux at the top,

$$q_{bnd\ top}(t_\ell) = q_{bnd}(t_\ell, H_\ell).$$

Subroutine CORE calculates the grid heights z'_0, z'_1 ...,z'_n at time $t_\ell + \Delta t_\ell$ of the moving grid which initially coincides with the stationary grid at time t_ℓ and moves with the liquid core during the time step Δt_ℓ. It then sets $z'_{n+1} = z_n$. The temperature $T_{c\ top}(t_\ell + \Delta t_\ell)$ at the liquid core top is calculated. The temperature $T_c(t_\ell + \Delta t_\ell, z)$ of the liquid core at the end of the time step Δt_ℓ is calculated as a staircase function in the moving grid, i.e.

$$T_c(t_\ell + \Delta t_\ell, z) = T'_{c,k}(t_\ell + \Delta t_\ell) \text{ for } z'_{k-1} < z < z'_k$$

for k = 1,2,...,n+1.

Subroutine LKUTTA updates the variables T_{wb} and $T_{ws,k}$ for k = 1,...,n by a time increment Δt_ℓ using a fourth-order Runge Kutta method to solve the system of ordinary differential equations for the variables. It obtains the first derivative with respect to time of these variables by calling subroutine DVL.

Subroutine DVL calculates the values of the first derivative with respect to time of the wetted wall temperatures T_{wb} and $T_{ws,k}$ for k = 1,2,...,n. It calls subroutine WL to evaluate other variables appearing in the differential equations for the wetted wall temperatures. The other variables are functionally dependent on the wetted wall temperatures and also on the core temperature $T_{c,k}$ for k = 1,2,...,n.

Subroutine WL calculates the variables $\dot{q}''_{rrob}$, $\dot{q}''_{c\ell b}$, $\dot{q}''_{rros,k}$, and $\dot{q}''_{c\ell s,k}$, which are functionally dependent on the wetted wall temperatures T_{wb}, $T_{ws,k}$ and the core temperature $T_{c,k}$ for k = 1,2,...,n.

Subroutine REZCORE takes the following staircase representation of the core temperature in a moving grid

$$T_c(t_\ell + \Delta t_\ell, z) = T'_{c,k}(t_\ell + \Delta t_\ell) \qquad \text{for } z'_{k-1} < z < z'_k$$

and converts it into the following staircase function in the stationary grid

$$T_c(t_\ell + \Delta t_\ell, z) = T_{c,k}(t_\ell + \Delta t_\ell) \qquad \text{for } z_{k-1} < z < z_k.$$

SECTION V
NUMERICAL RESULTS

The physical processes occurring inside a fire-exposed tank containing liquid flammables were identified and analyzed, and the corresponding governing thermohydrodynamic equations describing the physical phenomena were derived in Section III. Numerical solutions of the governing equations and modeling of the tank response prediction to an external thermal load were presented in Section IV. This section describes a special numerical scheme that was developed to calculate the response of the individual components comprising the fire tank system. An integrated response methodology was developed based on the response of wetted and unwetted wall temperatures, gas and liquid phases, convective turbulent boundary layer, interface mass evaporation, and the overall tank pressure rise.

Calculations are made to predict the response of a vented and an unvented 55-gallon (206-liter), 18-gage steel drum to a uniform external heating of 7 w/cm^2. For the vented cases, the vent diameter is 7.6 mm and the vent opening pressure is 41 kPa gage. The vent coefficient of discharge used in the calculations is 1.0 for the Freon™ tanks and 0.25 for the water tanks. The drums are filled up to 95 percent filling capacity either with water or Freon-113™. In the calculations, it is assumed that the drums are completely engulfed and the total incident heat consists of radiation as well as convection.

The response predictions of the wetted side wall and bottom wall temperatures for vented and unvented configurations are shown in Figures 9 and 10 and 11 and 12, respectively. The calculation shows that the temperature of the wetted walls strongly depends on the liquid in contact and is not at all affected by whether the tank is vented or unvented. It is also noted that the bottom wall invariably shows higher temperature than the side walls. Unlike the wetted walls, as might be expected, the temperature of the dry walls in the ullage volume is higher than the wetted wall temperature and remains the same for both liquids (Figures 13 and 14).

The predicted mass and heat fluxes for water and Freon-113™ in the boundary layer for vented and unvented tank configurations are shown in

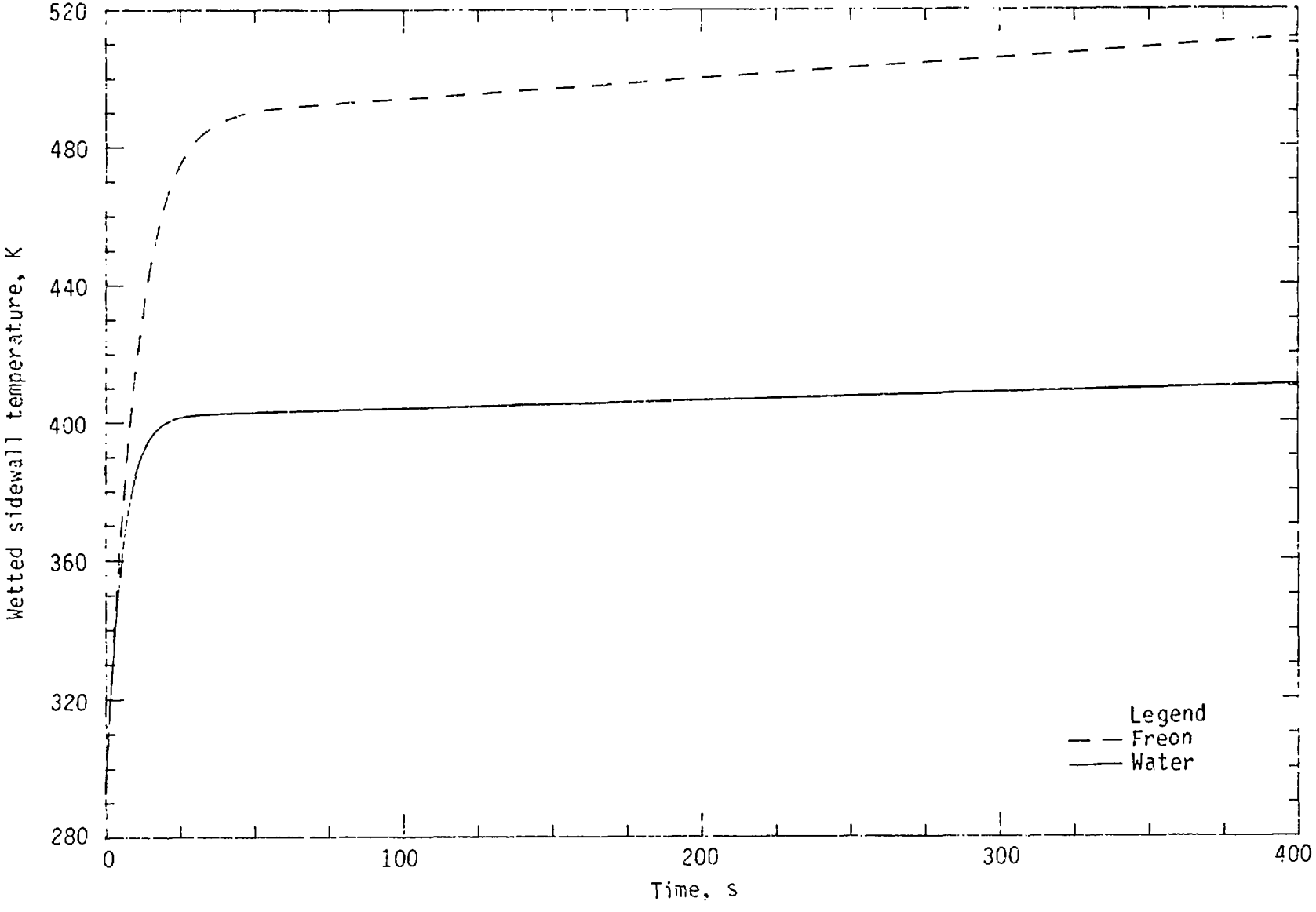

Figure 9. Wetted Sidewall Temperature Time Profile for Closed Vent Tank Configuration

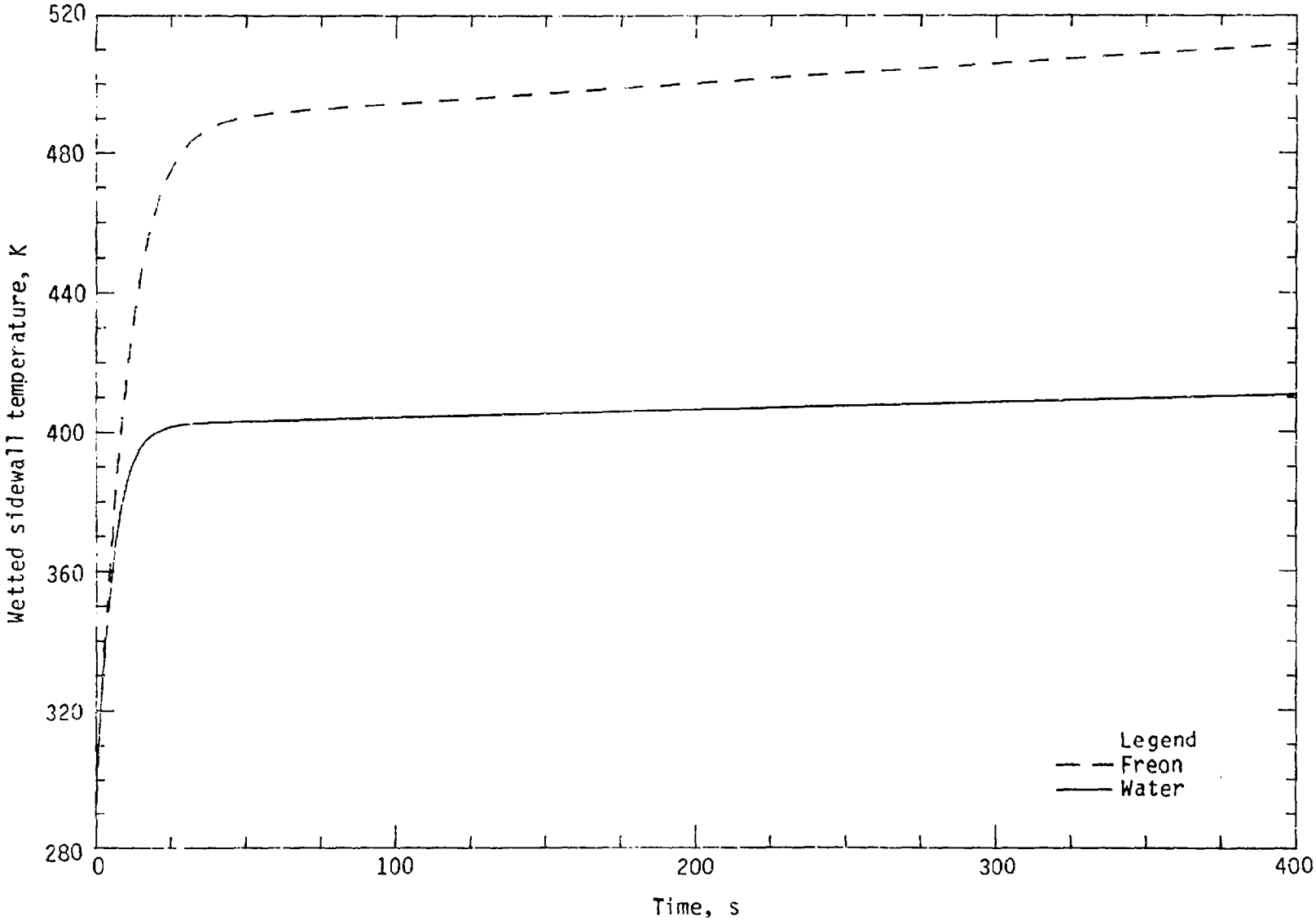

Figure 10. Wetted Sidewall Temperature Time Profile for Vented Tank Configuration

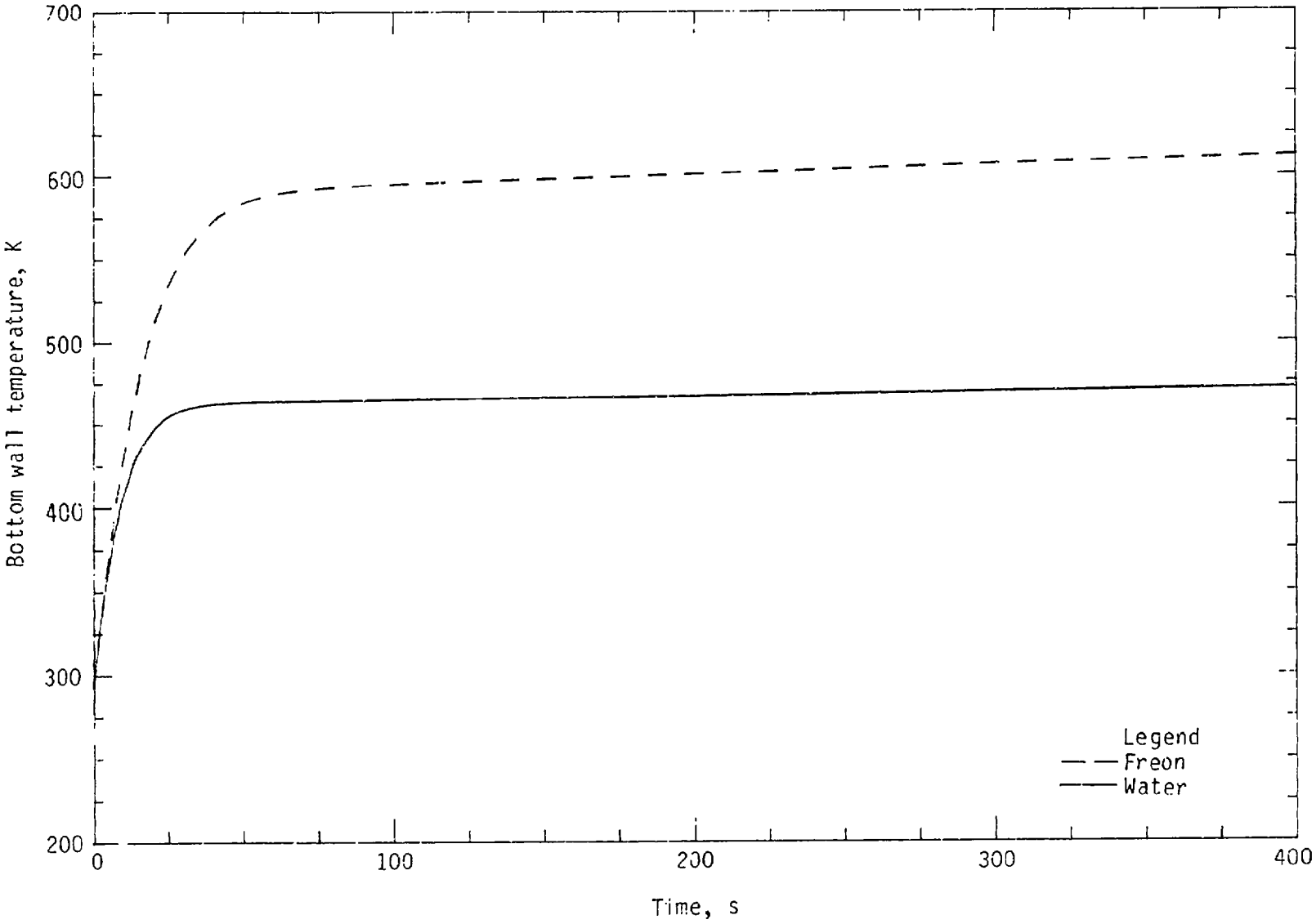

Figure 11. Bottom Wall Temperature Time Profile for Closed Tank Configuration

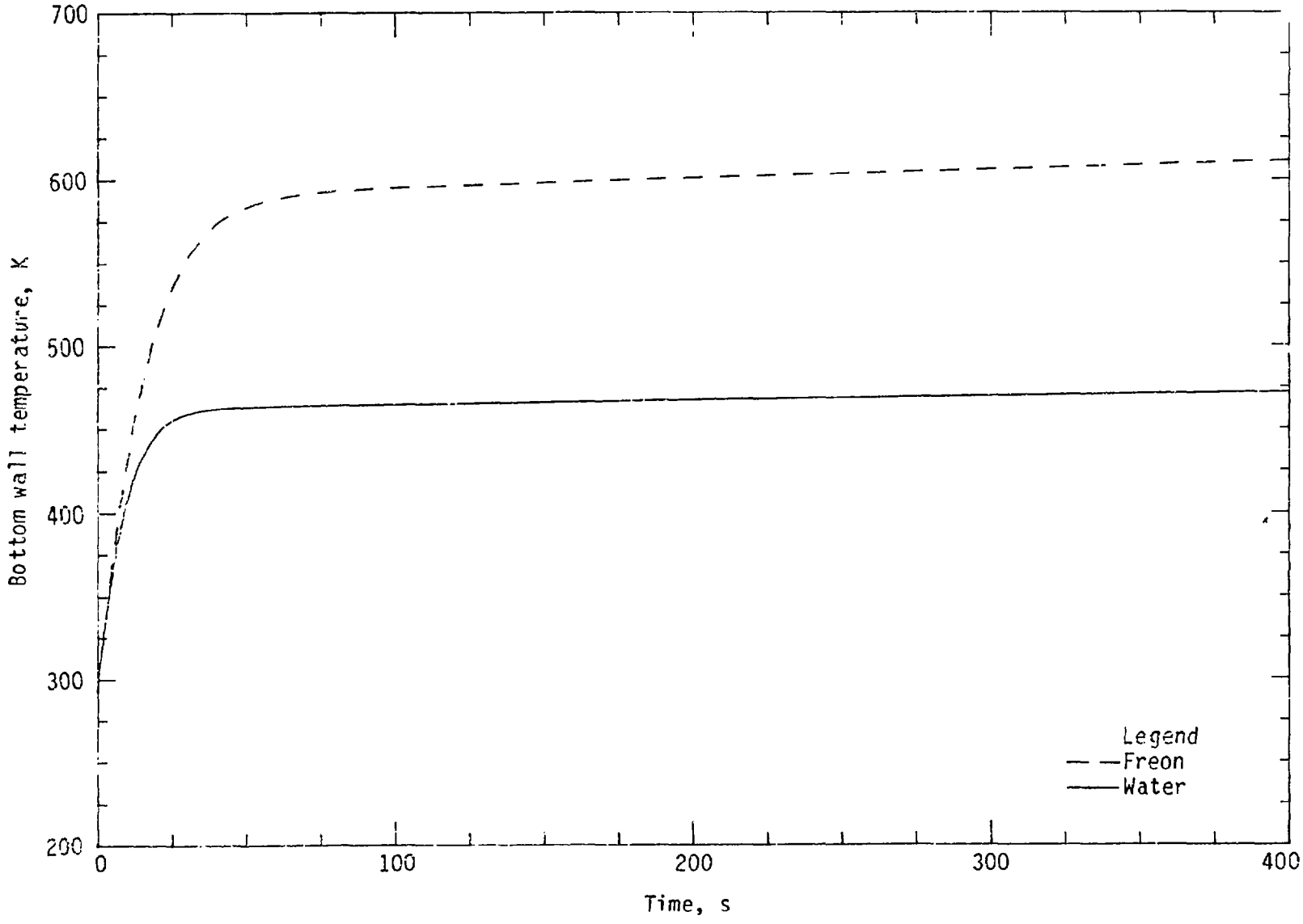

Figure 12. Bottom Wall Temperature Time Profile for Vented Tank Configuration

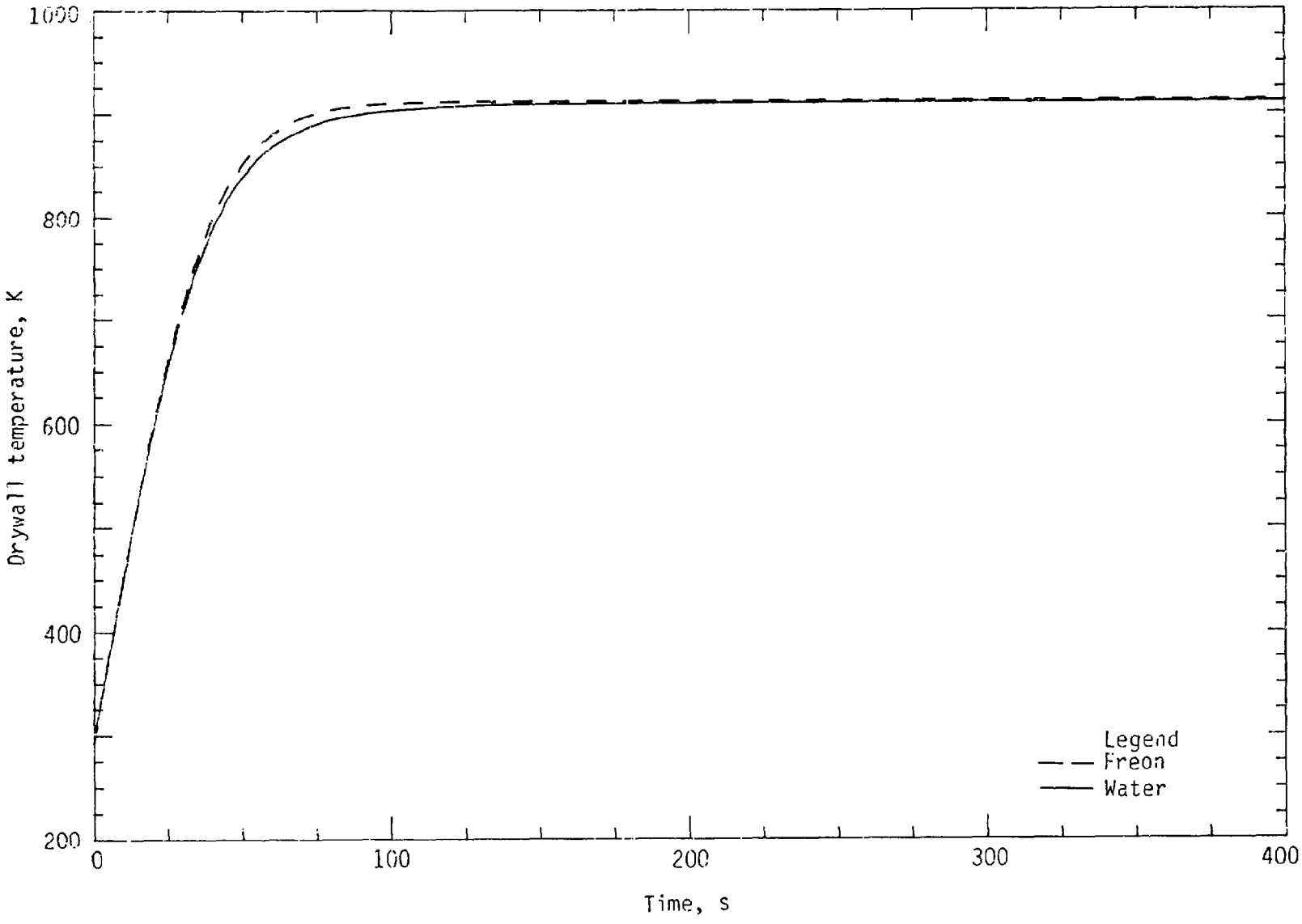

Figure 13. Dry Wall Temperature Time Profile for Closed Vent Configuration

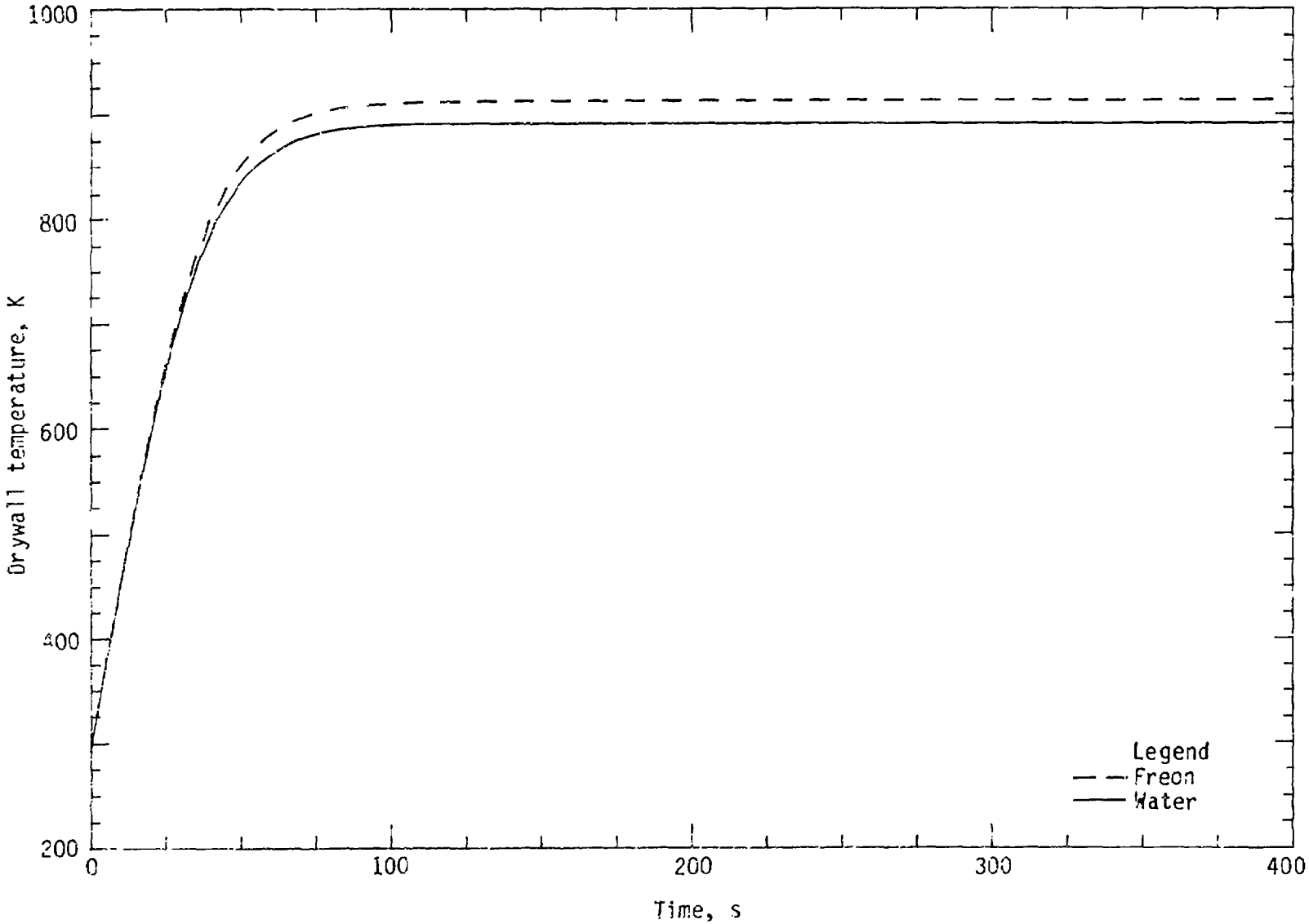

Figure 14. Dry Wall Temperature Time Profile for Vented Configuration

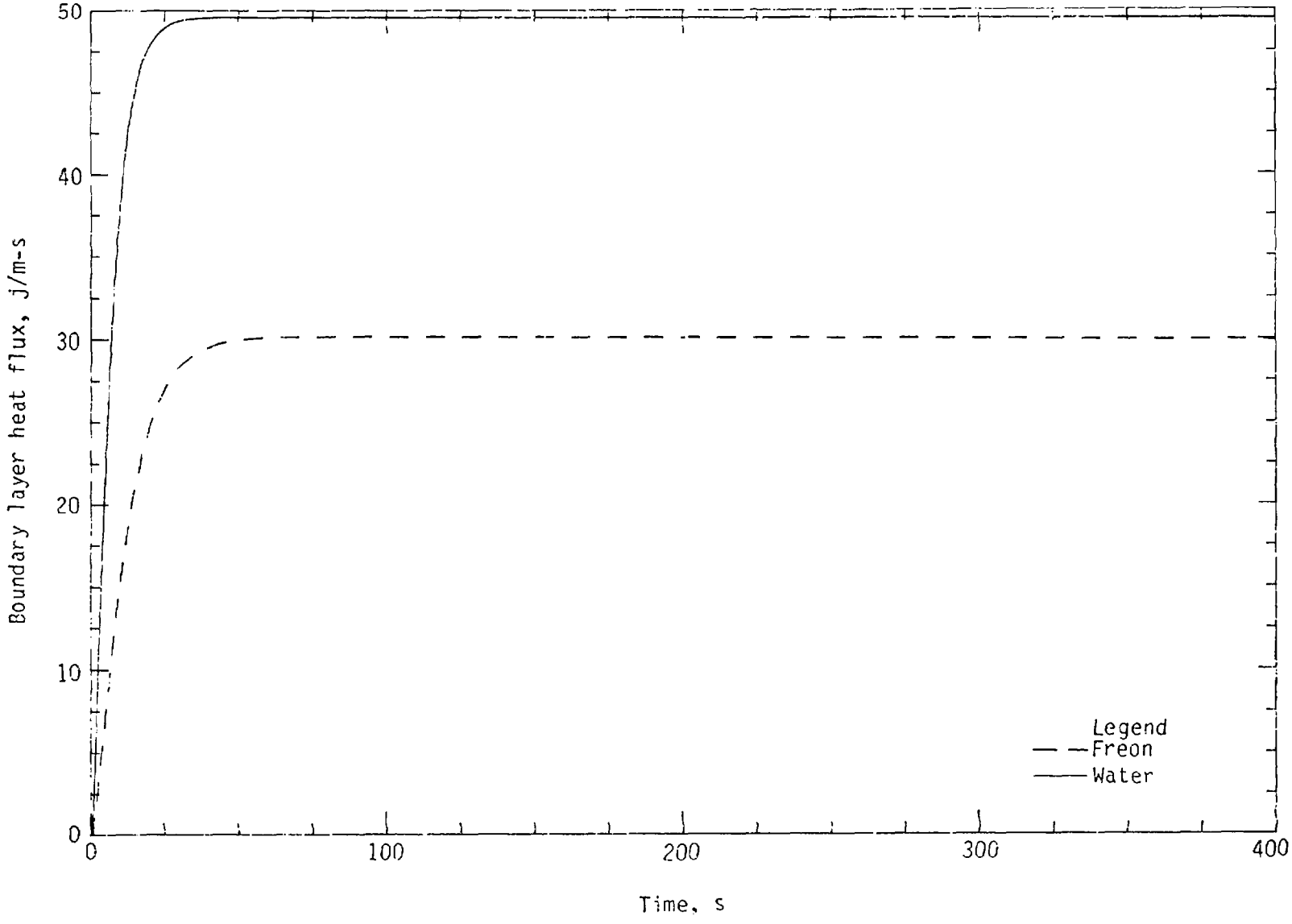

Figure 15. Boundary Layer Heat Flux Time Profile for Closed Vent Configuration

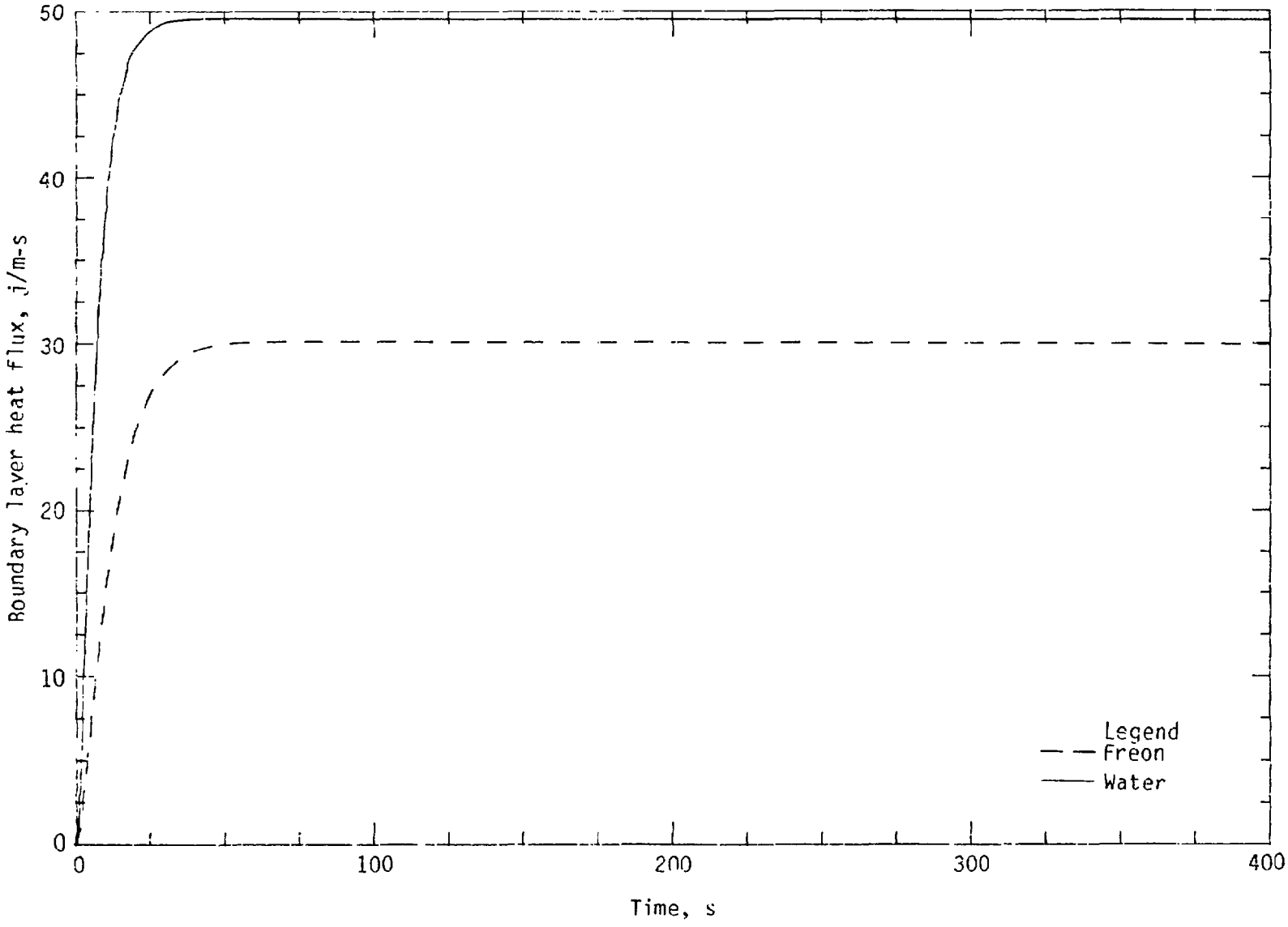

Figure 16. Boundary Layer Heat Flux Time Profile for Vented Configuration

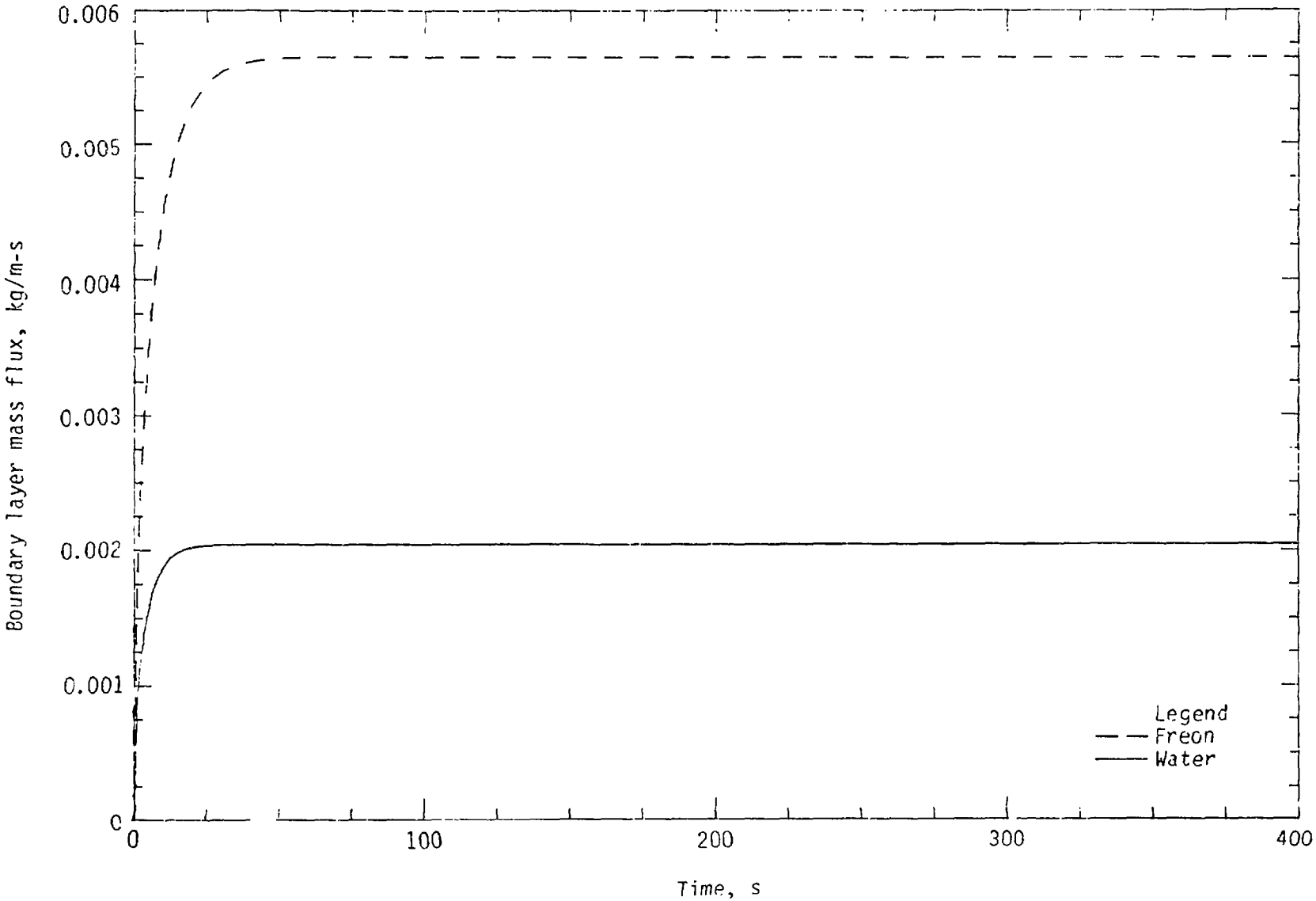

Figure 17. Boundary Layer Mass Flux Time Profile for Closed Vent Configuration

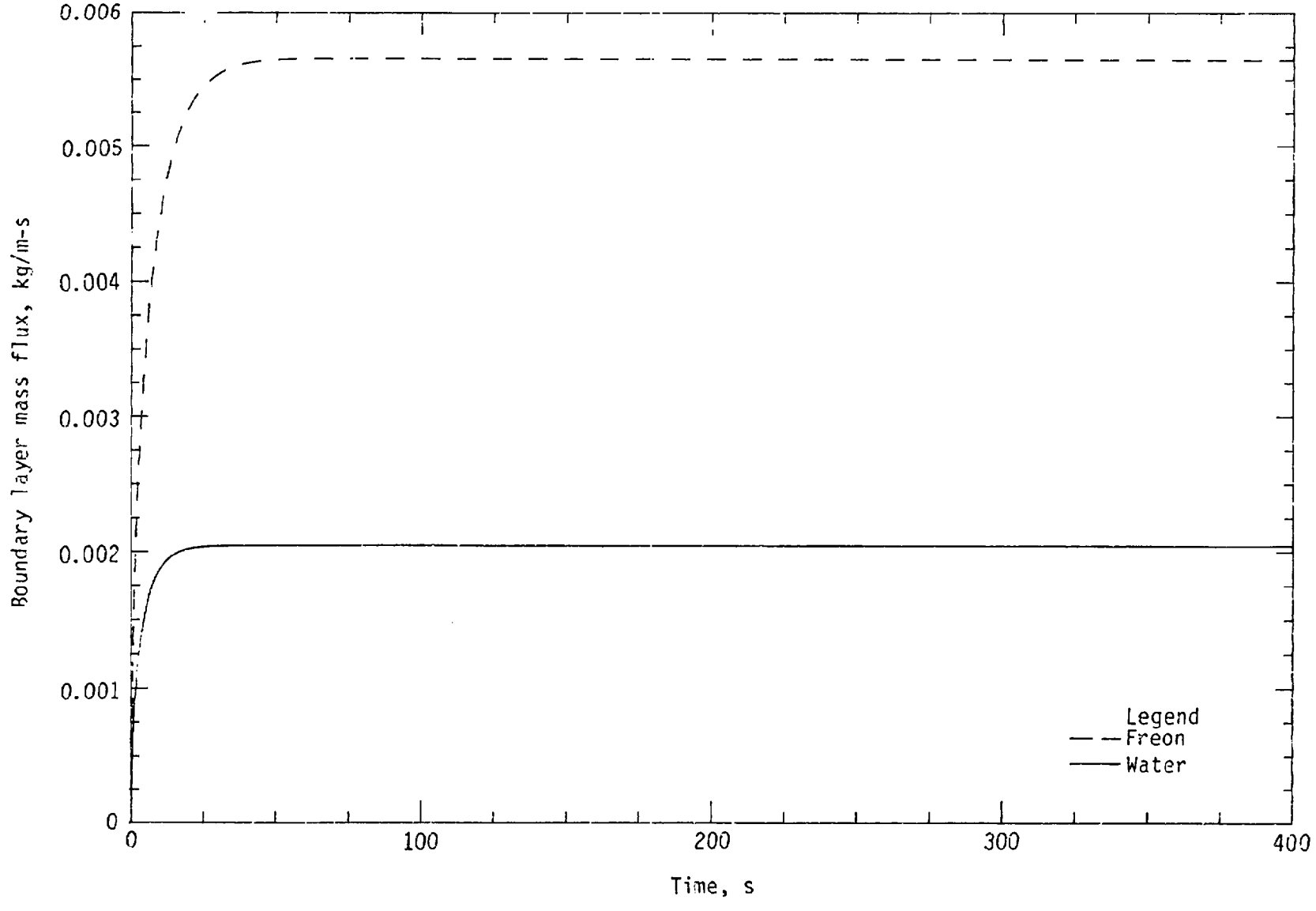

Figure 18. Boundary Layer Mass Flux Time Profile for Vented Configuration

Figures 15 and 16 and 17 and 18, respectively. Figures 15 and 17 show that the rate at which heat and mass are transported along the boundary layer is independent of the tank configuration and is controlled by the physical properties of the lading. It is noted that the Freon-113™ high rate of mass flux in comparison with water is evidence of this phenomenon.

The predicted pressure time profiles in the ullage volume are shown in Figures 19 and 20. As shown in Figure 19, in an unvented tank, the inside pressure rises quickly (in less than 1 minute) to a level that no ordinary container can withstand, and consequently the tank ruptures. However, the pressure rise inside a vented tank is more manageable. The pressure rises sharply until it reaches the vent operating pressure value at which venting takes place (Figure 20). The oscillation observed is caused by the opening and closing of the vent before it becomes stable. Beyond this point the pressure continues to rise, but at a slower rate because of the expulsion of the tank contents. With increasing time, the internal pressure rises steadily, causing the tank to rupture in less than 200 seconds. The dry wall temperature for both Freon™ and water was about 900 K for the closed vent tanks (Figure 13). For the vented tanks, the dry wall temperature was essentially the same as for the closed vent tanks for Freon-113™ and slightly less for water (Figure 14). The wetted sidewall temperatures were essentially the same for both the closed vent and vented tanks; that is, about 400 K for water and 500 K for Freon™ (Figures 9 and 10). The model prediction of other physical parameters such as mass of vapor in the ullage volume, boiling temperature, and gas temperature are shown in Figures 21-26.

The predictions from the calculations shown in Figures 9-25 are off as a result of inadvertent omission of a constant. The liquid density factor (RHOZ) was omitted from the expression for the constant CZ in both the water and Freon™ versions of subroutine INPUT1. This resulted in very small predicted boundary layer mass and heat fluxes. The code was corrected and was also improved to include the effect of venting on the rate of change of the gas temperature. The corrected code predicted a boundary layer mass flux that appears to be much too large. Because of project resource limitations, this was not investigated further.

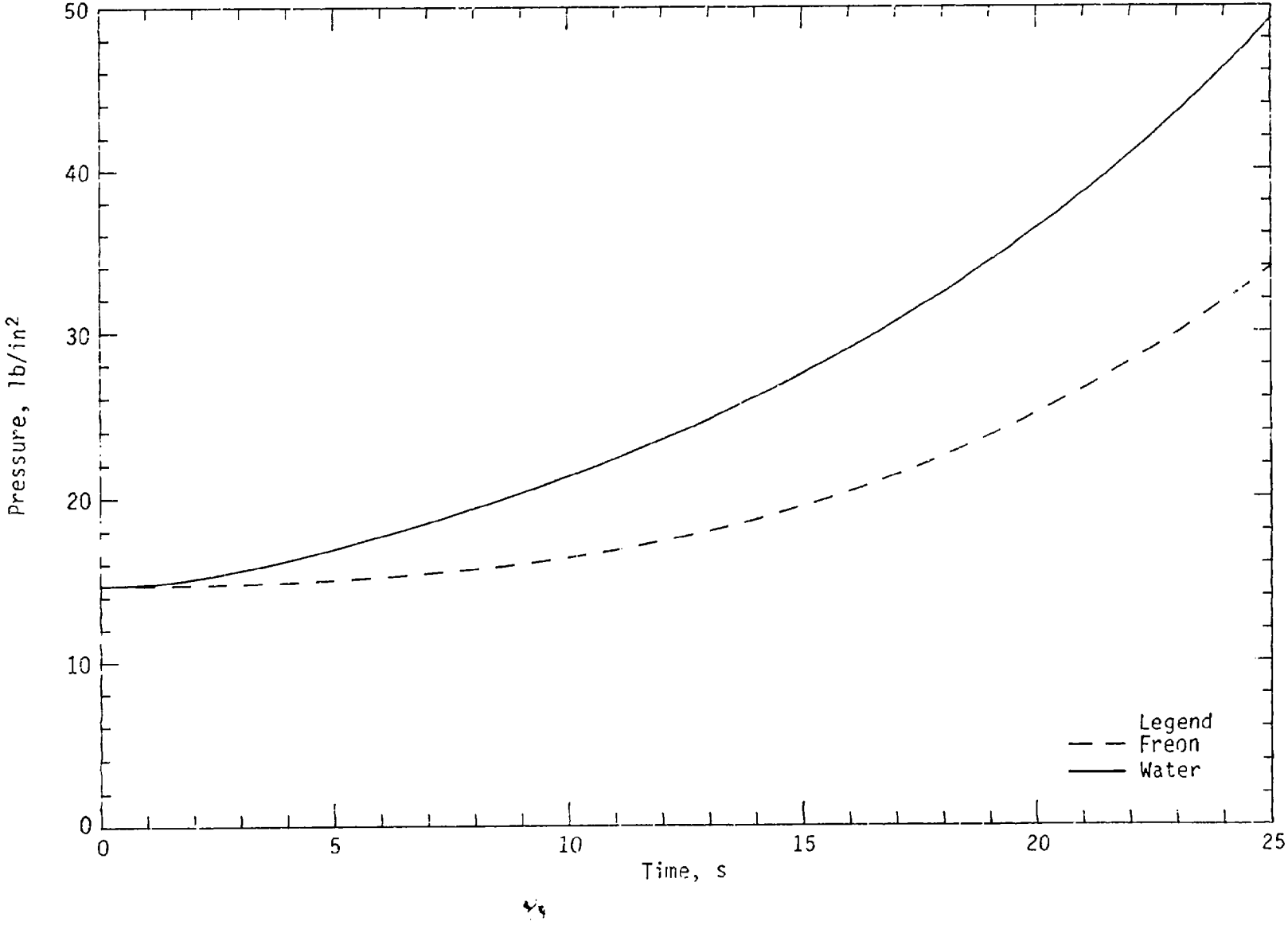

Figure 19. Pressure Time Profile for Closed Vent Configuration

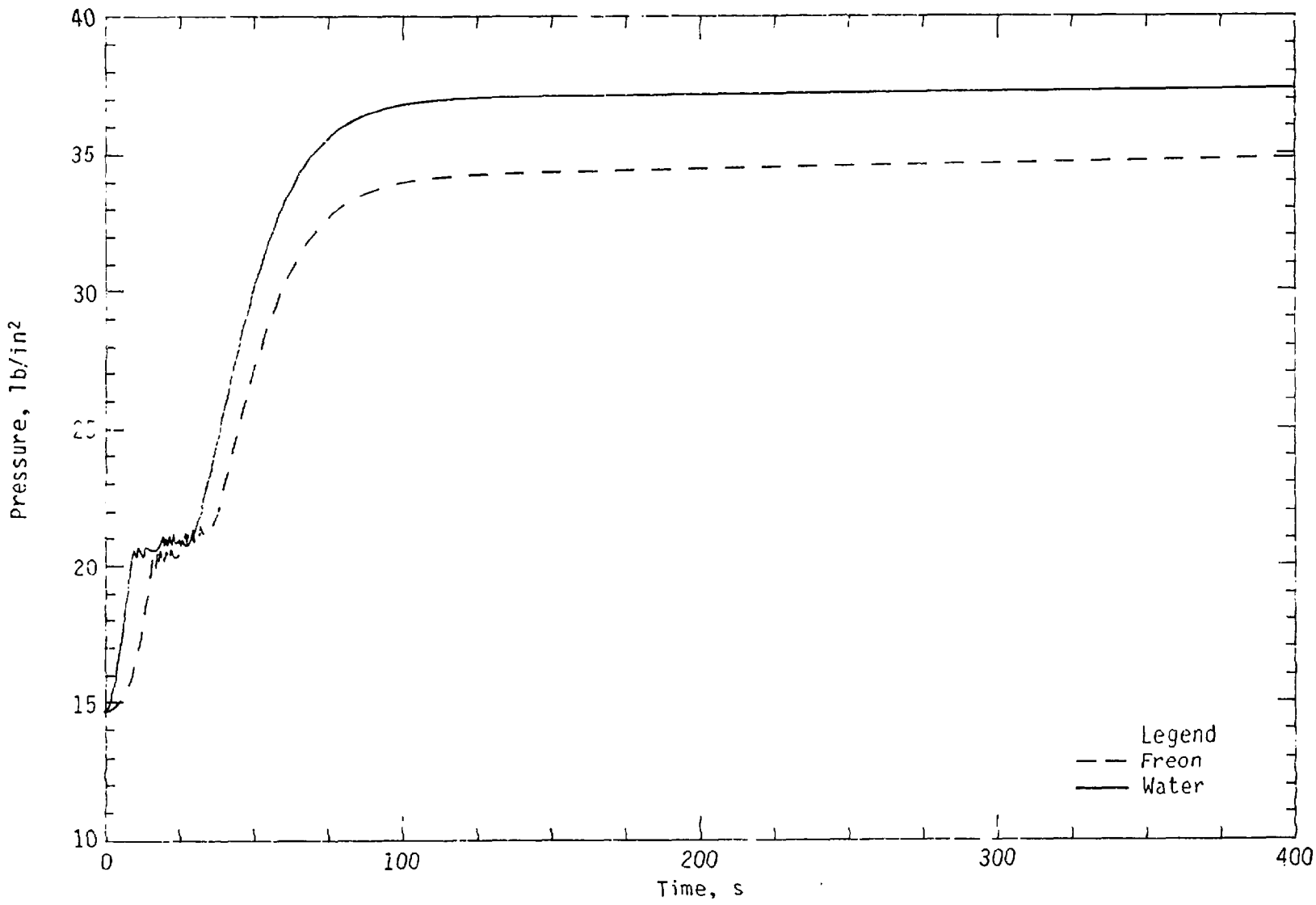

Figure 20. Pressure Time Profile for Vented Configuration

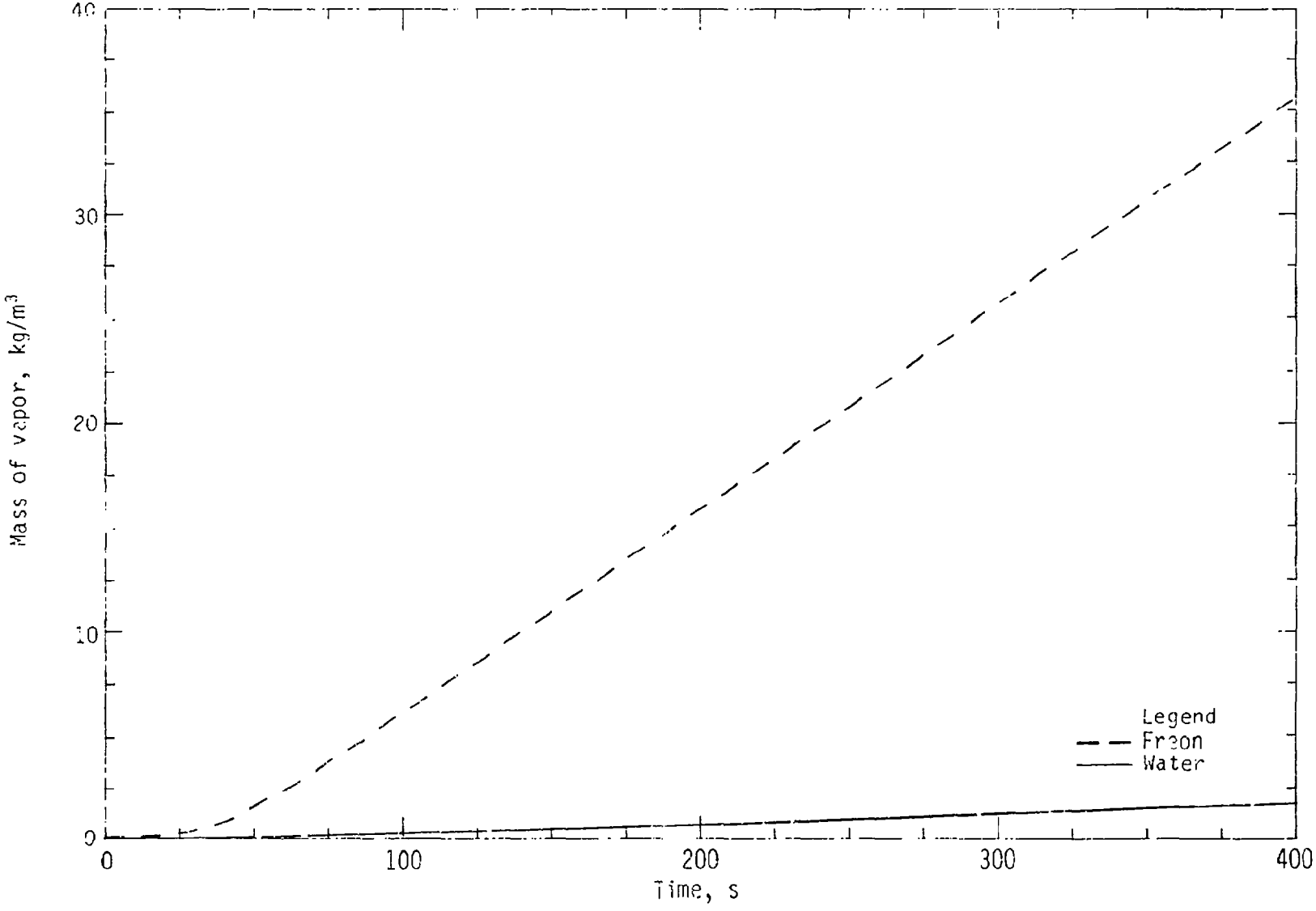

Figure 21. Mass of Vapor in Ullage Volume Time Profile for Closed Vent Configuration

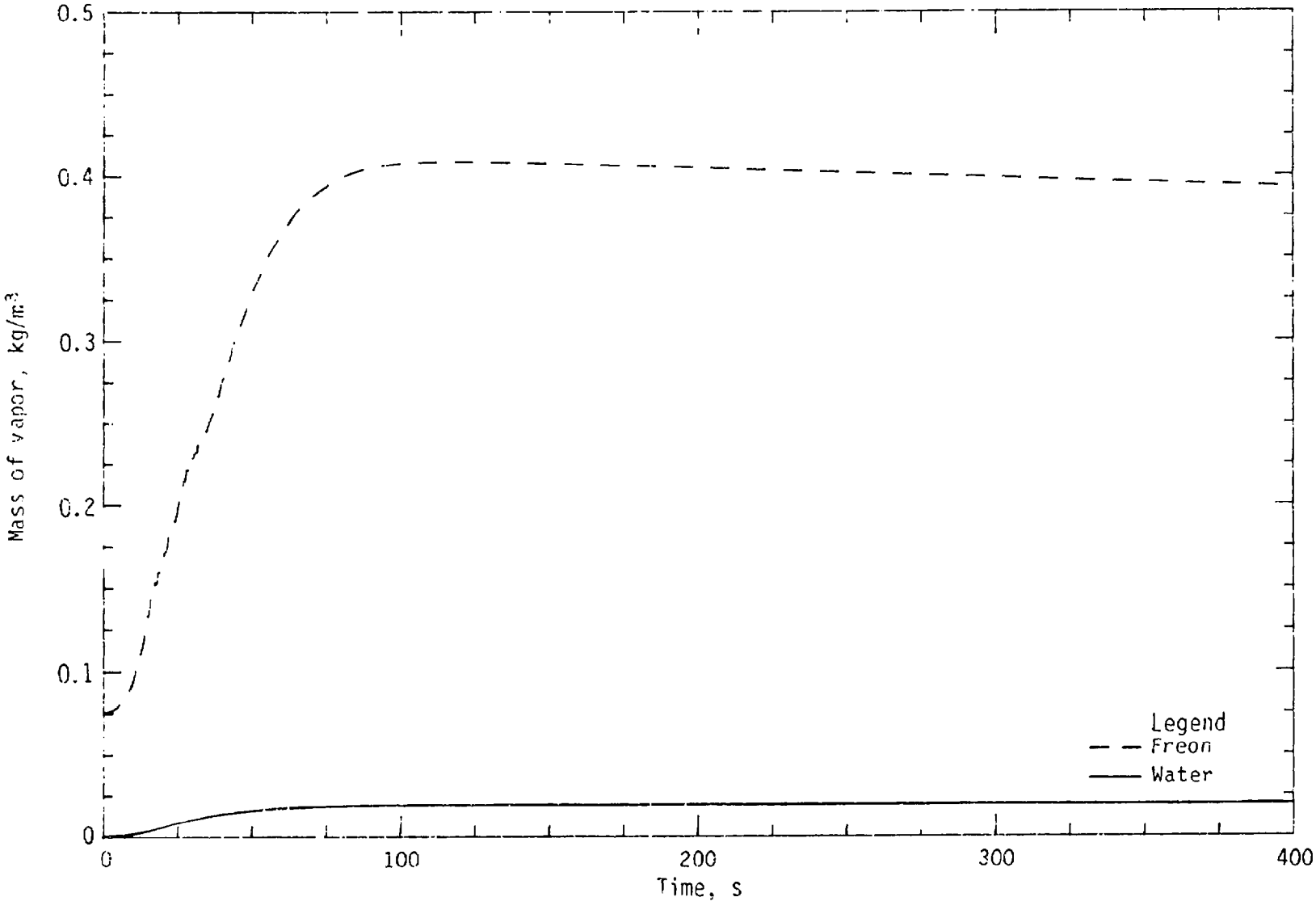

Figure 22. Mass of Vapor in Ullage Volume Time Profile for Vented Configuration

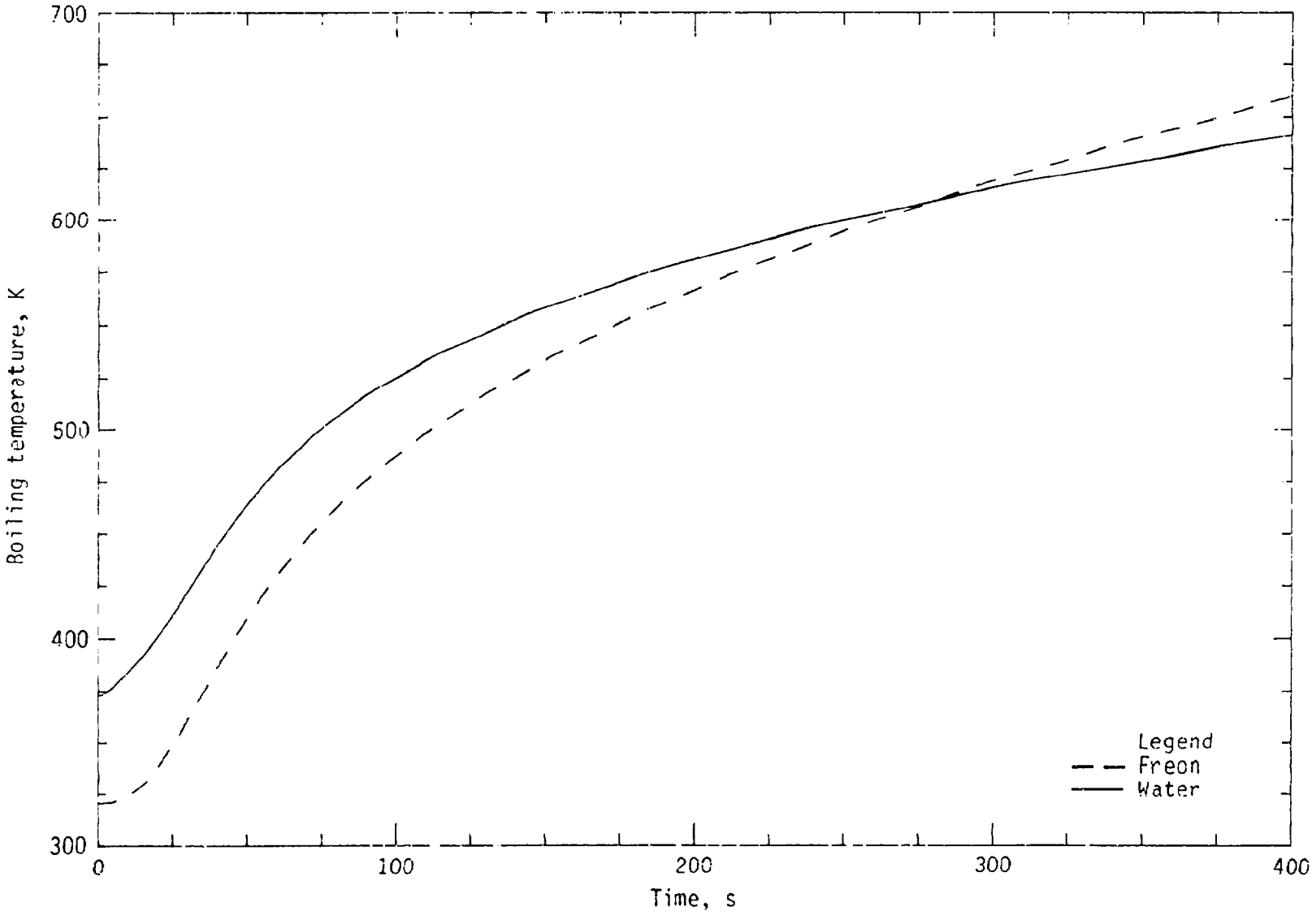

Figure 23. Boiling Temperature Time Profile for Closed Vent Configuration

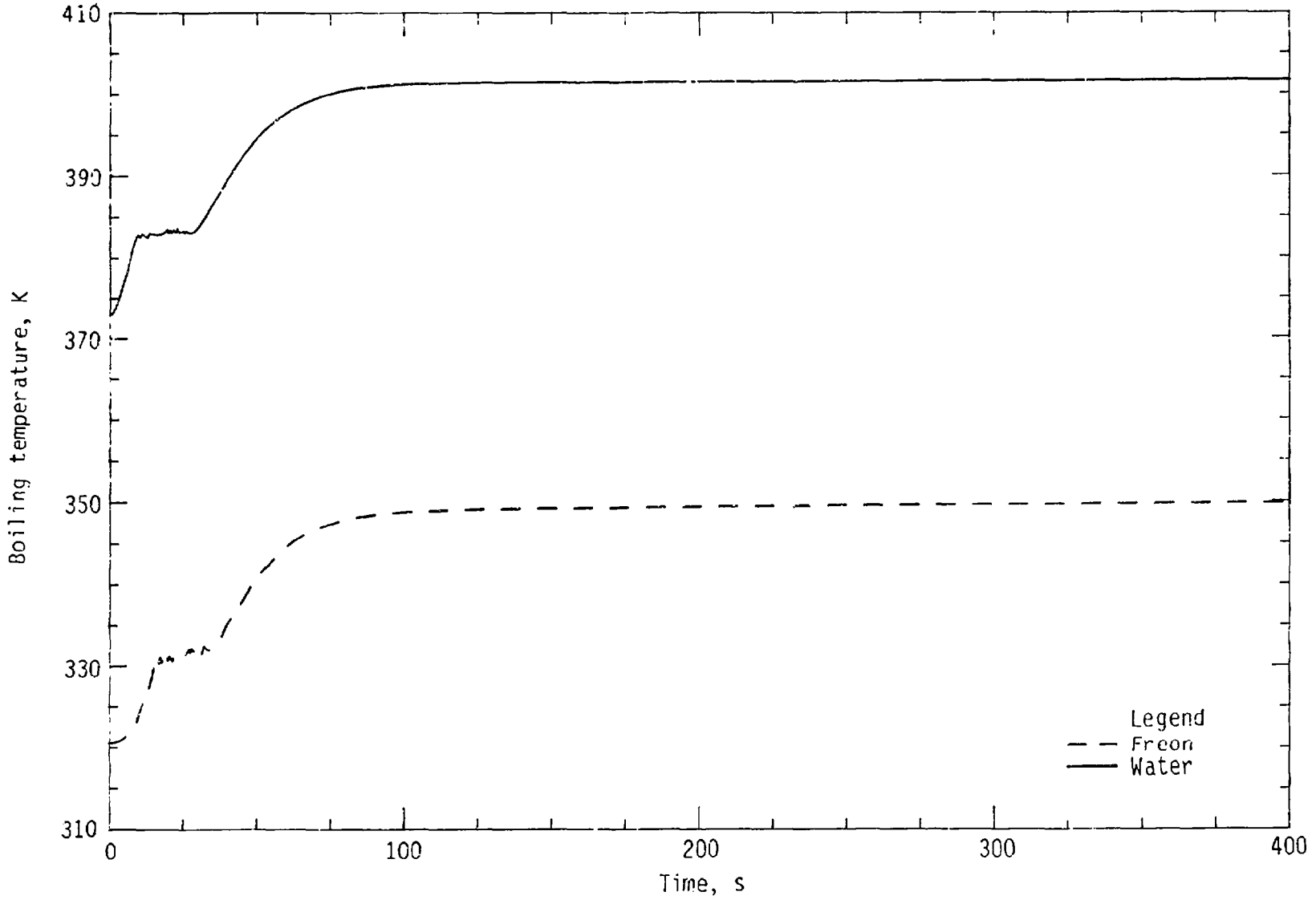

Figure 24. Boiling Temperature Time Profile for Vented Configuration

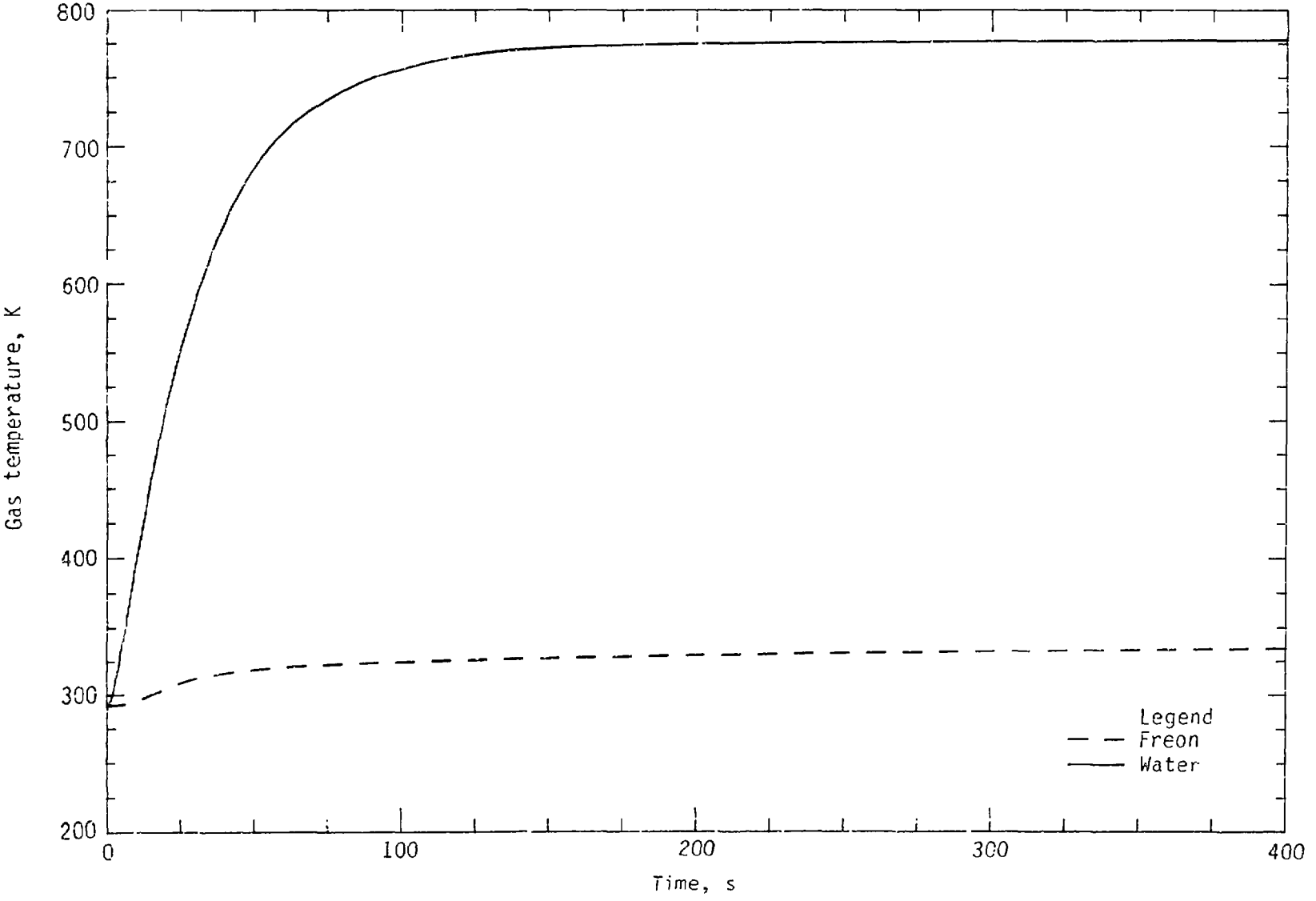

Figure 25. Gas Temperature Time Profile for Closed Vent Configuration

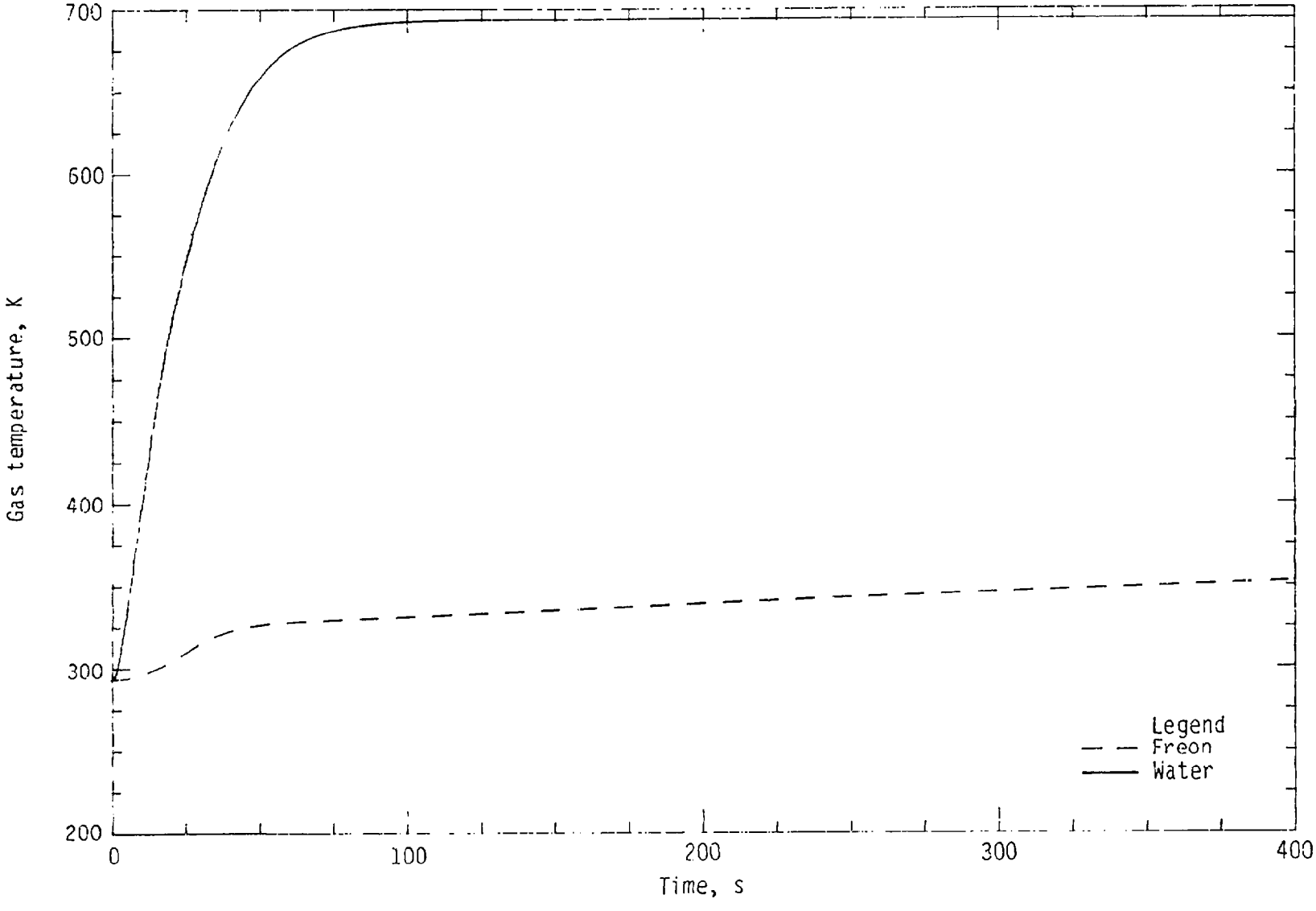

Figure 26. Gas Temperature Time Profile for Vented Configuration

SECTION VI
CONCLUSIONS

The governing equations describing the interactive processes occurring between the fire and the tank have been solved numerically, and a model predicting the thermofluid processes leading to occurrence of BLEVE has been developed. The calculations were made for vented and unvented tanks containing either water or Freon-113". The prediction demonstrated internal consistency amongst the parameters indicative of the model performance. Based on analysis of the calculated prediction, the following general observations are made:

1. The pressure rise in the ullage volume and occurrence of BLEVE strongly depend on the tank's initial filling density.

2. The physical properties of lading, especially the heat of vaporization, significantly contribute to the internal pressure rise.

3. The liquid/gas interface is the most thermally active region, and a decreasing temperature gradient exists in the downward direction.

4. Only the liquid boiling temperature is affected by configuration (vented or unvented) of the tank; all other temperatures remain unaffected, regardles of the tank configuration.

Specifically, to delineate several fundamental issues concerning this development, the following prediction case is considered. The calculated response for a vented 55-gallon, 18-gage steel drum, engulfed in an intense fire ($7.0 - \frac{W}{cm^2}$) and filled to 95 percent of its capacity with water showed that

1. The tank failure pressure is reached at about 200 seconds. The calculated pressure for a closed tank approached values much higher than for the vented tank for the same time.

2. The dry wall and wetted wall temperatures are changed very little by tank venting.

3. The internal pressure in a vented tank rises much more slowly than the pressure in a closed tank.

Similar calculations were made using Freon-113™ in place of water while maintaining the other variables. As was expected, the calculated response predictions for Freon-113™ were quite different when compared with the case for water.

The corrected code predicts a significantly higher boundary layer mass flux. Causes of this problem might be the simplifying assumptions made and the empirical fits used in the derivation of the model equations, or the numerical scheme used to solve the equations. Project resource limitations did not permit determination of the cause and the resulting effects on the predictions.

The failure response of the tank, and ultimately, the occurence of BLEVE also depend on the size, and the mechanical, thermal and physical integrity of the tank. Those, together with the variations in heat fluxes from various fire sizes, as well as differences in the heat input caused by the relative location of the tank with respect to the fire, indicate that every response prediction calculation requires a myriad of different inputs. This becomes a laborious and time-consuming operation, not consistent with the purpose for which the model was developed. The mission of this development is to quickly provide to the firefighters the essential predictions and the risk assessment data necessary for safe operations and successful extinguishment of a fire.

To achieve this goal without compromising accuracy of prediction, it is recommended, once the model is refined and verified, that prediction calculations be made for most probable ranges of fire tank situations and that a BLEVE prediction data base be created. The results from this data base could then be plotted into a series of reference charts, or stored in a computer and selected and displayed on the screen.

REFERENCES

1. Birk, A. M., and Oosthuizen, P. H., "Model for the Prediction of Radiant Heat Transfer to a Horizontal Cylinder Engulfed in Flames," ASME Paper No. 82 WA/HT-52, The American Society of Mechanical Engineers, National Heat Transfer Conference, 1982, New York, New York, 1983.

2. Collier, J. G., Convective Boiling and Condensation, McGraw-Hill, London, 1972.

3. Reid, R. C., "Possible Mechanisms for Pressurized Liquid Tank Explosions or BLEVEs," Science, Vol. 203, p. 1263, 1979.

4. Roberts, A. F., Cutler, D. P., and Billinge, K., "Fire-Engulfed Trails with LPG Tanks with a Range of Fire Protection Methods," Proceedings of the 4th International Symposium of Loss Prevention and Safety Promotion in the Process Industries, Vol. 3, Chemical Process Hazards, 1983.

5. Venart, J. E. S., Sousa, A. C. M., Steward, F. R., and Prasad, R. C., The Physical Behavior of Pressure Liquified Fuel Tanks Under Accident Conditions, Fire Science Center, University of New Brunswick, Fredericton, New Brunswick, Canada.

6. Hashemi, H. T., and Wesson, W. D., "Evaporation Rate of LNG," Hydrocarbon Processing, Vol. 50, No. 8, p. 117, 1971.

7. Garackat, H. Z., and Clark, J. A., "Laminar Natural Convection in a Cylindrical Tank," Proceedings of the Third International Heat Transfer Conference, Chicago, Illinois, 1966, p. 150.

8. Evans, L. B., and Reid, R. C., "Transient Natural Convection in a Vertical Cylinder," American Institute of Chemical Engineering (AICHE) Journal, Vol. 14, No. 2.

9. Aydemire, N. U., Sousa, A. C. M., and Venart, J. E. S., "Transient Thermal Stratification in Heated Partially Filled Horizontal Cylindrical Tanks," ASME Paper No. 84-HT-60, National Heat Transfer Conference, 1984, The American Society of Mechanical Engineers, New York, New York.

10. Virk, P. S., and Venkataramana, M., "Modeling of LNG Tank Dynamics," Department of Chemical Engineering, Massachusetts Institute of Technology, Cambridge, Massachusetts.

11. Birk, A. M., and Oosthuizen, P. H., A Thermodynamic Model of a Rail Tank-Car Engulfed in Fire, Canadian Institute of Guided Ground Transport, Queens University, Kingston, Ontario, Canada.

12. Delichatsios, M. A., "Exposure of Steel Drums to an External Spill Fire: Practical Tests of Requirements for the Storage of Drums Containing Flammable Liquids," Plant/Operation Progress, Vol. 1, pp. 37-45, 1982.

13. Rohsenow, W. M., and Choi, H., Heat, Mass, and Momentum Transfer, International Series in Engineering, Prentice-Hall, Englewood Cliffs, New Jersey, 1961.

14. Kanenetski, F., Diffusion and Heat Transfer in Chemical Kinetics, Plenum Press, New York, 1964, p. 184.

15. Baines, W. D., and Turner, J. S., "Turbulent Buoyant Convection from a Source in a Confined Region," Journal of Fluid Mechanics, Vol. 37, Part 1, pp. 51-80, 1969.

16. Schlichting, H., Boundary Layer Theory, 6th Edition, McGraw-Hill Series in Mechanical Engineering, New York, 1968.

17. Delichatsios, M. A., "Turbulent Convective Flows and Burning on Vertical Walls," Nineteenth International Symposium on Combustion, The Combustion Institute, 1982.

18. William, K. G., and Capp, S. P., "A Theory of Natural Convection Turbulent Boundary Layers Next to Heated Vertical Surfaces," Int. J. Heat and Mass Transfer, Vol. 22, p. 813, 1979.

19. Kutateladze, S., "The Model of Turbulent Free Convection Near a Vertical Heat Transfer Surface," Heat Transfer and Turbulent Buoyancy Convection (Spalding and Afgan, eds.), Vol. II, p. 487, Hemisphere Publishing, Washington, D.C., 1977.

20. Morto, B. R., Modeling of Fire Plumes, Tenth International Symposium on Combustion, The Combustion Institute, Pittsburgh, Pennsylvania, 1965, pp. 973-982.

21. Batchelor, G. K., Introduction to Fluid Mechanics, Cambridge University Press, 1970.

22. Hinze, J. O., The Theory and Mechanism of Turbulence, McGraw-Hill, New York, 1959.

23. Bary, K. N., and Libby, P. A., "Interaction Effects in Turbulent Premixed Flame," The Physics of Fluids, Vol. 19, 1976.

24. Kaplan, W., Advanced Differential Calculus, Vol. 19, p. 1687, Addison-Wesley Publishing Company, Inc., Reading, Massachusetts, 1959.

25. Delichatsios, A., "A New Integral Model For Turbulent Natural Convection Flows Next To The Heated Walls," Fifth Symposium on Turbulent Shear Flows, Ithaca, N.Y., 1985.

26. Germeles, A. E., "Forced Plumes and Mixing Of Liquid In Tanks," Journal of Fluid Mechanics, pp. 11, 601, 1975.

27. Carnahan, B., Luther, H. A., and Wilkes, J. O., Applied Numerical Methods, Wiley, New York, 1969.

28. Delichatsios, M. A., "A New Integral Method For Turbulent Natural Convection Flows Next To The Heated Walls," Fifth Symposium on Turbulent Shear Flows, Ithaca, New York, 1985.

29. Conte, S. D., and de Boor, C., Elementary Numerical Analysis: An Algorithmic Approach, 2nd ed., McGraw-Hill, New York, 1972.

(The reverse of this page is blank.)

APPENDIX A

DERIVATION OF EQUATION OF MASS TRANSFER
STAGNATION FILM THEORY

Consider a thin stagnant layer of fluid with thickness δ, Figure A-1 (Reference 14, p. 185).

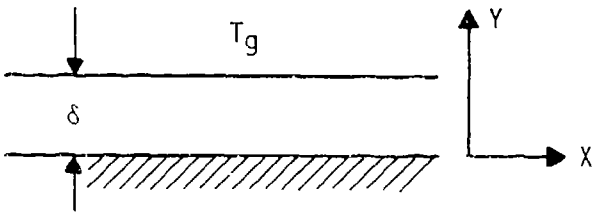

Figure A-1. Stagnant Film Layer

Assume that due to the high temperature gradient, mass is vaporizing at the free surface. Define the layer thickness so that

$$K/\delta = h_c \tag{A-1}$$

The conduction equation in this layer is

$$\rho C_p v \frac{\partial T}{\partial y} = K \frac{\partial^2 T}{\partial y^2} \tag{A-2}$$

If $\dot{m}''$ is the mass rate of vaporization per unit surface area, the conduction equation (A-2) can be modified using, $v = \dot{m}''/e$, to read

$$C_p \dot{m}'' \frac{\partial T}{\partial y} = K \frac{\partial^2 T}{\partial y^2} \tag{A-3}$$

The differential equation, Equation (A-3), is integrated. We have

$$T = C_1 \frac{k}{C_p \dot{m}''} \left[\exp\left(C_p \dot{m}'' y/k \right) - 1 \right] + C_2 \tag{A-4}$$

Applying the following boundary condition, one obtains

$$\text{at } y = o,\ T = T_i \quad ; \quad \text{at } y = \delta,\ T = T_g,$$

The solution then becomes

$$T_g - T_i = C_1 \frac{K}{C_p \dot{m}''} \text{Exp } (C_p \dot{m}'' \delta/k) - 1 \tag{A-5}$$

The energy balance at the surface gives

$$\dot{m}'' L_{eff} = \dot{q}''_{con} + \dot{q}''_{r,\ell} = k \left.\frac{\partial T}{\partial y}\right|_{y=o} + \dot{q}''_{r,\ell} \tag{A-6}$$

From equation (A-4)

$$K \left.\frac{\partial T}{\partial y}\right|_{y=o} = C_1 K$$

and hence from Equation (A-6) we have

$$C_1 K = \dot{m}'' L_{eff} - \dot{q}''_{r,\ell} \tag{A-7}$$

Substituting for C,K from Equation (A-7) into Equation (A-5) one obtains

$$C_p \left(T_g - T_i\right) = \left(L_{eff} - \frac{\dot{q}''_{r,\ell}}{\dot{m}''}\right) \left[\exp\left(C_p \dot{m}'' \delta/k\right) - 1\right] \tag{A-8}$$

Equation (A-8) describes the mass transfer rate which can be solved for $\dot{m}''$ to give Equation (22).

APPENDIX B

PROGRAM LISTING

```
*****************************************************************
****  [illegible] Code  (July [illegible], 1987)
****       The following program solves the partial differential
****  equations describing the thermohydrodynamic processes occurring
****  inside a tank resulting from fire impingement.  The program is
****  flexible enough to allow either heat flux or fire diameter to be
****  input.
****       This program is written in the FORTRAN 77 language.  The code
****  was developed on the VAX (VMS UNIX Environment) operating system
****  on a [illegible] 800 computer.  It consists of one main program and
****  seventeen subroutines.
*****************************************************************

      SUBROUTINE INPUT1
C          PRECM Version
      COMMON /PHYSCM/ G,G,PATM
      COMMON /GEOMCM/ HL,XLL,EL,AR,AB,V,VT
      COMMON /MATPRPCM/ XMOLA,XMOLV,RHOC,RHOZ,BETA,XLV,XL,T1,P1
      COMMON /HEATCPCM/ CP,CPL,CVP,CVV,CAV,CPG
      COMMON /HEATFLCM/ RCOW,EPSI,CZ,C2,CS,CG,CEV
      COMMON /INITCM/ TIMZ,TE,DF,TINF
      COMMON /VERTCM/ AVNT,COVNT,PVNT,DPVNT
      R = 8.30987
      G = 9.8
      PATM = 1.013E5
      HL = 0.71*1
      AL = 0.[illegible]
      XLL = 2.0*SQRT(3.14159*AL)
      HW = 0.4322
      EE = AL
      V = 0.0[illegible]
      VT = AL*HL
      XMOLA = 28.0
      XMOLV = 18.0
      XMOL[illegible] = 1.[illegible]
      CPL = [illegible]
      BETA = 0.[illegible]
      XL = 1.[illegible]
      XLV = XL
      T1 = 32[illegible].0
      P1 = 1.013[illegible]
      CPL = 0.[illegible]
      CP = CPL
      CVP = 1.0[illegible]
      CVV = 1.00[illegible]
      CAV = 7.[illegible]
      CPG = CVP
      XCON = 4.32E5
      EP = 0.9
      SI = 5.67E-8
      EPSI = EP*SI
      XNUC = 4.4E-7
      PR = 0.7
      CS = PR**2*CP*( XMUC*BETA*G/((5.3**4)*PR**2) )**(1.0/3.0)
      XKC = 7.63E-3
      BETAG = 3.1E-3
      XMUG = 1.42
      XMOALPH = 7.7
```

```
      CALPH = 0.711E5
      ALPHG = XKG/(RHOCALPH*CALPH)
      C1HT = C.06
      C1HI = C.0e
      CG = XKG*C1HT*( BETAG*G/(XNUG*ALPHG) )**(1.0/3.0)
      CEV = XKG*C1HI*( (BETAG*G/(XNUG*ALPHG))**(1.0/3.0) )/CPG
      XNUM = C.937*(5.3)**(4.C/3.C)
      CFAC1 = (XNUC**(1.C/12.C))/(XNUM*PR**(1.0/6.0))
      CFAC2 = 0.937*(XNUC**(1.0/4.0))*CP/(PR**(0.5))
      C2 = CFAC1*RHOZ
      C2 = CFAC2/(BETA*G)
      C1VS = C.11
      C1HB = C.06
      CS = CS*C1HB/C1VS
      TIMZ = C.0
      TZ = 293.0
      CF = 7.0E4
      TINF = 293.0
      AVNT = 4.5c1E-5
      CDVNT = 1.0
      PVNT = 1.4269E5
      DPVNT = 0.0
      RETURN
      END

      SUBROUTINE INPUT1
C          WATER Version
      COMMON /PHYSCM/ R,G,PATM
      COMMON /GEOMCM/ HL,XLL,AL,AW,AE,V,VT
      COMMON /MATPRPCM/ XMOLA,XMOLV,RHO,RHOZ,BETA,XLV,XL,T1,P1
      COMMON /HEATCPCM/ CP,CPL,CVP,CVV,CAV,CPG
      COMMON /HEATFLCM/ RCDW,EPSI,C2,C2,CB,CS,CG,CEV
      COMMON /INITCM/ TIMZ,TZ,CF,TINF
      COMMON /VENTCM/ AVNT,CDVNT,PVNT,DPVNT
      R = 8.3C9E3
      G = 9.8
      PATM = 1.0132E5
      HL = C.7191
      AL = 0.2534e
      XLL = 2.0*SQRT(3.14159*AL)
      AW = 0.4322
      AE = AL
      V = C.C25366
      VT = AL*HL
      XMOLA = 29.C
      XMOLV = 18.C
      RHOZ = 1.053
      RHO = RHOZ
      BETA = 1.2E-4
      XL = 2.253Ee
      XLV = XL
      T1 = 373.0
      P1 = 1.C132E5
      CPL = 4.1e93
      CP = CPL
      CVP = 1.905E3
      CVV = 1.44E3
      CAV = 7.953E2
      CPG = CVP
      RCDW = 4.32E3
      EP = 0.9
      SI = 5.67E-8
      EPSI = EP*SI
      XNUC = 9.8E-7
      PR = 6.8
      CS = RHOZ*CP*( XNUC*BETA*G/((5.3**4)*PR**2) )**(1.C/3.C)
```

```
      XKG = 0.001
      BETAG = 1.2E-4
      XNUG = 9.9E-7
      RHOALPH = 1.3e
      CALPH = CVP
      ALPHG = XKG/(RHOALPH*CALPH)
      C1HT = 0.06
      C1HI = 0.06
      CG = XKG*C1HT*( BETAG*G/(XNUG*ALPHG) )**(1.0/3.0)
      CEV = XKG*C1HI*( (BETAG*G/(XNUG*ALPHG))**(1.0/3.0) )/CPG
      XNUM = 0.937*(5.3)**(4.0/3.0)
      CFAC1 = (XNUG**(1.0/12.0))/(XNUM*PR**(1.0/6.0))
      CFAC2 = 0.937*(XNUG**(1.0/4.0))*CP/(PR**(0.5))
      CZ = CFAC1*RHOZ
      C2 = CFAC2/(BETA*G)
      C1VS = 0.11
      C1HS = 0.06
      CS = CS*C1HS/C1VS
      TIMZ = 0.0
      TZ = 293.0
      QF = 7.0E4
      TINF = 293.0
      AVNT = 4.5618-5
      CDVNT = 0.25
      PVNT = 1.+2e955
      DPVNT = 0.0
      RETURN
      END

      SUBROUTINE INPUT2
      COMMON /TIMCM/ TIMMX,DTIML,DTIMG,DTIMPR,TIML,TIMG,TIMPR
      COMMON /TOLCM/ TOFTOL,XTOL,FTOL,NTOL
      COMMON /NCM/ N
      COMMON /VENTCM/ AVNT,CDVNT,PVNT,DPVNT
      CHARACTER *1 VENTOPT
      CHARACTER *3 VOPT
      OPEN(55, FILE='2000CHAR*INTK')
      READ(55, *)
      READ(55, *) TIMMX
      READ(55, *)
      READ(55, *)
      READ(55, *) DTIML, DTIMG, DTIMPR
      READ(55, *)
      READ(55, *)
      READ(55, *) TOFTOL, XTOL, FTOL, NTOL
      READ(55, *)
      READ(55, *)
      READ(55, *) N
      READ(55, *)
      READ(55, *)
      READ(55, *) VENTOPT, PVNT, DPVNT
      IF(VENTOPT .EQ. "N") GO TO 10
      IF(VENTOPT .EQ. "n") GO TO 10
      VOPT = "YES"
      GO TO 15
   10 PVNT = 1.0E25
      VOPT = "NO"
   15 CONTINUE
      OPEN(65, FILE='2000CHAR*OUTTK')
      WRITE(65, *) "          TIMMX"
      WRITE(65, '(3X,E13.5)') TIMMX
      WRITE(65, *)
      WRITE(65, *) "          DTIML          DTIMG          DTIMPR"
      WRITE(65, '(3(3X,E13.5))') DTIML, DTIMG, DTIMPR
      WRITE(65, *)
      WRITE(65, '(  "          TOFTOL          XTOL          FTOL
```

```
     & NTGL")')
      WRITE(65, '(3(3X,E13.5),3X,I5)') TGFTGL, XTGL, FTGL, NTGL
      WRITE(65, *)
      WRITE(65, *) "      N"
      WRITE(65, '(3X,I5)') N
      WRITE(65, *)
      WRITE(65, *) "        VENTGFT              PVNT            DPVNT"
      WRITE(65, '(13X,A5,2(3X,E13.5))') VGFT,PVNT,DPVNT
      WRITE(65, *)
      RETURN
      END

      SUBROUTINE INPUT3
C         This subroutine obtains total heat fluxes from input fire
C     diameters by means of a fire diameter vs heat flux table (when
C     provided).  Also, this subroutine is flexible enough to input
C     the heat flux directly.
      COMMON /INITCM/ TIME,TZ,QF,TINF
      CHARACTER *1 AA
      DIAMF = -1.0
      PRINT *
      PRINT *, "INPUT Fire Diameter (meters)."
      READ *, DIAMF
      PRINT *
      IF(DIAMF .LE. 0.0) GO TO 15
C         The heat flux QF is obtained here from the fire diameter
C     vs heat flux table (when provided).
      PRINT '(" Fire Diameter (meters) = ",E13.5)', DIAMF
      PRINT '(" Imposed Heat Flux (watts/meter**2) = ",E17.5)', QF
      PRINT *
      WRITE(65, *) "          DIAMF                QF"
      WRITE(65, '(2(3X,E13.5))') DIAMF, QF
      WRITE(65, *)
      GO TO 20
   15 CONTINUE
      QF1 = -1.0
      PRINT *, "INPUT Imposed Heat Flux (watts/meter**2)."
      READ *, QF1
      IF(QF1 .GT. 0.0) QF=QF1
      PRINT *
      PRINT '(" Imposed Heat Flux (watts/meter**2) = ",E13.5)', QF
      PRINT *
      WRITE(65, *) "          DIAMF                QF"
      WRITE(65, '("             --", 3X,E13.5)') QF
      WRITE(65, *)
   20 CONTINUE
      PRINT *, "PRESS RETURN to Start Program."
      READ '(A1)', AA
      RETURN
      END

      SUBROUTINE INITVAL
      PARAMETER ( IDM=100 )
      COMMON /GEOMCM/ HL,XLL,AL,AW,AB,V,VT
      COMMON /INITCM/ TIME,TZ,QF,TINF
      COMMON /TIMCM/ TIMMX,DTIML,DTIMG,DTIMPR,TIML,TIMG,TIMPR
      COMMON /NCV/ N
      COMMON /VLCM/ TWB,TWS(IDM),TC(IDM),TPC(IDM+1),TINFB,TINFS
      COMMON /WLCM/ IFB,QRRO0,QCLS,QFS,QRROS(IDM),QCLS(IDM)
      COMMON /VGCM/ TWG,TG,XMV,XMA,TINFT
      COMMON /WGCM/ QFT,QRRO,QCG,PA,PV,P,QRRI,QRL,XLEFF,QXM,QCL
      COMMON /VICV/ I(0:IDM),PST(0:IDM),L(0:IDM),ZP(0:IDM+1)
      COMMON /TOPCV/ PSTTOP,LENDTOP,TCT,TI,Te
      TIML = TIME
      TWB = TZ
      DO 10 K=1,N
```

```
      TWS(K) = TZ
      TC(K) = TZ
   10 CONTINUE
      TIMG = TIMZ
      TWG = TZ
      TG = TZ
      TCT = TZ
      DXM = 0.0
      QFS = QF
      QFT = QF
      QFE = QF
      TINFS = TINF
      TINFT = TINF
      TINFE = TINF
      CALL INITM
      DO 20 K=0,N
      Z(K) = K*HL/N
   20 CONTINUE
      RETURN
      END

      SUBROUTINE INITM
      COMMON /PHYSCM/ R,G,PATM
      COMMON /GEOMCM/ HL,XLL,AL,AW,AE,V,VT
      COMMON /MATPROP/ XMOLW,XMOLV,RHO,RHOZ,BETA,XLV,XL,T1,P1
      COMMON /VGCM/ TWG,TG,XMV,XMA,TINFT
      COMMON /WGCM/ QFT,QRRO,QCG,PA,PV,P,QRRI,QRL,XLEFF,DXM,QCL
      PV = P1*EXP( (XMOLV*XLV/R)*(1.0/T1 - 1.0/TG) )
      XMV = (XMOLV*V/R)*PV/TG
      XMA = (XMOLA*V/R)*(PATM - PV)/TG
      RETURN
      END

      PROGRAM TANK
      PARAMETER ( IDM=100 )
      COMMON /INITCM/ TIMZ,TZ,QF,TINF
      COMMON /TIMCM/ TIMMX,DTIML,DTIMG,DTIMPR,TIML,TIMG,TIMPR
      COMMON /NCM/ N
      COMMON /VLCM/ TWS,TWS(IDM),TC(IDM),TPC(IDM+1),TINFR,TINFS
      COMMON /WLCM/ QFS,QRRO,QCLE,QFS,QRROS(IDM),QCLS(IDM)
      COMMON /VGCM/ TWG,TG,XMV,XMA,TINFT
      COMMON /WGCM/ QFT,QRRO,QCG,PA,PV,P,QRRI,QRL,XLEFF,DXM,QCL
      COMMON /TOPCM/ PSTTOP,QENDTOP,TCT,TI,TB
      COMMON /DVGCM/ DTWG,DTG,DXMV,DXMA,DXMO,DXMI
      PPSI = 1.450E-4
      CALL INPUT1
      CALL INPUT2
      CALL INPUT3
      CALL INITVAL
      OPEN(65, FILE='2DCCHAR*OUTL')
      OPEN(66, FILE='2DCCHAR*OUTG')
      OPEN(67, FILE='2DCCHAR*OUT1')
      WRITE(65,*)"          TIML          TWS(1)          TWS(N)
     &TC(1)          TC(N)"
      WRITE(65,*)
      WRITE(66,'("          TIMG          TWG          TG
     &  XMV          XMA          P(PSI)          DXMI          DXMO"
     &)')
      WRITE(66,*)
      WRITE(67,'("       PSTTOP       QENDTOP          TCT
     &   TB          TWS          TIML          TIMG")')
      WRITE(67,*)
      TIMPR = -0.001 * TIMZ
   10 CONTINUE
C     PRINT *," 4 "
      CALL WL
```

```
C       PRINT *," 5 "
        CALL OVG
C       PRINT *," 6 "
        WRITE(66,'(5(2X,E13.5))') TIML, TWS(1), TWS(K), TC(1), TC(N)
        WRITE(66,'(5(2X,E13.5))') TIMG, TWG, TG, XMV,XMA,P*PPSI,DXMI,DXMO
        WRITE(67,'(7(2X,E13.5))') PSTTOP,QENDTOP,TCT,TB,TWB,TIML,TIMG
        TIMPR = TIMPR + DTIMPR
        IF(TIMPR .GE. TIMMX) STOP
   20 CONTINUE
C       PRINT *," 7 "
        CALL SKETCH
        TIMG = TIMG + DTIMG
        IF(TIMG .LT. (TIML+0.999*DTIML)) GO TO 20
   30 CONTINUE
C       PRINT *," 8 "
        CALL BUOY
C       PRINT *," 9 "
        CALL CORE
C       PRINT *," 10 "
        CALL SKETCH
C       PRINT *," 11 "
        CALL RELEASE
C       PRINT *," 12 "
        TIML = TIML + DTIML
        IF(TIML .LT. (TIMG-0.001*DTIMG)) GO TO 30
        IF(TIML .LT. TIMPR) GO TO 20
        GO TO 10
        END

        SUBROUTINE BUOY
        PARAMETER ( IDM=100 )
        COMMON /PHYSCM/ P,G,PATM
        COMMON /MATPRPCM/ XMOLA,XMOLV,RHO,RHOZ,BETA,XLV,XL,T1,P1
        COMMON /HEATPLCM/ RGAS,EPSI,C1,C2,CB,CS,CG,CEV
        COMMON /NCM/ N
        COMMON /VLCM/ TWS,TWS(IDM),TC(IDM),TPC(IDM+1),TINFB,TINFS
        COMMON /VYCM/ Z(0:IDM),PST(0:IDM),L(0:IDM),ZF(0:IDM+1)
        COMMON /TOPCM/ PSTTOP,QENDTOP,TCT,TI,TB
        PST(0) = 0.0
        DO 10 K=1,N
        DLTW = G*BETA*(TWS(K)-TC(K))
        C2C2 = C2*(Z(K)-Z(K-1))
        PST(K) = ( PST(K-1)**(3.0/4.0) + C2C2*DLTW**(1.0/3.0) )**(4.0/3.0)
   10 CONTINUE
        PSTTOP = PST(N)
        DLTW = G*BETA*(TWS(N)-TC(N))
        QENDTOP = C2*DLTW*PSTTOP**(3.0/4.0)
        RETURN
        END

        SUBROUTINE CORE
        PARAMETER ( IDM=100 )
        COMMON /GEOMCM/ HL,XLL,QL,AW,AB,V,VT
        COMMON /MATPRPCM/ XMOLA,XMOLV,RHO,RHOZ,BETA,XLV,XL,T1,P1
        COMMON /HEATCPCM/ CP,CPL,CVP,CVV,CAV,CPG
        COMMON /TIMCM/ TIMMX,DTIML,DTIMG,DTIMPR,TIML,TIMG,TIMPR
        COMMON /NCM/ N
        COMMON /VLCM/ TWS,TWS(IDM),TC(IDM),TPC(IDM+1),TINFB,TINFS
        COMMON /DVLCM/ DTWB,DTWS(IDM),DTPC
        COMMON /WLCM/ QF,QR,QS,QCLB,QFS,QRADS(IDM),QCLS(IDM)
        COMMON /VYCM/ Z(0:IDM),PST(0:IDM),L(0:IDM),ZF(0:IDM+1)
        COMMON /TOPCM/ PSTTOP,QENDTOP,TCT,TI,TB
        DTPC = (48/(RHO*CP*VT))*QCLB
        TCT = TC(N) + DTIML*DTPC
        IF(PSTTOP .GE. 1.0E-30) TCT=TCT+(QENDTOP/PSTTOP)/CP
        DO 10 K=1,N
```

```
      TPC(K) = TC(K) + DTIML*DTPC
   10 CONTINUE
      TPC(N+1) = TCT
      U(0) = 0.0
      ZP(0) = Z(0)
      DO 20 K=1,N
      U(K) = -PST(K)*XLL/(RHOI*AL)
      ZP(K) = Z(K) + DTIML*U(K)
   20 CONTINUE
      ZP(N+1) = Z(N)
      DO 30 K=1,N+1
      IF(ZP(K) .LT. ZP(K-1)) GO TO 40
   30 CONTINUE
      RETURN
   40 CONTINUE
      WRITE(05,*) "STOP IN SUBROUTINE CORE.  ZP(K) NOT INCREASING."
      STOP
      END

      SUBROUTINE INTCOR
      PARAMETER ( IDM=100 )
      COMMON /NCM/ N
      COMMON /VLCM/ TWB,TWS(IDM),TC(IDM),TPC(IDM+1),TIMPB,TIMPS
      COMMON /VYCM/ Z(0:IDM),PST(0:IDM),U(0:IDM),ZP(0:IDM+1)
      K = 0
      IH = 0
   10 CONTINUE
      K = K+1
      IG = IH
   20 CONTINUE
      IF(IH .GE. N) GO TO 30
      IF(ZP(IH+1) .GT. Z(K)) GO TO 30
      IH = IH+1
      GO TO 20
   30 CONTINUE
      IF(IH .NE. IG) GO TO 40
      TC(K) = TPC(IH+1)
      GO TO 90
   40 CONTINUE
      S = 0.0
      J = IG+2
   50 CONTINUE
      IF(J .GT. IH) GO TO 60
      S = S + (ZP(J)-ZP(J-1))*TPC(J)
      J = J+1
      GO TO 50
   60 CONTINUE
      S = S + (ZP(IG+1)-Z(K-1))*TPC(IG+1) + (Z(K)-ZP(IH))*TPC(IH+1)
      TC(K) = S/(Z(K)-Z(K-1))
   90 CONTINUE
      IF(K .LT. N) GO TO 10
      RETURN
      END

      SUBROUTINE RKUTTA
      PARAMETER ( IDM=100 )
      COMMON /TIMCM/ TIMMX,DTIML,DTIMG,DTIMPR,TIML,TIMG,TIMPR
      COMMON /NCM/ N
      COMMON /VLCM/ V(IDM+1)
      COMMON /DVLCM/ DV(IDM+1)
      DIMENSION V1(IDM+1), S(IDM+1)
      M = N+1
      H = DTIML
      DO 10 K=1,M
      V1(K) = V(K)
   10 CONTINUE
```

```
      CALL DVL
      DO 20 K=1,N
      S(K) = DV(K)
      V(K) = V1(K) + DV(K)*H/2.0
   20 CONTINUE
      CALL DVL
      DO 30 K=1,N
      S(K) = S(K) + 2.0*DV(K)
      V(K) = V1(K) + DV(K)*H/2.0
   30 CONTINUE
      CALL DVL
      DO 40 K=1,N
      S(K) = S(K) + 2.0*DV(K)
      V(K) = V1(K) + DV(K)*H
   40 CONTINUE
      CALL DVL
      DO 50 K=1,N
      V(K) = V1(K) + (S(K)+DV(K))*H/6.0
   50 CONTINUE
      RETURN
      END

      SUBROUTINE DVL
      PARAMETER ( IDM=100 )
      COMMON /HEATFLOW/ RODW,EPSI,C2,C2,CB,CS,CG,CEV
      COMMON /NOW/ N
      COMMON /DVLOW/ DTWB,DTWS(IDM),DTPC
      COMMON /WLOW/ QFB,QRROB,QCLB,QFS,QRROS(IDM),QCLS(IDM)
      CALL WL
      DTWB = (QFB - QRROB - QCLB)/RODW
      DO 10 K=1,N
      DTWS(K) = ( QFS - QRROS(K) - QCLS(K) )/RODW
   10 CONTINUE
      RETURN
      END

      SUBROUTINE WL
      PARAMETER ( IDM=100 )
      COMMON /HEATFLOW/ RODW,EPSI,C2,C2,CB,CS,CG,CEV
      COMMON /NOW/ N
      COMMON /VLOW/ TWB,TWS(IDM),TC(IDM),TPC(IDM+1),TINFB,TINFS
      COMMON /WLOW/ QFB,QRROB,QCLB,QFS,QRROS(IDM),QCLS(IDM)
      QRROB = EPSI*(TWB**4 - TINFB**4)
      TDIFF = MAX(0.0, TWB-TC(1))
      QCLB = CB*TDIFF**(4.0/3.0)
      DO 10 K=1,N
      QRROS(K) = EPSI*(TWS(K)**4 - TINFS**4)
      TDIFF = MAX(0.0, TWS(K)-TC(K))
      QCLS(K) = CS*TDIFF**(4.0/3.0)
   10 CONTINUE
      RETURN
      END

      SUBROUTINE GRUTTA
      COMMON /VGOM/ V(4)
      COMMON /DVGOM/ DV(4)
      COMMON /TIMOM/ TIMMX,DTIML,DTIMG,DTIMPR,TIML,TIMG,TIMPR
      DIMENSION V1(4), S(4)
      H = DTIMG
      DO 10 K=1,4
      V1(K) = V(K)
   10 CONTINUE
      CALL DVG
      DO 20 K=1,4
      S(K) = DV(K)
      V(K) = V1(K) + DV(K)*H/6.0
```

```
      CONTINUE
      CALL DVG
      DO 30 K=1,4
      S(K) = S(K) + 2.0*DV(K)
      V(K) = V1(K) + DV(K)*H/2.0
   30 CONTINUE
      CALL DVG
      DO 40 K=1,4
      S(K) = S(K) + 2.0*DV(K)
      V(K) = V1(K) + DV(K)*H
   40 CONTINUE
      CALL DVG
      DO 50 K=1,4
      V(K) = V1(K) + (S(K)+DV(K))*H/6.0
   50 CONTINUE
      RETURN
      END

      SUBROUTINE DVG
      COMMON /GEOMCM/ RL,XLL,AL,AW,AE,V,VT
      COMMON /HEATPCM/ CP,CPL,CVP,CVV,CAV,CPG
      COMMON /HEATFLCM/ RCOW,EPSI,C1,C2,CS,CS,CG,CEV
      COMMON /VGCM/ TWG,TG,XMV,XMA,TINFT
      COMMON /DVGCM/ DTWG,DTG,DXMV,DXMA,DXMC,DXMI
      COMMON /WGCM/ QFT,QRRC,QCG,PA,PV,P,QRRI,QRL,XLEFF,DXM,QCL
      COMMON /TOPCM/ PSTTOP,QENDTOP,TCT,TI,TB
      COMMON /PHYSCM/ R,G,PATM
      COMMON /VENTCM/ AVNT,CDVNT,PVNT,DPVNT
      CALL WG
      DTWG = (QFT - QRRC - QRRI - QCG)/RCOW
      DXMTRM = AL*DXM*(CVP*TI - CVV*TG)
      DTG = (QCG*AW - QCL*AL + DXMTRM)/(XMA*CAV + XMV*CVV)
      DXMI = AL*DXM
      DXMC = 0.0
      DXMV = DXMI
      DXMA = 0.0
      IF(P .LE. PVNT) RETURN
      DXMC = AVNT*CDVNT*SQRT(2.0*(P-PATM)*(XMV+XMA)/V)
      IF(P .LT. (PVNT+DPVNT)) DXMC = DXMC*(P-PVNT)/DPVNT
      DXMV = DXMV - DXMC*XMV/(XMV+XMA)
      DXMA = -DXMC*XMA/(XMV+XMA)
      DTG = DTG - DXMC*P*V/( (XMV+XMA)*(XMA*CAV+XMV*CVV) )
      RETURN
      END

      SUBROUTINE WG
      COMMON /PHYSCM/ R,G,PATM
      COMMON /GEOMCM/ RL,XLL,AL,AW,AE,V,VT
      COMMON /MATPRPCM/ XMOLA,XMOLV,RHO,RHOZ,BETA,XLV,XL,T1,P1
      COMMON /HEATPCM/ CP,CPL,CVP,CVV,CAV,CPG
      COMMON /HEATFLCM/ RCOW,EPSI,C1,C2,CS,CS,CG,CEV
      COMMON /VGCM/ TWG,TG,XMV,XMA,TINFT
      COMMON /WGCM/ QFT,QRRC,QCG,PA,PV,P,QRRI,QRL,XLEFF,DXM,QCL
      COMMON /TOPCM/ PSTTOP,QENDTOP,TCT,TI,TB
      QRRC = EPSI*(TWG**4 - TINFT**4)
      TDIFF = MAX(0.0, TWG-TG)
      QCG = CG*TDIFF**(4.0/3.0)
      PA = (XMA/XMOLA)*(R/V)*TG
      PV = (XMV/XMOLV)*(R/V)*TG
      P = PA + PV
      TB = 1.0/( (1.0/T1) - (R/(XMOLV*XLV))*LOG(P/P1) )
      CALL SURFTEMP
      QRRI = EPSI*(TWG**4 - TI**4)
      QRL = QRRI*AW/AL
      XLEFF = XL + CPL*(TI-TCT)
      CALL EVAP
```

```
      WCL = DXM*XLEFF - GRL
      RETURN
      END

      SUBROUTINE EVAP
      COMMON /HEATCPCM/ CP,CPL,CVP,CVV,CAV,CPG
      COMMON /HEATFLCM/ RCOM,EPSI,CI,C2,CB,CS,CG,CEV
      COMMON /TOLCM/ TOFTOL,XTOL,FTOL,NTOL
      COMMON /VGCM/ TWG,TG,XMV,XMA,TINFT
      COMMON /WGCM/ QFT,GRRO,GCG,PA,PV,P,GRRI,GRL,XLEFF,DXM,GCL
      COMMON /TOPCM/ PSTTOP,GENDTOP,TCT,TI,TB
      TDIFF = MAX(0.0, TG-TI)
      A = CEV*TDIFF**(1.0/3.0)
      B = CPG*TDIFF/XLEFF
      C = GRL/XLEFF
      IF(TDIFF .GE. TOFTOL) GO TO 10
      DXM = C
      RETURN
   10 CONTINUE
      CALL EVNEWT(A,B,C,DXM,I1FL,I2FL)
      IF((I1FL+I2FL) .LT. NTOL) RETURN
      WRITE(6,*) "STOP IN SUBROUTINE EVAP.  NTOL EXCEEDED."
      STOP
      END

      SUBROUTINE EVNEWT (A, B, C, X, I1FL, I2FL)
      COMMON /TOLCM/ TOFTOL,XTOL,FTOL,NTOL
      IF(A .GT. XTOL) THEN
      AVAR = A*SQRT(B*C/(A+A*C+B*C))
      X = C + MAX(AVAR,0.99*FTOL)
      ELSE
      X = C + 0.99*FTOL
      ENDIF
      I1FL = 0
      I2FL = 0
      DO 20, N=1,NTOL
      F = X - A*LOG(1.0+B*X/(X-C))
      DF = 1.0 + A*( ( B*C/((1.0+B)*(X-C)+B*C) )/(X-C) )
      DX = F/DF
      IF (F .GT. 0.0) THEN
      I1FL = I1FL+1
      IF((X-C) .LT. FTOL) RETURN
      DX = MIN(DX, 0.5*(X-C))
      ELSE
      I2FL = I2FL+1
      END IF
      IF (ABS(F) .LT. FTOL) RETURN
      X = X-DX
   20 CONTINUE
      RETURN
      END

      SUBROUTINE SURFTEMP
      COMMON /VGCM/ TWG,TG,XMV,XMA,TINFT
      COMMON /WGCM/ QFT,GRRO,GCG,PA,PV,P,GRRI,GRL,XLEFF,DXM,GCL
      COMMON /TOPCM/ PSTTOP,GENDTOP,TCT,TI,TB
      TI = MIN(0.5*(TG+TCT),TB)
      RETURN
      END

*****************************************************************
****  VGS TITLE INTX
*****************************************************************

      TIMMX
      400.0
```

DTZML	DT1MG	DTMPR	
0.5	0.5	0.5	
TOFTOL	XTOL	FTOL	NTOL
2.0	1.0E-25	1.0E-3	20

N (Number of cells)
6

VENTOPT	PVNT	DPVNT
"Y"	1.4269E5	0.0

APPENDIX C
EXPERIMENTAL EFFORT

Specially designed fire/tank tests were conducted to measure the response of a tank containing liquid to fire impingement. This experimental effort consisted of measuring effects of the heat input from a large-scale turbulent sooty fire on a partially filled liquid solvent container. The goals of this task were: (1) to evaluate the fire/tank interaction environment, and (2) to obtain the data necessary for preliminary validation of the numerical computer prediction model.

In these tests, commercially available 55-gallon, 18-gage steel drums were used. The drums were instrumented to monitor the internal pressure and temperature rise of a fire-engulfed tank. The drums were equipped with a network of chromel alumel thermocouples for measuring the variation of the liquid temperature (Figure C-1). A pressure gage (0-30 lb/in^2) was used to monitor the pressure rise resulting from expansion of the vapor (Figure C-2) and manually vent the tanks before rupture. The tanks were placed about 0.15 m above the surface of a 4.3-m-diameter JP-4 fuel pool fire in both vertical and horizontal orientations. Prior to the start of the fire, the tanks were filled with water up to 12 centimeters (5 inches) from the top of the tank. The temperatures were read by a datalogger at 5-second intervals, and each event was recorded continously, using video and still photographs. Figures C-3 and C-4 show the fire pit and the orientations of the tank with respect to the pool fire. Figures C-5 and C-6 show the temperature profiles for two tests with the tanks oriented vertically.

General analysis of the temperature data and postfire inspection of the tank shell revealed the following:

1. The tank initial pressure rise is predominantly due to the expansion of vapor in the ullage volume,

2. The radiation heat emitting from the dry wall in the ullage volume is the main heat flux mechanism in the gaseous phase,

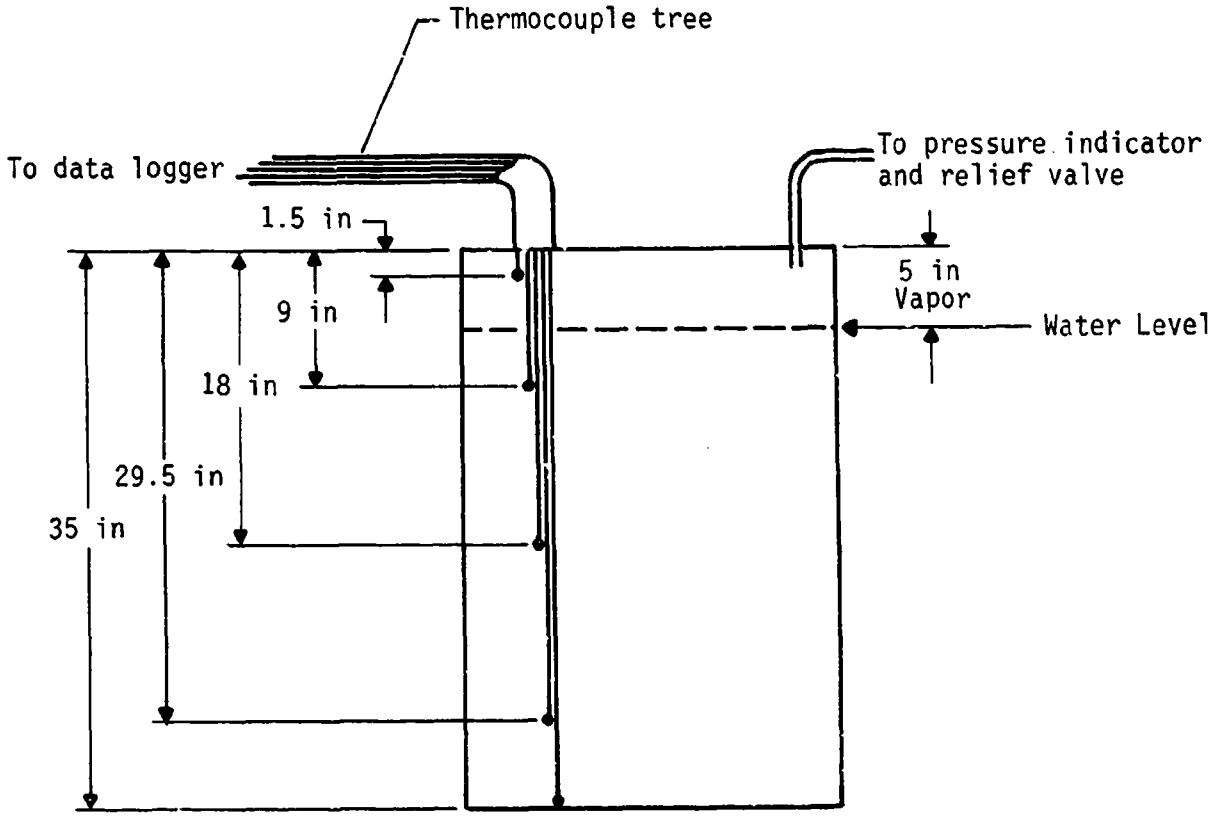

Figure C-1. Water-filled 55-gallon Drum

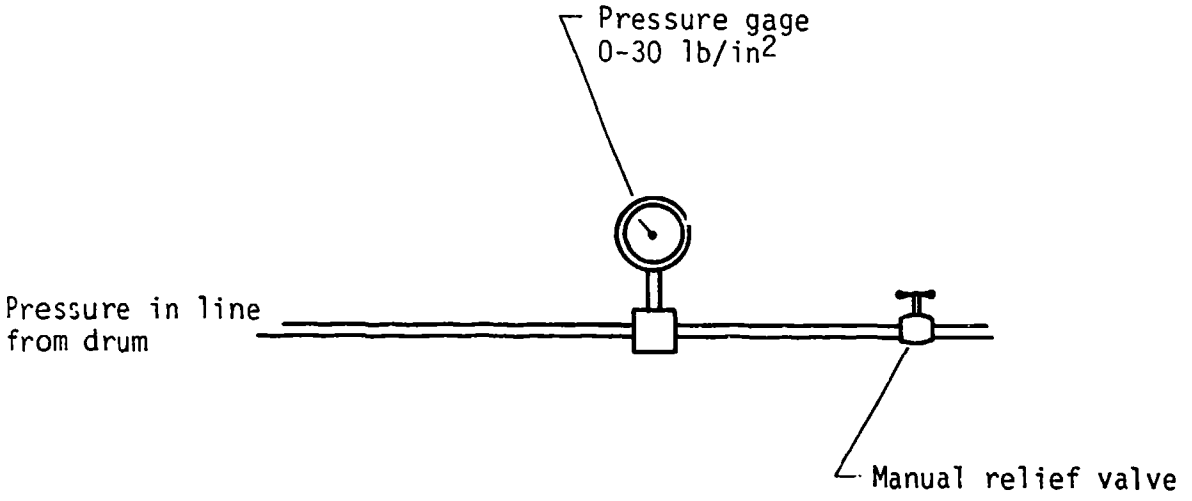

Figure C-2. Pressure Monitoring Assembly

(a) Vertical orientation tank fire

(b) Horizontal orientation tank fire

Figure C-3. Tank Fires with Different Orientations

(a) Vertical orientation test

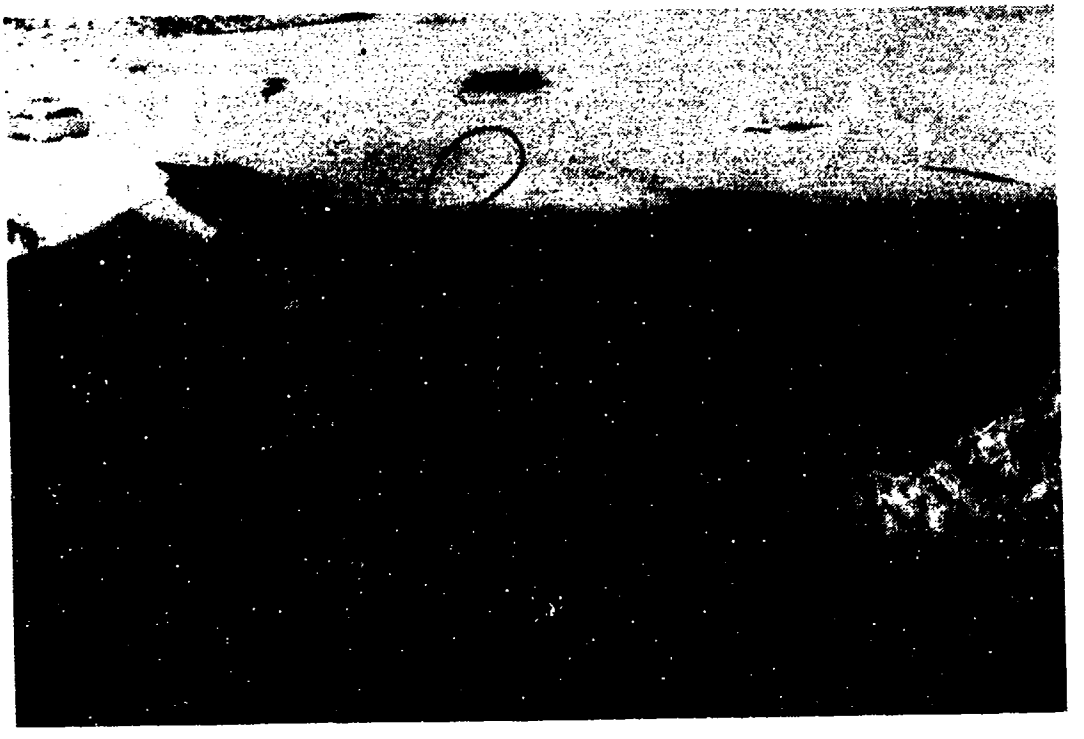

(b) Horizontal orientation test

Figure C-4. Vertical and Horizontal Orientation Tests

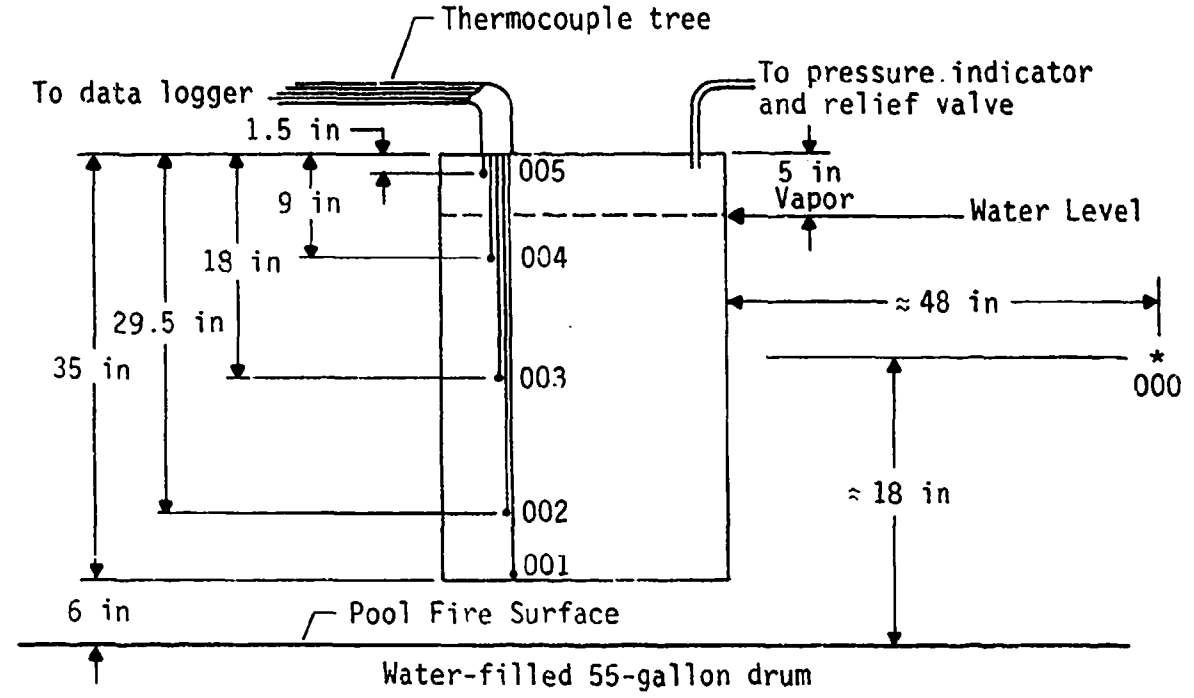

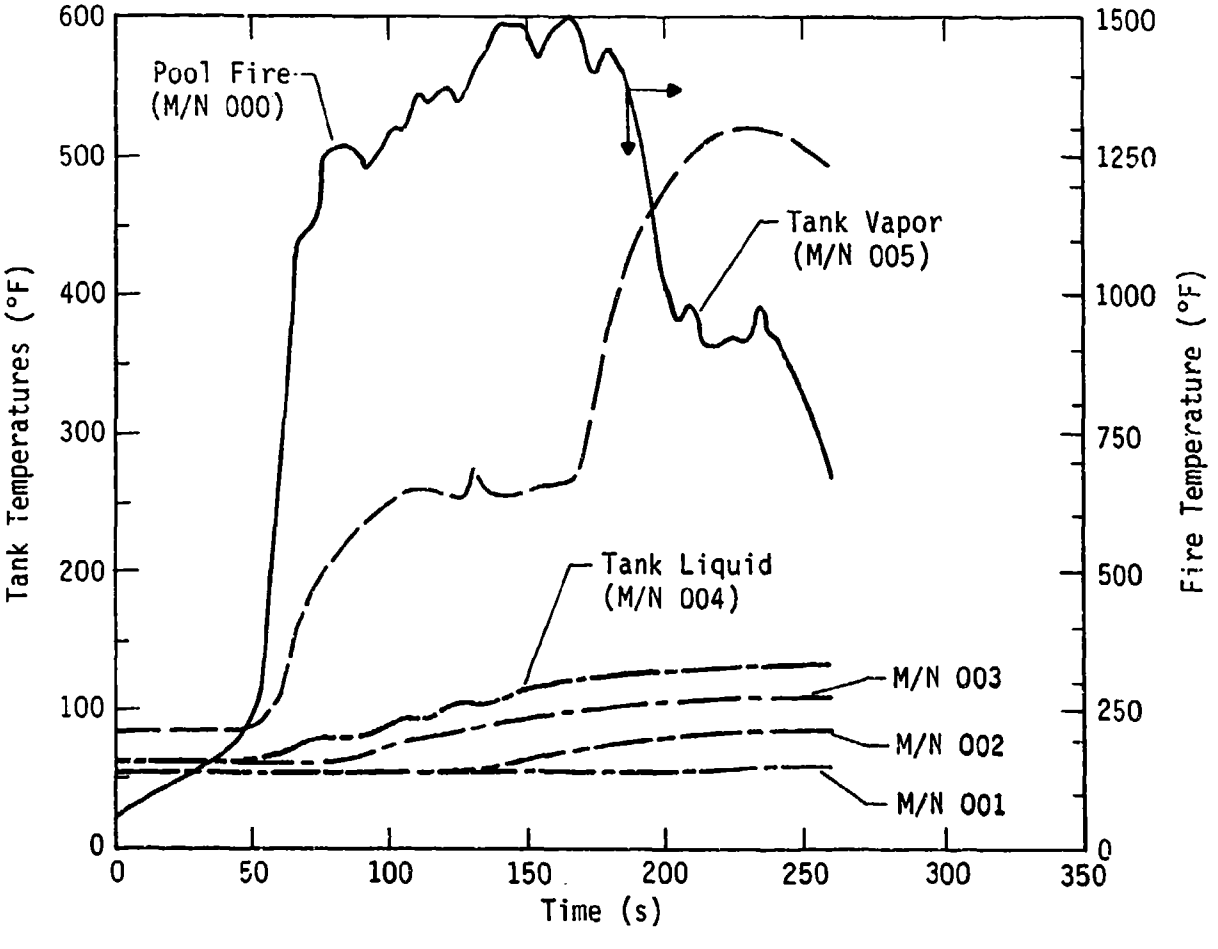

Figure C-5. Fire/Tank Test No. 1 Temperature Profiles

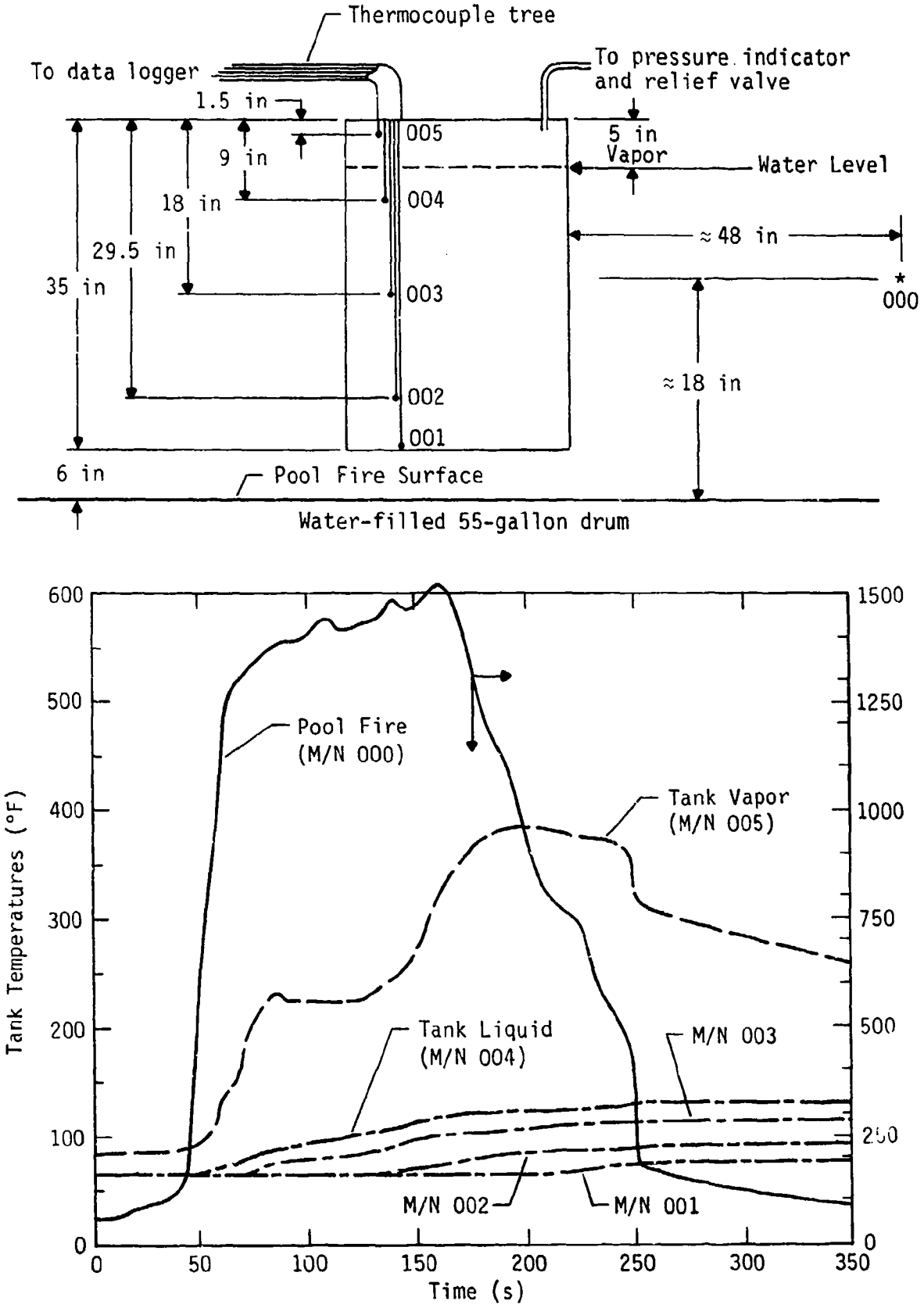

Figure C-6. Fire/Tank Test No. 2 Temperature Profiles

3. Discoloration of the wall next to the vapor compared to the wall in contact with the liquid is indicative of a large temperature difference across the vapor/liquid interface, and

4. The thermocouples placed at various elevations along the height of the tank showed a decreasing temperature gradient downward from the top of the tank.

The discoloration of the tank shell suggests a strong conduction heat transfer in the tank wall at the liquid meniscus which contributes to the overall thermal activity of the interface and should be considered in the model.

The predictions of the model proved to be consistent with physical intuition and agreed well with the overall trend of the experimental data. However, the predictions from the calculations consistently showed higher values than the corresponding experimental data. This variation, sometimes as high as 200 percent, persisted during all test events.

The factors that might cause or contribute to the discrepancy between the simulation predictions and the tests were evaluated. The assumption of constant heat flux over the entire tank in the simulation may not have been duplicated in the tests as a result of wind effects and the overall test configuration. Also, because of safety considerations the tank was vented manually, which could have affected the tank response. Project resource limitations did not permit further testing and validation of the tank response model.